

Characterization of Parkinson's disease associated DJ-1 mutants
and influence of α -synuclein on glial cells

Dissertation

zur Erlangung des Grades eines
Doktors der Naturwissenschaften

der Mathematisch-Naturwissenschaftlichen Fakultät
und
der Medizinischen Fakultät
der Eberhard-Karls-Universität Tübingen

vorgelegt

von

Emmy Helena Rannikko
aus Pargas, Finnland

November - 2013


Tag der mündlichen Prüfung:	10.02.2014
Dekan der Math.-Nat. Fakultät:	Prof. Dr. W. Rosenstiel
Dekan der Medizinischen Fakultät:	Prof. Dr. I. B. Autenrieth
1. Berichterstatter:	Prof. Dr Philipp Kahle
2. Berichterstatter:	Prof. Dr Olaf Rieß
Prüfungskommission:	Prof. Dr Philipp Kahle Prof. Dr Olaf Rieß Prof. Dr Thilo Stehle Prof. Dr Ulrike Naumann

To my grandpa, who was diagnosed with Parkinson's disease
and passed away during my graduate time

“Your songs and stories I carry with me,
Your warm heart, always open for me,
Your proud smile smiling at me,
Thank you, dear Moffa”

I hereby declare that I have produced the work entitled: "*Characterization of Parkinson's disease associated DJ-1 mutants and influence of α -synuclein on glial cells*", submitted for the award of a doctorate, on my own (without external help), have used only the sources and aids indicated and have marked passages included from other works, whether verbatim or in content, as such. I swear upon oath that these statements are true and that I have not concealed anything. I am aware that making a false declaration under oath is punishable by a term of imprisonment of up to three years or by a fine.

Tübingen, 15.10.2013
Date


Signature

Parts of this work has been presented in

Original article

- **Rannikko EH**, Vesterager LB, Shaik JH, Weber SS, Cornejo Castro EM, Fog K, Jensen PH, Kahle PJ. "Loss of DJ-1 protein stability and cytoprotective function by Parkinson's disease-associated proline-158 deletion" *J Neurochem.* 2012 Dec 14 doi:10.1111/jnc.12126. [Epub ahead of print]

Oral presentation

- 5th Annual Meeting of NGFN-Plus and NGFN-Transfer in the Program of Medical Genome Research in Heidelberg, 11-13 December 2012

Abstracts and poster presentation

- NGFNplus network "Functional genomics of Parkinson's disease" in Tübingen, 18-20 April 2013

- "5th conference on advances in molecular mechanisms underlying neurological disorders" organized by the European Society for Neurochemistry and the Biochemical Society in Bath, UK, 23-26 June 2013

Contents

Contents	I
Figures	IV
Tables	V
Abbreviations	VI
1 Introduction	1
1.1 Parkinson's disease and multiple system atrophy are synucleinopathies.....	1
1.1.1 PD is the most common neurodegenerative movement disorder.....	1
1.1.2 MSA patients have oligodendroglial cytoplasmic inclusions	2
1.2 Neuroinflammation	4
1.2.1 Increased cytokine signaling is proinflammatory	4
1.2.2 Cyclooxygenase	4
1.2.3 Nitric oxide is a stress induced signaling molecule in the brain	5
1.2.4 Toll-like receptor 4 signaling pathway	5
1.3 α -syn is an aggregation-prone protein	7
1.3.1 The (Thy1) ^h [A30P]SNCA transgenic mouse line as a PD animal model	9
1.3.2 The hypothesis of α -syn transmission	9
1.4 DJ-1 is a multifunctional cytoprotective protein	15
1.4.1 DJ-1 is a highly conserved dimeric protein	16
1.4.2 DJ-1 animal models are more sensitive to mitochondrial toxins and oxidative stress	19
1.4.3 DJ-1 is multifunctional	19
1.5 ASK1 is a mitogen activated protein kinase kinase kinase	21
1.5.1 ASK1 is activated in response to stress.....	21
1.6 Objectives.....	25
2 Material and methods	26
2.1 Material	26
2.1.1 Devices	26
2.1.2 Consumables	26
2.1.3 Chemicals	27
2.1.4 Antibodies.....	29
2.1.5 Electrocompetent bacteria	29
2.1.6 Constructs	30
2.1.7 Preparation of recombinant α -synuclein	31
2.2 Animals.....	32
2.2.1 Mouse maintenance	32
2.3 Cell culture	33
2.3.1 Preparation of primary astrocytes	33
2.3.2 Cell line maintenance	34
2.3.3 Transfection.....	34
2.4 Protein biochemistry.....	34
2.4.1 SDS-Polyacrylamide Gel Electrophoresis (SDS-PAGE).....	34
2.4.2 Sensitive coomassie staining.....	35
2.4.3 Immunoblot	35

2.4.4	Immunofluorescence staining.....	35
2.4.5	Semi quantitative PCR.....	36
2.4.6	Steady state protein levels.....	36
2.4.7	Cycloheximide treatment.....	37
2.4.8	Pulse Chase.....	37
2.4.9	Size exclusion chromatography and co-immunoprecipitations.....	37
2.4.10	Daxx translocation.....	38
2.4.11	OLN AS viability assays.....	38
2.4.12	In vitro immunocomplex kinase assay.....	39
2.4.13	NO assay.....	39
2.4.14	NF- κ B nuclear translocation.....	39
2.4.15	Uptake of extracellular α -syn.....	40
2.4.16	Statistical analyses.....	40
3	Results.....	41
3.1	Characterization of the PD associated DJ-1 ^{A179T} , DJ-1 ^{P158Δ} and DJ-1 ^{A107P} mutants.....	41
3.1.1	The steady state protein levels of DJ-1 ^{P158Δ} and DJ-1 ^{A107P} are decreased compared to the protein levels of DJ-1 ^{wt} and DJ-1 ^{A179T}	41
3.1.2	DJ-1 ^{P158Δ} and DJ-1 ^{A107P} have decreased protein half-life times compared to DJ-1 ^{wt} and DJ-1 ^{A179T}	43
3.1.3	DJ-1 ^{P158Δ} and DJ-1 ^{A107P} forms dimers with DJ-1 ^{wt} , but no homodimers of the mutants were detected.....	43
3.1.4	DJ-1 ^{P158Δ} binds to ASK1 also in absence of oxidative stress.....	46
3.1.5	DJ-1 ^{P158Δ} inhibits Daxx nuclear export less efficiently than DJ-1 ^{wt} and DJ-1 ^{A179T}	49
3.1.6	DJ-1 ^{wt} , but not mutants, decrease p25 α dependent MT retraction in an α -syn overexpressing oligodendroglial cell line.....	51
3.1.7	ASK1 is involved in p25 α dependent MT retraction in OLN AS cells.....	53
3.2	Induction of inflammation by and uptake of extracellular α -syn in primary astrocytes.....	55
3.2.1	Quality control of the purified recombinant synuclein proteins.....	55
3.2.2	Treatment with recombinant α -syn induces cytokine expression in primary astrocytes.....	57
3.2.3	Treatment with recombinant α -syn up-regulates the iNOS expression in astrocytes.....	59
3.2.4	Extracellular recombinant α -syn induces a possibly TLR4 dependent astroglial NO production.....	60
3.2.5	Induction of cytokine and iNOS expression by α -syn treatment is decreased in Tlr4 ^{-/-} astrocytes.....	61
3.2.6	Induction of p38 and JNK phosphorylation by α -syn treatment is decreased in Tlr4 ^{-/-} astrocytes.....	62
3.2.7	NF- κ B nuclear translocation after treatment with α -syn is inhibited in Tlr4 ^{-/-} astrocytes.....	64
3.2.8	The recombinant α -syn is taken up by the astrocytes in a TLR4 independent manner and is not phosphorylated in the astrocytes...	65
3.2.9	The internalized extracellular α -syn is possibly degraded via the proteasome in astrocytes.....	68
3.3	Onset of motorical symptoms in <i>Dj-1^{-/-}/Thy1h[A30P]SNCA</i> mice.....	70
4	Discussion.....	72

4.1	P158 and A107 are important for the stability of the DJ-1 dimer	72
4.1.1	A179 to T mutation does not affect the stability and binding behavior of DJ-1	72
4.1.2	Deletion of P158 and mutation of A107 affect stability and dimerization ability of DJ-1.....	73
4.1.3	DJ-1 ^{P158Δ} and DJ-1 ^{A107P} show an altered binding behavior towards ASK1.....	74
4.1.4	DJ-1 protection and ASK1 activation in a MSA cell culture model	76
4.2	Elevated secretion of α -syn possibly cumulates the neuronal stress.....	78
4.2.1	TLR4 involved activation of inflammation induced by extracellular α -syn	79
4.2.2	DJ-1 as protector against α -syn induced stress.....	80
4.2.3	Astrocytes as removers of extracellular α -syn	81
4.2.4	Transmission of pathogenic α -syn during disease progression	83
4.3	Perspectives.....	85
5	Summary	89
6	References	90
7	Acknowledgments	103
	Appendix – Declaration of co-authorship	

Figures

Figure 1.1	The basal ganglia circuit in a healthy brain compared to the circuit in a PD brain.....	2
Figure 1.2	TLR4 signaling pathway (modied from Kawai and Akira, 2007, Lu et al., 2008)	6
Figure 1.3	Schematic view of human α -syn protein (modified from Recchia et al., 2004)	8
Figure 1.4	A possible model of the transmission of α -syn.....	14
Figure 1.5	Multiple sequence alignment of eukaryotic DJ-1 homologues	16
Figure 1.6	DJ-1 protein structure.....	17
Figure 1.7	Schematic overview of ASK1 and its regulation.....	22
Figure 3.1	DJ-1 ^{P158Δ} and DJ-1 ^{A107P} show decreased protein steady state levels compared to DJ-1 ^{wt} and DJ-1 ^{A179T}	42
Figure 3.2	Inhibition of protein translation with cycloheximide reveals that DJ-1 ^{P158Δ} and DJ-1 ^{A107P} degrade faster than DJ-1 ^{wt} and DJ-1 ^{A179T}	44
Figure 3.3	The protein protein half-life time of DJ-1 ^{P158Δ} is significantly shorter than the half-life times of DJ-1 ^{wt} and DJ-1 ^{A179T}	45
Figure 3.4	The dimerization ability of DJ-1 ^{P158Δ} and DJ-1 ^{A107P} is altered.....	45
Figure 3.5	DJ-1 ^{P158Δ} binds also in absence of oxidative stress to ASK1 ^{FL} , whereas DJ-1 ^{A107P} seems to behave almost as DJ-1 ^{wt}	47
Figure 3.6	Size exclusion chromatography confirmed the binding behavior of DJ-1 ^{P158Δ} to ASK1	49
Figure 3.7	Five times more cDNA of DJ-1 ^{P158Δ} than of DJ-1 ^{wt} and DJ-1 ^{A179T} is needed in order to decrease Daxx nuclear translocation upon induction of oxidative stress	50
Figure 3.8	DJ-1 ^{wt} , but not mutant DJ-1, decrease MT retraction induced by co-expression of α -syn and p25 α in rat oligodendrocytes.....	51
Figure 3.9	DJ-1 ^{A107P} is to some extent able to decrease the MT retraction after p25 α transfection in OLN AS cells.....	52
Figure 3.10	Regulation of ASK1 is influencing the MT retraction in p25 α and α -syn expressing OLN cells	54
Figure 3.11	Quality control of the purified recombinant synucleins showed that they were absent of other contaminating proteins and contained very low levels of endotoxins.....	56
Figure 3.12	Treatment with recombinant α -syn induces expression of COX-2, IL-1 β and IL-6 in primary astrocytes from littermate <i>Dj-1</i> ^{+/+} and <i>Dj-1</i> ^{-/-} mice.....	58
Figure 3.13	Treatment with α -syn induces iNOS mRNA expression in primary astrocytes from littermate <i>Dj-1</i> ^{-/-} and <i>Dj-1</i> ^{+/+} mice.....	60
Figure 3.14	Treatment with α -syn induces NO production and release in astrocytes, the induction can be reduced with a TLR4 specific inhibitor	61
Figure 3.15	Induction of iNOS and cytokine expression after treatment with recombinant α syn is greatly reduced in <i>Tlr4</i> ^{-/-} primary astrocytes.....	63
Figure 3.16	Treatment with recombinant α -syn induces p38 and JNK phosphorylation to a lesser extent in <i>Tlr4</i> ^{-/-} than in <i>Tlr4</i> ^{+/+} primary astrocytes.....	65
Figure 3.17	Treatment with recombinant α -syn induces NF- κ B nuclear translocation in <i>Tlr4</i> ^{+/+} , but not in <i>Tlr4</i> ^{-/-} astrocytes.....	66
Figure 3.18	Extracellular α -syn is internalized by primary astrocytes in a TLR4 independent manner.....	67

Figure 3.19 The internalized recombinant α -syn is not phosphorylated in the astrocytes.....	68
Figure 3.20 The amount of α -syn taken up by the astrocytes decrease with time, possibly via proteasomal degradation	69
Figure 3.21 Knock out of <i>Dj-1</i> does not accelerate the onset of motorical symptoms in Thy1h[A30P]SNCA transgenic mice	71
Figure 4.1 Suggested model of mutant DJ-1 regulation of ASK1 signalosome activation.....	78
Figure 4.2 Model of how extracellular monomeric α -syn may influence astrocytes..	82

Tables

Table 1.1 Genes associated with autosomal recessive and dominant PD.....	3
Table 1.2 Mutations in DJ-1 associated with PD	15
Table 2.1 Mutagenesis primers	31
Table 2.2 Mouse lines and genotyping primers.....	33
Table 2.3 Semi quantitative PCR primers	36

Abbreviations

α -syn	α -synuclein
APS	Ammonium persulfate
ASK1	Apoptosis signal regulating kinase 1
β -syn	β -synuclein
BCA	Bicinchoninic acid
BSA	Bovine serum albumin
CCC	C-terminal coil-coiled region (of ASK1)
CCL	C-C motif chemokine
COX	Cyclooxygenase
CX3CL	Chemokine (C-X3-C motif) ligand
CXCL	C-X-C motif chemokine ligand
CXCR	C-X-C chemokine receptor
DAMP	Death/Damage associated molecular pattern
Daxx	Death domain-associated protein
DMAT	2-dimethylamino-4,5,6,7-tetrabromo-1H-benzimidazole
DMEM	Dulbecco's minimal essential medium
DMSO	Dimethyl sulfoxide
ECL	Enhanced chemiluminescence
EDTA	Ethylene diamine tetraacetic acid
EGTA	Ethylene glycol tetraacetic acid
eNOS	Epithelial nitric oxide synthase
ERK	Extracellular signal regulating kinase
FCS	Fetal calf serum
FL	Full length
FPLC	Fast protein liquid chromatography
GAPDH	Glyceraldehyde-3-phosphate dehydrogenase
GICs	Glial cytoplasmic inclusions
GST	Glutathione S-transferase
HEK	Human embryonic kidney
HIPK1	Homeodomain-interacting protein kinase 1
hPBGD	Human porphobilinogen deaminase
HRP	Horseradish peroxidase
ICAM	Intracellular adhesion molecule
IFN	Interferon
iNOS	Inducible nitric oxide synthase
I κ -B α	Nuclear factor κ B inhibitor α
IKK	Inhibitor of nuclear factor κ B kinase
IL	Interleukin
IPTG	Isopropyl β -D-1-thiogalactopyranoside
IRAK	Interleukin-1 receptor-associated kinase
IRF	Interferon regulatory factor
JNK	c-Jun N-terminal kinase
Keap1	Kelch-like ECH-associated protein 1
LB	Luria-Bertani (media)
LBP	LPS binding protein
LPS	Lipopolysaccharide
MAP3K	Mitogen activated protein kinase kinase kinase
MAPK	Mitogen activated protein kinase
MBP	Myelin basic protein
MEF	Mouse embryonic fibroblasts
MEK1/2	Mitogen activated protein kinase kinase 1/2
MMP	Matrix metalloproteinase
MKK	Mitogen activated protein kinase kinase
MSA	Multiple system atrophy
MT	Microtubules/Microtubuli
MPTP	1-methyl-4-phenyl-1,2,3,6-tetrahydropyridine
MyD88	Myeloid differentiation primary response gene
NAC	Non-amyloid component

NCC	N-terminal coil-coiled region (in ASK1)
NGF	Nerve growth factor
NF- κ B	Nuclear factor κ B
nNOS	Neuronal nitric oxide synthase
NO	Nitric oxide
NP-40	Nonident P-40
Nrf2	Nuclear factor erythroid-2 related factor 2
OLN AS	Rat oligodendroglial cells stably overexpressing human α -syn
PAGE	Polyacrylamide gel electrophoresis
PAMP	Pathogen associated molecular pattern
PBS	Phosphate buffered saline
PCR	Poly chain reaction
PD	Parkinson's disease
PI3 K	Phosphoinositide 3-kinase
PP5	Protein phosphatase 5
PSF	Polyoyrimidine tract binding protein-associated splicing factor
PTEN	Phosphate and tensin homolog deleted from chromosome 10
PVDF	Polyvinylidene difluoride
RIP	Receptor interacting protein
ROS	Reactive oxygen species
SAP	Shrimp alkaline phosphatase
SARM1	Sterile α and TIR motif-containing protein 1
SDS	Sodium dodecyl sulfate
SNARE	Soluble N-ethylmaleimide-sensitive-factor attachment receptor
TAB	Transforming growth factor β -activated kinase 1 binding protein
TAK1	Transforming growth factor β -activated kinase 1
TBK1	Serine/threonine-protein kinase TANK-binding kinase 1
TBST	Tris buffered saline with tween
TEMED	N,N,N',N'-Tetramethylethyldiamine
TGF	Transforming growth factor
TH	Tyrosine hydroxylase
TIR	Toll-interleukin-1 receptor
TIRAP (Mal)	TIR domain-containing adaptor protein
TLR	Toll-like receptor
TNF	Tumor necrosis factors
TRAF	TNF receptor associated factor
TRAM	TRIF-related adaptor molecule
TRIF	TIR domain containing adaptor inducing IFN- β
Trx	Thioredoxin
UV	Ultra violet radiation
v/v	Volume per volume
VCAM	Vascular cell adhesion protein
w/v	Weigth per volume

1 Introduction

1.1 Parkinson's disease and multiple system atrophy are synucleinopathies

Pathological examinations of brains from Parkinson's disease (PD) patients have revealed abnormal amounts of intraneuronal protein aggregates. These aggregates, called Lewy bodies or Lewy neurites, are the hallmark of PD. Lewy bodies have the size of 5-25 μm and are eosinophilic, round inclusions located in the cytoplasm of the neuron (Spillantini et al., 1997). Over 70 different proteins have been identified to be present in Lewy bodies, but the main component is α -synuclein (α -syn) (Shults et al., 2005, Wakabayashi et al., 2007). Aggregates of α -syn are found in a subset of other diseases as well, for example multiple system atrophy (MSA) and dementia with Lewy bodies. Diseases with α -syn positive inclusions are commonly called synucleinopathies.

1.1.1 PD is the most common neurodegenerative movement disorder

PD was first described by James Parkinson in 1817 in the work "An Essay on the Shaking Palsy" (Parkinson, 2002). Many years later the disease was named after him. PD is the most common neurodegenerative movement disorder affecting about two percent of the population over 70 years. Age is an important risk factor; the common age of onset is between 50 and 80 years. The main clinical symptoms of PD are rigidity, bradykinesia or akinesia, resting tremor and postural instability. In addition, depression, sleep disorders, dementia, psychosis and reduced sense of smell are common among PD patients (Reviewed in Jankovic, 2008). The disease is caused by degeneration of neurons, especially the dopaminergic neurons, in *substantia nigra pars compacta* in the midbrain. The loss of these neurons in this region affects the signaling in the basal ganglial circuit leading to decreased output from cortex and brainstem (Fig 1.1). Up to date there is no cure for PD and therefore the clinical treatment is focused on reduction of the symptoms, for example by administration of a precursor of dopamine, levodopa, or deep brain stimulation. In deep brain stimulation a brain pulse generator is used to stimulate the firing of the neurons in the basal ganglia to compensate for the loss of the signaling from *substantia nigra pars compacta*. The most used target is the subthalamic nucleus.

1 Introduction

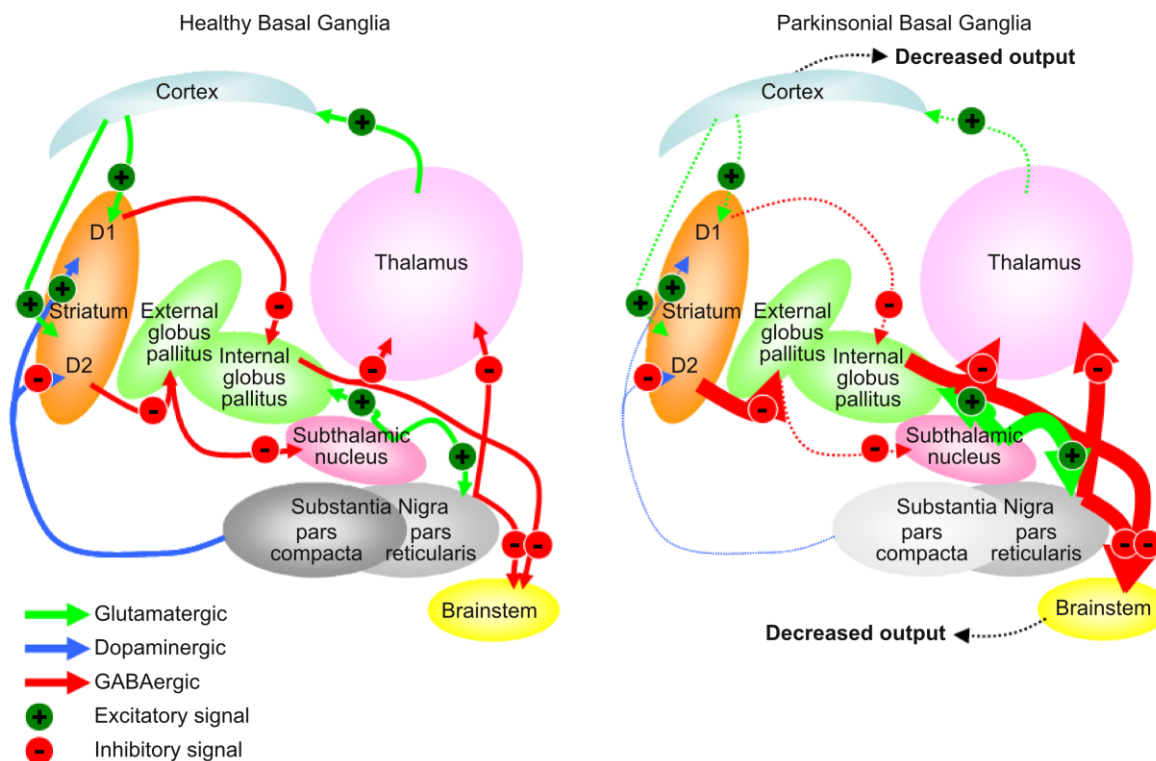


Figure 1.1 The basal ganglia circuit in a healthy brain compared to the circuit in a PD brain. The input from dopaminergic neurons in substantia nigra pars compacta to striatum decreases during PD disease progression, which leads to decreased activation of cortex and increased inhibition of the brainstem. Thick arrows in the Parkinsonian circuit indicate increased neuronal activity compared to healthy circuit and thin dotted arrows decreased neuronal activity.

Most cases of PD are considered idiopathic. However, 5-10 percent of the cases can be explained by a familiar inheritance. Table 1.1 presents the genes, which are associated with autosomal recessive or dominant PD. These genes code for proteins in fairly different pathways and their PD-associated mutations lead to either a gain or a loss of their protein function. It is still actively examined how mutations in these genes can cause PD. Moreover, increased protein aggregation, mitochondrial dysfunction, oxidative stress, disturbed ubiquitin-proteosomal and lysosome-autophagosomal functions and increased cellular calcium levels are proposed to contribute to the neurodegeneration in PD (Reviewed in Alberio et al., 2012). This work focuses on the protein products of two of the PD associated genes, namely SNCA and DJ-1, which code for the proteins α -syn and DJ-1, respectively. These two proteins are described in more detail later on.

1.1.2 MSA patients have oligodendroglial cytoplasmic inclusions

MSA is a ruthless neurodegenerative disorder with adult onset. The major clinical hallmarks are variable combinations of parkinsonism, cerebellar ataxia, autonomic

dysfunction and mood and executive function deficits (Reviewed in Ubhi et al., 2011). Due to absence of diagnostic biomarkers the patients are often misdiagnosed and a neuropathological confirmation is needed for confident MSA diagnosis. MSA patients show neuronal loss and gliosis in the brainstem and in other parts of the brain. The neuropathological hallmark of MSA is α -syn containing filamentous glial cytoplasmic inclusions (GCIs) (Papp et al., 1989, Wakabayashi et al., 1998). In addition, the GCIs contain the microtubule (MT) associated protein p25 α , which is also called tubulin polymerization-promoting protein (Lindersson et al., 2005). p25 α is an unstructured protein that is primarily expressed in oligodendroglia (Takahashi et al., 1993). It has been shown to interact with tubulin and to promote the polymerization and stability of the MT (Tirian et al., 2003). Moreover p25 α causes the MT to form aberrant bundles (Hlavanda et al., 2002). In contrast to its normal oligodendroglial localization, p25 α is also found in a subset of the neuronal Lewy bodies (Lindersson et al., 2005). Furthermore, the oligodendroglial cells with GCIs have been shown to have elevated amounts of the PD related protein DJ-1 (Neumann et al., 2004).

Table 1.1 Genes associated with autosomal recessive and dominant PD

PARK locus	Inheritance	Gene	Gene Product	Reference
PARK1/4	Dominant	<i>SNCA</i>	α -syn	Polymeropoulos et al, 1997, Singleton et al, 2003
PARK2	Recessive	<i>PRKN</i>	parkin	Kitada et al., 1998
PARK5	Dominant	<i>UCHL1</i>	Ubiquitin carboxyl-terminal hydrolase isozyme L1	Leroy et al., 1998
PARK6	Recessive	<i>PINK1</i>	PTEN-Induced Putative Kinase 1	Valente et al. 2004
PARK7	Recessive	<i>DJ-1</i>	DJ-1	Bonifati et al., 2003
PARK8	Dominant	<i>LRRK2</i>	Leucin-Rich Repeat Kinase 2	Zimprich et al., 2004
PARK9	Recessive	<i>ATP13A2</i>	Probable cation-transporting ATPase 13A2	Ramirez et al, 2006
PARK11	Dominant	<i>GIGYF2</i>	Grb10-Interacting GYF Protein 2	Lautier et al. 2008
PARK13	Dominant	<i>HTRA2</i>	HtrA2/Omi	Strauss et al., 2005
PARK14	Recessive	<i>PLA2G6</i>	85 kDa calcium-independent phospholipase A2	Paisan-Ruiz et al., 2009
PARK15	Recessive	<i>FBXO7</i>	F-box only protein 7	Di Fonzo et al., 2009
PARK17	Dominant	<i>VPS35</i>	Vacuolar protein sorting-associated protein 35	Vilarino-Guell et al., 2011
PARK18	Dominant	<i>EIF4G1</i>	Eukaryotic translation initiation factor 4 gamma 1	Chartier-Harlin et al., 2011
Gaucher's locus	Recessive	<i>GBA</i>	Glucosylceramidase	Sidransky et al, 2009

1 Introduction

1.2 Neuroinflammation

The innate immune system can be induced to protect the brain against damage caused by trauma, infection, stroke or neurotoxins. Inflammation in the central nervous system is characterized by increased activation of microglia and astrocytes, elevated pro-inflammatory cytokine concentration, enhanced blood-brain-barrier permeability and hence increased leukocyte invasion. However, long-lasting formation and accumulation of proinflammatory mediators can initiate neuronal damage, neuronal circuit impairments and neurodegeneration. Postmortem studies have shown an increase in neuroinflammatory signals in brains from PD patients. Activated microglia are found in the substantia nigra of PD patients (McGeer et al., 1988) and PD brains show a higher density of CD8⁺ and CD4⁺ T-cells than healthy control brains (Brochard et al., 2009). Correspondingly, the neuroinflammatory pathology found in brains of PD patients has been reproduced in several PD animal models (Reviewed in Hirsch and Hunot, 2009).

1.2.1 Increased cytokine signaling is proinflammatory

Cytokines are small signaling molecules that can be produced and secreted by most cell types, but are mostly produced in the cells of the immune system. They diffuse to neighboring cells, where they bind and activate specific receptors. Cytokines can induce either pro- or anti-inflammatory reactions, for example, they can activate cyclooxygenases (COX) and nitric oxide synthases (NOS). Usually cytokine production is cell protective. However, excess and sustained proinflammatory cytokine signaling may lead to cell damage. Tumor necrosis factors (TNF), interleukins (IL), interferons (IFN) and chemokines are pro-inflammatory cytokines. Notably, postmortem investigations of brains from PD patients have revealed increased levels of IFN- γ , TNF α and IL-1 β in substantia nigra. In addition, the cytokine levels have also been found to be elevated in striatum, in cerebrospinal fluid and in the blood serum. Moreover, genetic association studies have found a relation between certain polymorphisms in cytokine genes and increased risk of developing PD (Reviewed in Hirsch and Hunot, 2009).

1.2.2 Cyclooxygenase

The expression of COX-2 in astrocytes is induced by proinflammatory substances. COX-2 catalyses the rate limiting step when prostaglandins are formed from

arachidonic acid. High levels of prostaglandins are proinflammatory, since they induce proinflammatory responses in neighboring cells (Reviewed in Phillis et al., 2006).

1.2.3 Nitric oxide is a stress induced signaling molecule in the brain

Nitric oxide (NO) can function as a signaling molecule between adjacent cells. It can freely diffuse across membranes from one cell to another. In addition, NO is used by the cells of the immune system to cause nitrosylative stress in intruding pathogens. The short lived NO is easily oxidized to non-reactive nitrite (NO_2^-), which can be oxidized by OH^\bullet , resulting in reactive NO_2^\bullet radicals. These can nitrosylate and thus disturb proteins, lipids and DNA. Moreover, under oxidative stress conditions NO can react with the O_2^\bullet superoxide radical and form highly reactive peroxynitrite (ONOO^-) species, which also can nitrosylate macromolecules. Elevated levels of nitrosylated proteins have been found in postmortem PD brain (Reviewed in Nakamura et al., 2013).

There are three NOS proteins in the brain. The neuronal NOS (nNOS) and the epithelial NOS (eNOS) are constantly expressed and are activated by calcium increase in the cell. In contrast to what its name says, nNOS is a ubiquitously expressed protein. nNOS and eNOS are important for the production of NO when it is used as a signaling substance. In contrast, the expression of inducible NOS (iNOS) is increased in response to various stress signals, for example in response to cytokines (Stuehr, 1999). When it is expressed iNOS produces continuously NO, it is only regulated by transcription and its short protein half-life time (Kolodziejcki et al., 2004). Thus dysregulation of cytokine expression leads to increased iNOS expression, which generates elevated NO levels, resulting in nitrosylative stress and increase in nitrosylated proteins. Interestingly, iNOS positive microglia cells have been identified in PD brains (Hunot et al., 1996).

1.2.4 Toll-like receptor 4 signaling pathway

Toll-like receptors (TLRs) are expressed by cells that belong to the innate immune system. They are activated by pathogen associated molecular patterns (PAMP), which are structural motifs of proteins and lipids characteristically expressed by fungi, bacteria and viruses. TLRs can also be activated by certain endogenous molecular patterns, these are sometimes termed DAMPs, where D stand for death or damage. Activation of TLRs induces activation of different signaling pathways and expression of different cytokines. Over ten different TLRs are known and they differ both in which pathways they activate as well as in which PAMPs and DAMPs they recognize. TLR4 is

1 Introduction

activated by lipopolysaccharide (LPS), but also by the fusion protein from respiratory syncytial virus and the envelope protein from mouse mammary tumor virus (Poltorak et al., 1998, Kurt-Jones et al., 2000, Rassa et al., 2002). In addition, some DAMPs, for example heat-shock proteins, hyaluronic acid and β -defensin 2, have been shown to either directly or indirectly activate TLR4 (Ohashi et al., 2000, Biragyn et al., 2002, Termeer et al., 2002).

TLR4 is a transmembrane protein. The recognition of LPS involves three extracellular proteins in addition to TLR4, namely CD14, MD-2 and LPS binding protein (LBP) (Fig 1.2). LPS binds to LBP, which facilitates the association between LPS and CD14. CD14 promotes the transfer of LPS to the MD-2/TLR4 receptor complex. Upon activation TLR4 undergoes oligomerization and recruits intracellular proteins through interactions with its intracellular toll-interleukin-1 receptor (TIR) domain. There are five proteins that interact with the activated TIR domain; myeloid differentiation primary response gene 88 (MyD88), TIR domain-containing adaptor protein (TIRAP or Mal), TIR domain containing adaptor inducing IFN- β (TRIF), TRIF-related adaptor molecule (TRAM) and sterile α and TIR motif-containing protein 1 (SARM1). TLR4 can interact with all of the-

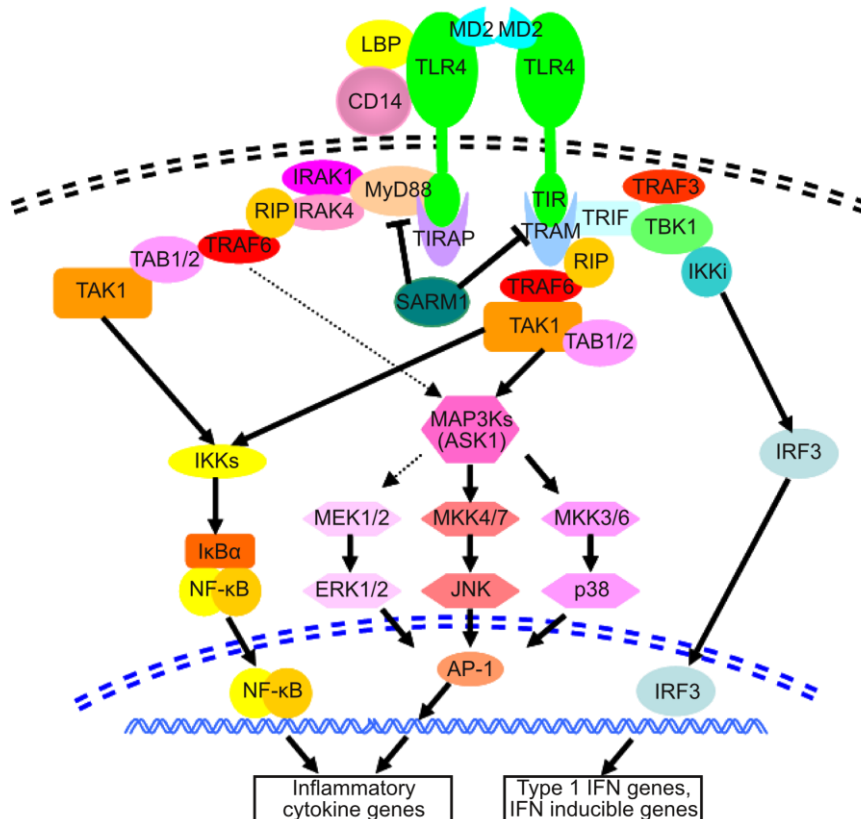


Figure 1.2 TLR4 signaling pathway. The MyD88 dependent pathway is illustrated on the left and the MyD88 independent pathway on the right. Dashed arrows are less known associations. Full names of proteins are written in the list of abbreviations (Modified from Kawai and Akira, 2007, Lu et al., 2008).

se adaptor proteins. Activation of TLR4 can induce a MyD88 dependent pathway, which leads to induction in proinflammatory cytokine expression. In addition, TLR4 can induce a MyD88 independent pathway, which induces the expression of Type 1 IFN and IFN-inducible genes (Fig 1.2) (Reviewed in Lu et al., 2008).

1.3 α -syn is an aggregation-prone protein

α -syn is highly abundant in the brain, but it is also present in other tissues, for example it is also present in red blood cells (Barbour et al., 2008). It is associated with synaptic vesicles (Maroteaux et al., 1988) and may also associate with other membranes (Davidson et al., 1998, Jo et al., 2000, Fortin et al., 2004). The physiological functions of α -syn are still not fully understood, but it is suggested that it affiliates the soluble N-ethylmaleimide-sensitive-factor attachment receptor (SNARE) complex assembly in synaptic vesicles and thereby it can influence the neurotransmitter release (Burre et al., 2010). In addition, it has been suggested in computer molecular simulation studies that α -syn may stabilize the unfavourable curved form of small phospholipid micelles by filling the fissures at the surface (Perlmutter et al., 2009). The curvature stress in small lipid micelles favors fusion of the micelles with flat target membranes (Chernomordik et al., 1995). Thus it is possible that α -syn functions as a regulator of a controlled fusion of synaptic vesicles with membranes by preventing unwanted fusion of the vesicles and by facilitating the Ca^{2+} /SNARE mediated fusion.

The length of α -syn is 140 amino acids (Fig 1.3). There are three proteins in the family of synucleins, α -, β -, and γ -syn. The N-terminal domains of the synucleins are reminiscent, whereas the C-terminal parts differ. The non-amyloid component (NAC)-domain (amino acids 65-95) of α -syn has been shown to be essential for its ability to form fibrils (Fig 1.3). The NAC domain is partly absent in both β -syn and γ -syn and therefore α -syn is more aggregation prone than its family members (Giasson et al., 2001, el-Agnaf and Irvine, 2002). The synucleins lack an organized peptide structure. However, it is shown *in vitro* that at least lipid-bound α -syn adopts an α -helical structure where the C-terminal domain of α -syn bends towards the NAC domain thereby blocking the domain from interaction with other α -syn monomers (Ulmer and Bax, 2005). Truncated and cleaved forms of α -syn that lack the C-terminus are more prone to aggregate than the full length α -syn (Crowther et al., 1998, Murray et al., 2003). Also other posttranslational modifications of α -syn, for example, nitrosylation

1 Introduction

and phosphorylation, seem to promote fibril formation (Fujiwara et al., 2002, Takahashi et al., 2002). In addition, α -syn tends to aggregate more easily in vesicles that often have high calcium concentrations, low pH and where glycosaminoglycans are present (Cohlberg et al., 2002, Hoyer et al., 2002, Lowe et al., 2004). Moreover, aggregation of α -syn to β -sheet rich aggregates is shown to accelerate when preformed fibrillar aggregate seeds are present. This nucleation property is a common feature of fibrillar, amyloid aggregate formation (Wood et al., 1999). Oligomeric α -syn is still soluble, but fibrillar α -syn becomes insoluble. Currently it is generally thought that the oligomers are likely to be the more cytotoxic α -syn species and that aggregation may be a cytoprotective function.

Point mutation, duplication or triplication of the gene for α -syn, *SNCA*, has been found in a few families with familial autosomal dominant PD (Fig 1.3) (Polymeropoulos et al., 1997, Singleton et al., 2003). The point mutations A53T and A30P are well studied (Polymeropoulos et al., 1997, Kruger et al., 1998). These two mutants have been shown to accelerate the α -syn fibril formation (Narhi et al., 1999). In other hand, duplication and triplication of the gene has been shown to increase the α -syn protein amount in the cells (Farrer et al., 2004). More recently, polymorphisms in the *SNCA* promoter region have been found in autosomal-dominant PD and in the genome-wide association studies several single nucleotide polymorphisms in *SNCA* were found to increase the risk of developing sporadic PD (Satake et al., 2009, Simon-Sanchez et al., 2009, Edwards et al., 2010, Mata et al., 2010). In other words, there is a strong correlation between alterations in the expression and function of α -syn and PD.

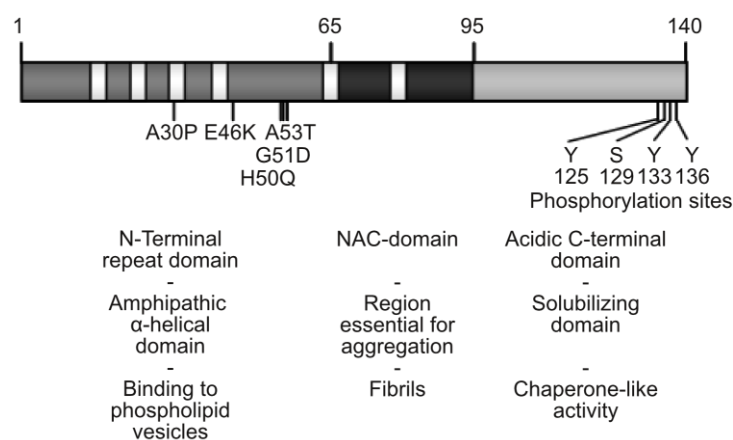


Figure 1.3 Schematic view of human α -syn protein. White boxes show imperfect KTKEGV repeats. PD associated point mutants are indicated. (Modified from Recchia et al., 2004).

1.3.1 The (Thy1)*h*[A30P]SNCA transgenic mouse line as a PD animal model

Different animal models that assumingly mimic synucleinopathies have been generated. The (Thy1)*h*[A30P]SNCA mouse line that was used here has been well characterized (Kahle et al., 2000, Kahle et al., 2001, Neumann et al., 2002, Freichel et al., 2007, Schell et al., 2009). In this mouse line human α -syn^{A30P} is overexpressed under the control of the *Thy1*-promoter, which is specific for the neurons in the central nervous system. These mice form already at young age somatodendritic, detergent insoluble α -syn accumulations throughout the brain and the spinal cord (Kahle et al., 2000, Kahle et al., 2001). Only in aged brains (over 16 months) the α -syn accumulations in the brainstem, midbrain and olfactory bulb are thioflavine S positive and proteinase K resistant, which implies fibrillar amyloid inclusions. However, in substantia nigra the α -syn expression seem to be relatively low and no dopaminergic neuron loss is seen (Neumann et al., 2002). With age the mice develop phenotypic cognitive impairment and motoric symptoms, which lead to a motoric endstage at the age around 1.5 years (Freichel et al., 2007, Schell et al., 2009). Interestingly, S129 phosphorylated α -syn positive staining can be found in many cortical areas, hippocampus and in the basolateral amygdala. This correlates with difficulties in emotional learning in aged mice (Freichel et al., 2007, Schell et al., 2009). In conclusion, this mouse line shows several relevant signs that mimic human synucleinopathies – mostly reminiscent to dementia with Lewy bodies – and can thus be considered as a useful animal model.

1.3.2 The hypothesis of α -syn transmission

Braak and colleagues studied the α -syn pathology in 110 brains – 41 brains were from patients with clinically diagnosed PD and 69 brains were from individuals with no or only some clinical markings of PD symptoms (Braak et al., 2003). All brains showed α -syn pathology in the dorsal motor nucleus. If α -syn pathology was found in cortical regions, it was also found in the dorsal motor nucleus, coeruleus–subcoeruleus complex, midbrain and mesocortex. Based on the results Braak suggested a staging model, where the α -syn pathology spreads in a specific pattern from the the dorsal motor nucleus via *substantia nigra* to the cortex. In this model the areas affected in a certain stage correlates with the motorical symptom severity (Braak et al., 2003). Thus, it has been in recent years actively discussed if progression of the pathological protein misfolding and aggregation during PD disease development is caused by

1 Introduction

transmission of misfolded α -syn between adjacent cells. This hypothesis is supported by the *in vivo* findings that α -syn containing Lewy body-like inclusions have been found in transplanted embryonic midbrain tissue in PD patient brains (Kordower et al., 2008, Li et al., 2008). The transmission of α -syn pathology from host to transplanted tissue has also been observed in *in vivo* mouse models (Desplats et al., 2009, Hansen et al., 2011). However, if α -syn itself can act as a disease spreading agent it needs to be able to fulfill some requirements. First α -syn needs to exit the donor neuron and be transferred to a recipient cell. Moreover, it has to either enter the recipient cell and/or act via a receptor on the cell membrane. Importantly the transmitted α -syn has to cause cellular stress and damage the recipient cell and this should cause the recipient cell to further transfer the pathological α -syn. More evidence is currently appearing that α -syn may be able to perform these actions. However, there are still many deficits and inconsistencies in this hypothesis and the exact mechanisms are still intensively investigated and discussed.

Secretion of α -syn

Predominantly, α -syn is located in the cell body or synapses of neurons, but even though α -syn lacks a cell secretory signaling sequence it is found in the cerebrospinal fluid and blood plasma both in PD patients and healthy controls (El-Agnaf et al., 2003, Lee et al., 2006, Tokuda et al., 2006). Moreover, both monomeric and fibrillar forms of α -syn have been shown to be secreted to the growth media from cultured neurons and cell lines (El-Agnaf et al., 2003, Lee et al., 2005, Sung et al., 2005, Danzer et al., 2011). Dying cells that release their cellular content can be a source of the extracellular α -syn, but the concentration of extracellular α -syn does not correlate with that of other cytosolic proteins (Lee et al., 2005). Thus it is very likely that α -syn is secreted from the cells. However, the mechanism how α -syn is secreted is not fully understood. Cellular stress conditions that facilitate accumulation of misfolded and damaged proteins have been shown to increase vesicular α -syn and thus the release of α -syn (Fig 1.4) (Jang et al., 2010). For example, inhibition of the lysosome or the proteasome, serum deprivation and oxidative stress have been suggested to increase the vesicular translocation of α -syn and subsequently the secretion (Lee et al., 2005, Jang et al., 2010). Dopamine has been suggested to induce the α -syn aggregation in the vesicles and increase the secretion (Lee et al., 2011). The export of α -syn is proposed to be a non-classical, ER/Golgi-independent secretion pathway (Lee et al., 2005, Jang et al., 2010). In addition, a fraction of α -syn has been implied to be

secreted in exosomes in a calcium dependent manner (Fig 1.4) (Emmanouilidou et al., 2010). The exosomal secretion was proposed to be increased upon lysosomal inhibition (Alvarez-Erviti et al., 2011). Normally exosomes allow adjacent cells to exchange proteins and RNA, for example they can supply the recipient cell with material for protection against oxidative stress (Eldh et al., 2010). Although exosomal vesicles play an important role in cell protection they have also been shown to be involved in prion protein transmission (Fevrier et al., 2004, Rajendran et al., 2006, Vella et al., 2007). However, the exosomal secretion seems to be a minor contributor to the extracellular α -syn, since fractionation of cell culture media from α -syn overexpressing SH-SY5Y cells did not show enriched levels of α -syn in the exosomal fraction (Hasegawa et al., 2011).

Transfer of α -syn to recipient cells

The part of the extracellular α -syn that is not surrounded by a protective exosomal membrane can either be taken up by other cells or alternatively be degraded. Three extracellular proteases, namely matrix metalloproteinase 3 (MMP3), neurosin and plasmin, have been shown to cleave α -syn and thus decrease its extracellular concentration (Fig 1.4) (Sung et al., 2005, Kasai et al., 2008, Tatebe et al., 2010, Kim et al., 2012). Interestingly, phosphorylated and α -syn^{A30P} were less efficiently cleaved by neurosin than non phosphorylated wild type (wt) α -syn (Kasai et al., 2008). In addition, it has been proposed that α -syn can be transferred directly between cells in so called tunneling nanotubes, which are long, thin extensions of the surface membrane and interconnect cells over long distances (Fig 1.4) (Agnati et al., 2010). For example, the prion protein is also shown to be transferred between cells in these tubes (Gousset et al., 2009).

Uptake of extracellular α -syn

How and if α -syn enters the recipient cells is rather unclear. Different mechanisms and explanations have been proposed by a variety of groups. The mechanism of the uptake of oligomeric and fibrillar α -syn may differ from the uptake of the monomeric protein. As mentioned previously, α -syn can interact with membranes and lipids (Davidson et al., 1998, Jo et al., 2000, Fortin et al., 2004). Thus it is possible that extracellular α -syn can directly associate with the cell membrane. Accordingly, it has been shown that α -syn can be taken up in cells at very low temperatures and in presence of endocytic inhibitors, which would indicate that α -syn is able to passively

1 Introduction

diffuse through the cell membrane (Fig 1.4) (Ahn et al., 2006, Lee et al., 2008a). It is also possible that α -syn associates with lipid rafts and thus it may enter cells nonspecifically during the renewal of membrane proteins (Fig 1.4) (Fortin et al., 2004). The ganglioside GM1, which is an essential component of lipid rafts, has been suggested to interact with α -syn (Martinez et al., 2007). Accordingly, lipid raft-mediated endocytosis has been proposed for microglial uptake of α -syn (Park et al., 2009). Furthermore, it is suggested that oligomeric and fibrillar α -syn is taken up by the cells in a classical Rab5a-dependent endocytic pathway (Fig 1.4). This is suggested since the uptake of the fibrils has been shown to be abated at low temperature, in presence of a dominant negative dynamin variant and when potential endocytosis receptor proteins were removed with trypsin (Sung et al., 2001, Lee et al., 2008a). Both TLR4 and TLR2 have been suggested to mediate the internalization of α -syn in microglia (Fellner et al., 2013, Kim et al., 2013). However, more data is still needed to explain the mechanism of the uptake.

Cellular mischief made by secreted α -syn

Depending on how a protein enters a recipient cells it is either directly cytosolic (for example after passive diffusion) or in membrane surrounded vesicles (for example after endocytosis). If and how α -syn is able to exit the vesicles and get access to the cytosol is unclear. Nevertheless, α -syn inclusions have been found in cells that had been treated either with α -syn, which had been produced in cultured cells (Hansen et al., 2011), or with *in vitro* generated, recombinant α -syn oligomers and fibrils (Fig 1.4) (Danzer et al., 2009, Luk et al., 2009, Nonaka et al., 2010, Waxman and Giasson, 2010). The inclusions were shown to be thioflavine S and ubiquitin positive, mainly perinuclear and they were shown to contain misfolded and phosphorylated α -syn (Luk et al., 2009, Nonaka et al., 2010, Waxman and Giasson, 2010). Both exogenous and endogenous α -syn was found in the inclusions. The exogenous α -syn seemed to be located in the core and the endogenous α -syn in the outer layers of the inclusions (Luk et al., 2009, Hansen et al., 2011, Angot et al., 2012). In addition, α -syn variants, which do not form fibrils, did not lead to formation of such inclusions (Waxman and Giasson, 2010). This would favor the nucleation theory for the α -syn fibril formation and propagation.

A second hypothesis is that α -syn, which is taken up by the cells, leads to an α -syn overload and thus aggregation. This may be relevant since misfolded, aggregated and abnormal forms of α -syn have been shown to impair the ubiquitin-proteasome system

(Stefanis et al., 2001, Snyder et al., 2003). The hypothesis is further supported by a study where introduction of exogenous α -syn fibrils led to impairment of proteasomal activity and subsequently to formation of inclusions (Nonaka et al., 2010). Thus the internalized α -syn may be especially aggregation prone and may lead to proteotoxic stress.

In addition, treatment of primary rat cortical neurons with exogenous α -syn fibrils was shown to induce reactive oxygen species (ROS) production and nuclear factor κ B (NF- κ B) nuclear translocation (Tanaka et al., 2002). An other study showed that exogenous α -syn led to an NMDA receptor-dependent increase in nNOS expression and NO production in cultured rat brain slices (Fig 1.4) (Adamczyk et al., 2009). Moreover, studies have proposed that cells that had received extracellular α -syn show disruption of the *cis*-Golgi and an increase in cell death (Sung et al., 2001, Desplats et al., 2009, Luk et al., 2009, Danzer et al., 2011). Thus it seems like transmitted extracellular α -syn can induce stress-associated intracellular pathways in recipient neurons and other cells.

Besides the neurotoxic responses, extracellular α -syn is suggested to be able to induce neuroinflammation by activating glial cells (Fig 1.4). *In vitro* studies have shown that exposure of microglial cells to extracellular α -syn can increase their activation, production of NO and expression of cytokines and TLRs (Zhang et al., 2005b, Klegeris et al., 2008, Su et al., 2008, Beraud et al., 2011). Furthermore, injection of human α -syn into the substantia nigra of mice led to an induced expression of pro-inflammatory cytokines and microglial activation (Couch et al., 2011). It was shown that α -syn can regulate the microglial activity through activation of the CD36 scavenger receptor and the Mac-1 receptor (Zhang et al., 2007, Su et al., 2008). Microglial cells can be effective removers of extracellular α -syn, but their activation seems to decrease the α -syn degradation ability, which could further lead to accumulation of the protein in these cells (Lee et al., 2008a, Lee et al., 2008b). In other words, it is possible that increasing amounts of extracellular α -syn in PD brains can progressively slow down the α -syn disposal by microglial cells and thus further enhance the pathological effects. Moreover, one study suggested a transfer of α -syn from neuronal cells to astrocytes (Fig 1.4). The transmission was demonstrated both in cell culture and in vivo, it was suggested to be endocytosis dependent and it was shown to lead to α -syn inclusions followed by inflammatory responses in the astrocytes (Lee et al., 2010).

1 Introduction

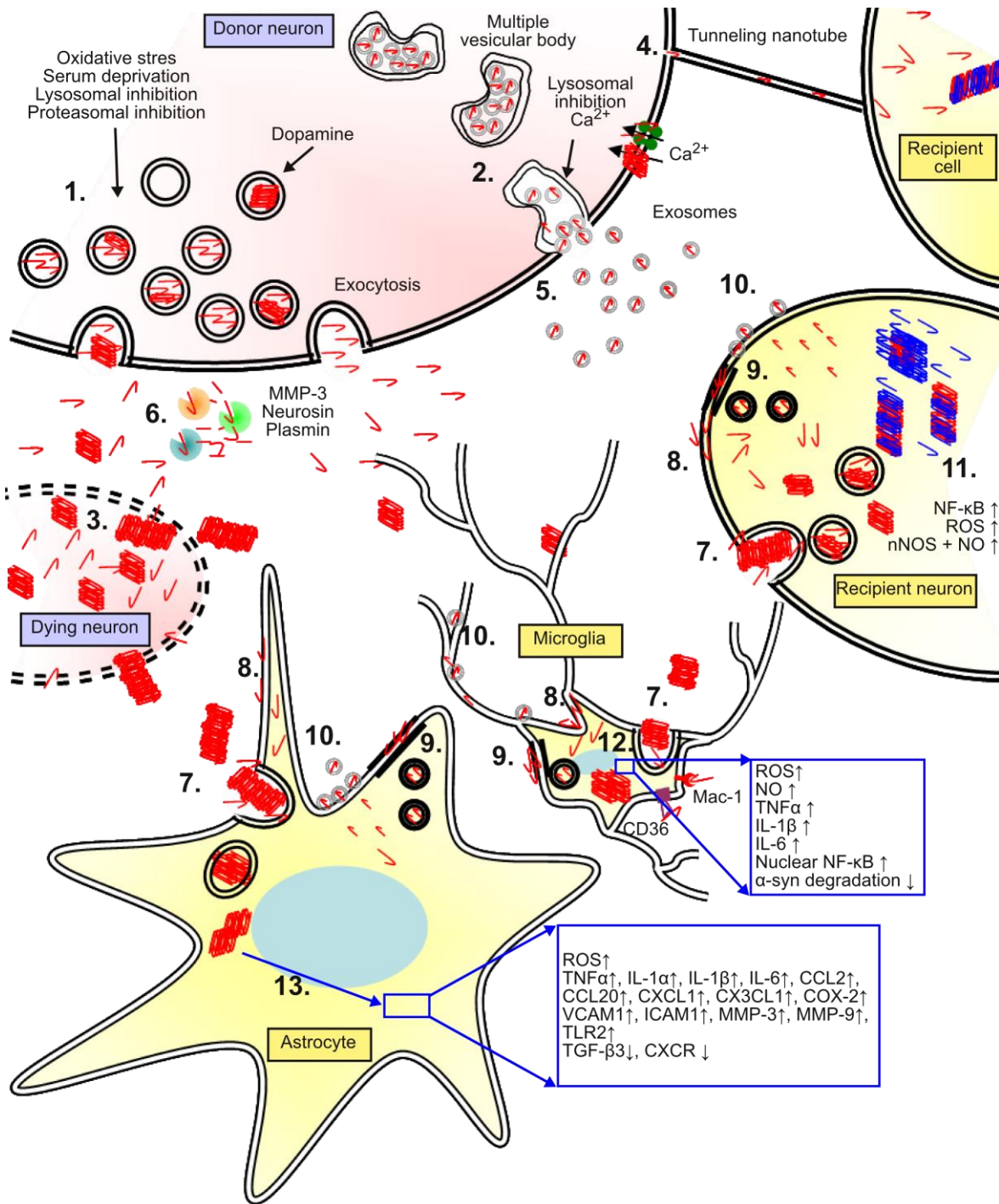


Figure 1.4 A possible model of the transmission of α -syn. The extracellular α -syn may derive from secretion through exocytosis (1.), exosomes (2.) or dying neurons (3.). Transmission may also happen directly through tunneling nanotubes (4.). The α -syn in the exosomes (5.) is protected from the extracellular proteases (6.). Oligomeric and fibrillar α -syn is suggested to be taken up by receptor dependent endocytosis (7.), whereas monomeric α -syn may enter the cells by passive diffusion (8.) or via lipid raft mediated endocytosis (9.). The exosomes can fuse with the cell membrane (10.). The internalized α -syn may aggregate and induce different cellular and inflammatory responses in recipient neurons (11.), microglia (12.) and astrocytes (13.). Full names of proteins are written in the list of abbreviations.

Table 1.2 Mutations in DJ-1 associated with PD

Mutations	Inheritance	Effect	Reference
L166P	Homozygous	Protein instability	Bonifati et al., 2003
14-kb del	Homozygous	Loss of protein	Bonifati et al., 2003
M26I	Homozygous	Decreased protein stability	Abou-Sleiman et al., 2003
D149A	Heterozygous	Unknown	Abou-Sleiman et al., 2003
IVS6-1 G-C	Heterozygous	Altered splicing	Hague et al., 2003
c.56delC c.57G→A	Heterozygous	Frameshift	Hague et al., 2003
g.168_185del	Both	Polymorphism	Hague et al., 2003
R98Q	Heterozygous	Polymorphism	Hague et al., 2003
A104T	Heterozygous	Polymorphism	Hague et al., 2003
Ex5-7del	Heterozygous	Altered transcript	Hedrich et al., 2004
IVS5+2-12del	Heterozygous	Altered splicing	Hedrich et al., 2004
c.192G>C	Homozygous	Altered splicing	Hering et al., 2004
E163K	Homozygous	Decreased function	Annesi et al., 2005
g.168_185dup	Homozygous	Unknown	Annesi et al., 2005
L10P	Homozygous	Decreased protein stability	Guo et al., 2008
P158del	Homozygous	Decreased protein stability	Macedo et al., 2009
A179T	Heterozygous	Unknown	Macedo et al., 2009
Ex1-5dup	Heterozygous	Altered transcript	Macedo et al., 2009
A107P	Homozygous	Unknown	Ghazavi et al., 2011
c.91-2AG	Homozygous	Altered splicing	Ghazavi et al., 2011

In conclusion it is suggested that different stress conditions can increase the secretion of α -syn into the extracellular space. The fate of the extracellular α -syn may be either degradation by proteases or uptake by neighboring cells. Elevated levels of extracellular α -syn are proposed to lead to microglial and astroglial activation, intracellular Lewy-body-like inclusions, neuroinflammation and cell death (Fig 1.4).

1.4 DJ-1 is a multifunctional cytoprotective protein

DJ-1 is a 20 kDa ubiquitously expressed, cytoprotective, multifunctional protein. Its localization is mostly cytosolic, but it is also found in the nucleus and associated with mitochondria (Zhang et al., 2005a, Junn et al., 2009). *DJ-1* was first described as an oncogene (Nagakubo et al., 1997) and shortly thereafter it was found to regulate male fertility (Welch et al., 1998). Later mutations in the *DJ-1* gene were found in a Dutch and an Italian family with frequent occurrence of early onset PD (Bonifati et al., 2003). Today 23 *DJ-1* variants have been identified in PD patients (Table 1.2.). Many of them are predicted or shown to be loss of function mutations and cause PD with early onset and slow progression of the disease. Nonetheless, mutations in the *DJ-1* gene are very rare; they cause less than 1% of the familiar early onset recessive PD cases.

1 Introduction

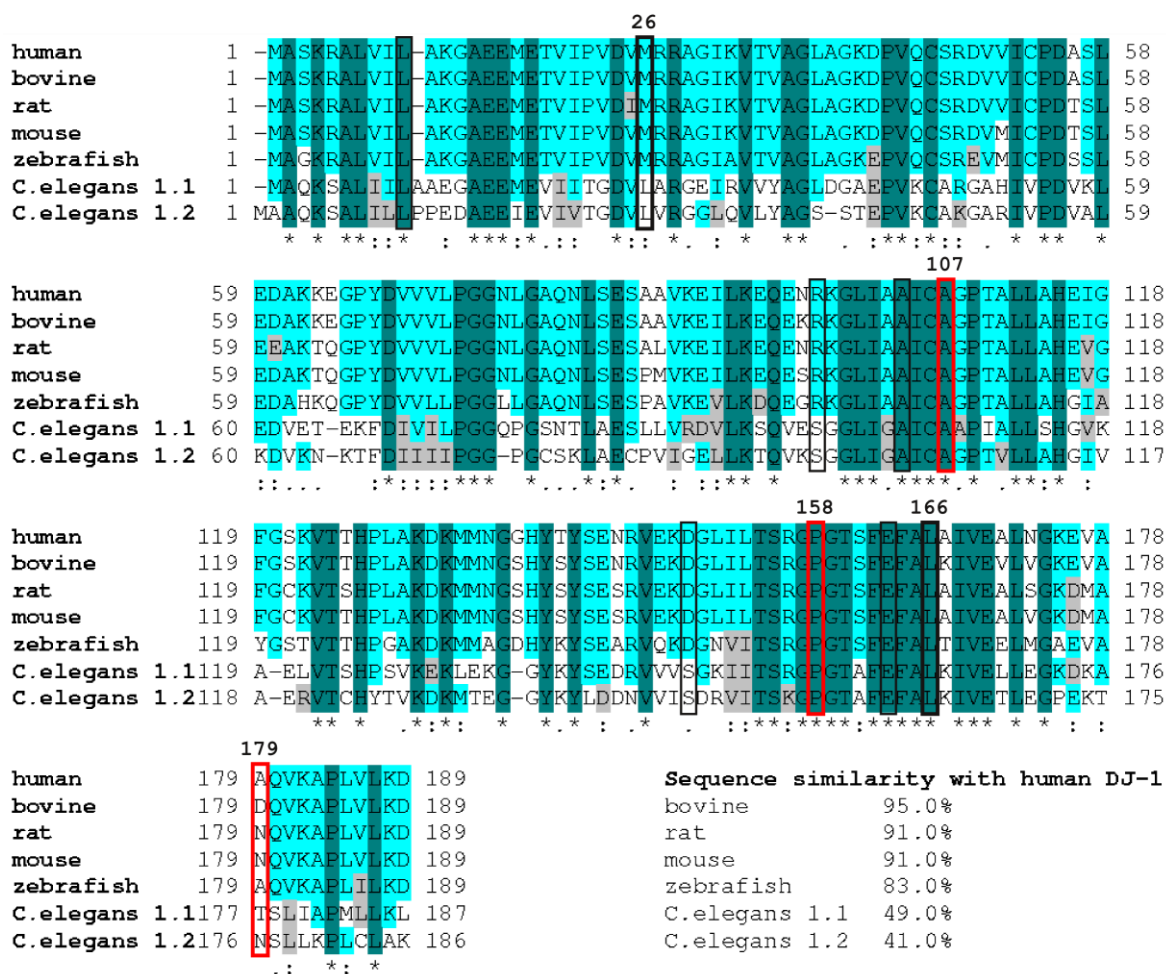


Figure 1.5 Multiple sequence alignment of eukaryotic DJ-1 homologues. Boxed residues have been found mutated in patients with PD. Red boxes mark the residues which are studied in this work. The alignment was performed with ClustalW.

DJ-1 is expressed in almost all cells and tissues (Nagakubo et al., 1997). The expression is upregulated upon oxidative stress (Yanagida et al., 2009). Correspondingly, in brains from patients with PD and other neurodegenerative diseases extensive DJ-1 staining has been observed in reactive astrocytes (Bandopadhyay et al., 2004, Neumann et al., 2004, Rizzu et al., 2004). An interesting finding is that in PD brain DJ-1 is found in its oxidized form (Bandopadhyay et al., 2004). Since the known cases have not reached autopsy, the pathology in human PD patients with *DJ-1* mutations is not known.

1.4.1 DJ-1 is a highly conserved dimeric protein

DJ-1 consists of 189 amino acids and belongs to the Thj1/Pfp1 superfamily. It is highly conserved among species (Fig 1.5). Resolution of the crystal structure revealed that the monomer has an α/β -sandwich-fold with eleven β -strands and eight α -helices organized in a structure, which is similar to the Rossmann fold (Fig 1.6 A) (Honbou et al., 2004).

al., 2003, Tao and Tong, 2003, Wilson et al., 2003). The DJ-1 structure is very similar to the bacterial protease Pfp1 family, which catalytic sites consist of a C/H/E triade. However, in DJ-1 the putative active site that consists of the E18/C106/H126 triade (Fig 1.6 B) is distorted. In addition, DJ-1 possesses an additional C-terminal H- α -helix, which projects out of the rest of the protein and masks the entry to the putative active site.

In solution DJ-1^{wt} exist as a dimer (Fig 1.6 C) (Honbou et al., 2003, Wilson et al., 2003). The dimerization interface area between the monomers is large and excludes

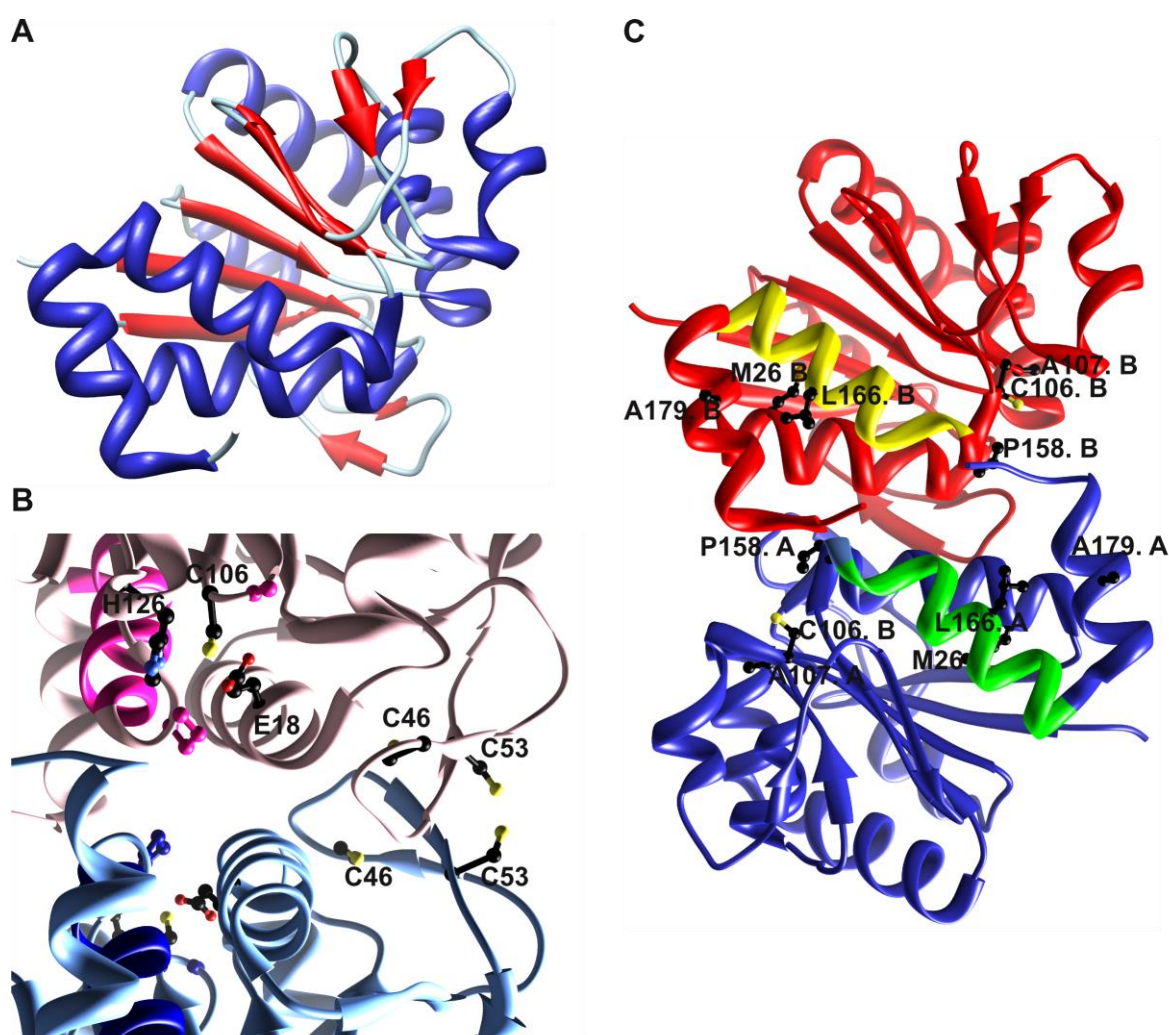


Figure 1.6 DJ-1 protein structure. A shows the DJ-1 monomer, which has an α/β -fold. B shows the putative active center of DJ-1 that is made up by E18, C106 and H126. In addition C46, C53, A107 and P158 are shown in ball and stick. The sulfur atoms of the cysteines are yellow, oxygen atoms of E18 are red and the nitrogen atom of H126 is blue. C shows the DJ-1 dimer. The A-monomer is blue and B-monomer is red. The side chains of residues M26, C106, A107, P158, L166 and A179 are shown as ball and stick in black. The structurally important G- α -helix is shown in green (monomer A) and yellow (monomer B). The molecular models were drawn with Chimera (www.cgl.ucsf.edu/chimera) using the DJ-1 crystal structure data published by Tao and Tong in 2003 with the PDB accession code 1PDW.

1 Introduction

water molecules. Several hydrogen bonds and ionic interactions are present, but the dimer is mostly stabilized by hydrophobic interactions. Not surprisingly, the residues within this area are highly conserved. The amount of hydrophobic residues on the surface of the monomeric DJ-1 makes it very unlikely for this protein to exist as a monomer in solution (Honbou et al., 2003, Tao and Tong, 2003, Wilson et al., 2003). In addition, the C-terminal helix-kink-helix motif has been shown to be essential for the stability of the dimer (Gorner et al., 2007). This can explain the severe instability of the PD associated DJ-1^{L166P} point mutant (Macedo et al., 2003, Moore et al., 2003, Gorner et al., 2004), since introduction of a proline into the G- α -helix is very likely to disrupt the helix and thereby the helix-kink-helix motif.

The putative active site E18/C106/H126 triade is located close to the dimer interface. The monomers are in a head-to-tail fashion, so that the active sites of each monomer are on opposite sites of the dimer (Tao and Tong, 2003). Mutation of C106 is implied with loss of DJ-1 function (Canet-Aviles et al., 2004, Taira et al., 2004, Meulener et al., 2006, Waak et al., 2009a). The C106 is located in a strained backbone conformation in a “nucleophilic elbow”, which likely contributes to the high oxidizability of this residue (Wilson et al., 2003). Indeed, under oxidizing conditions the C106 is oxidized to SOH, SO₂H and then to SO₃H (Canet-Aviles et al., 2004, Kinumi et al., 2004), from which DJ-1^{C106-SO₃H} is suggested to be destabilized and inactivated (Zhou et al., 2006, Hulleman et al., 2007). Importantly, E18 lowers the pK_a of C106 and thus stabilizes the oxidized sulfinic acid (Witt et al., 2008). Moreover, are G75 and A107 shown to form an amide pocket, which can bind an ordered water molecule that forms a hydrogen bond with C106 (Witt et al., 2008). The small size of these side chains enables the water molecule to form hydrogen bonds with the peptide backbone. This ordered water molecule has not been present in all published DJ-1 crystal structures and thus the authors hypothesized that it plays a role when the C106 is oxidized (Witt et al., 2008). Despite the important role of oxidation of C106, the crystal structures of the C106-reduced and oxidized DJ-1 are remarkably similar (Canet-Aviles et al., 2004). In addition, the accessibility of C106 to the solvent is blocked by the helix-kink-helix motif. Here the two other cysteines, C46 and C53, from which C53 is in direct contact with the solvent, may play a role in the activation of DJ-1 (Waak et al., 2009a).

In addition to oxidation, DJ-1 might be sumoylated (Shinbo et al., 2006), S-nitrosylated (Ito et al., 2006) or phosphorylated (Rahman-Roblick et al., 2008). However, the roles of these posttranslational modifications are not clarified up to date.

1.4.2 DJ-1 animal models are more sensitive to mitochondrial toxins and oxidative stress

To study the effects of loss of DJ-1 function knock out animal models have been created. Interestingly, in contrast to humans, knock out of *DJ-1* homologues in mouse (Chen et al., 2005, Yamaguchi and Shen, 2007, Pham et al., 2010), zebrafish (Bretaud et al., 2007) and fruit fly (Meulener et al., 2005, Park et al., 2005) do not lead to excessive degeneration of dopaminergic neurons under basal conditions. However, the knock out animals are shown to be more sensitive to certain stress conditions, for example to the mitochondrial toxin 1-methyl-4-phenyl-1,2,3,6-tetrahydropyridine (MPTP) and to oxidative stress (Kim et al., 2005b, Meulener et al., 2005, Bretaud et al., 2007). Contradictory to the earlier observations a recent study showed an age dependent neurodegeneration and motor deficits in a *Dj-1*^{-/-} mouse line (Rousseaux et al., 2012).

The *Dj-1*^{-/-} mice used in this work has been showed to have a slightly reduced number of dopaminergic neurons (~6% reduction) in the ventral tegmental area (Pham et al., 2010). However, the decrease of these neurons with age is not accelerated when compared to littermate wt mice and no decrease in dopaminergic neurons in substantia nigra was detected. Moreover, the *Dj-1*^{-/-} mice showed a minor increase in activity of mitochondrial respiratory enzymes, which is possibly a compensatory mechanism for the absence of DJ-1 (Pham et al., 2010).

1.4.3 DJ-1 is multifunctional

DJ-1 is very important for the protection against oxidative stress. It is shown to be able to directly quench ROS and oxidation is important for its activation (Taira et al., 2004). However, the peroxidase activity of DJ-1 is very low (Andres-Mateos et al., 2007) and thus it is probably not its main cytoprotective function. Accordingly, variable functions have been described for DJ-1. It has been suggested to function as a protease (Chen et al., 2010), chaperone (Shendelman et al., 2004), regulator of mitochondrial fusion (Krebiehl et al., 2010), transcriptional regulator (Takahashi et al., 2001, Zhou and Freed, 2005), direct regulator of signaling pathways, glyoxalase (Lee et al., 2012) and metal sequestering protein (Bjorkblom et al., 2013). Many of these

1 Introduction

functions are quite vague and it is unclear if they are all physiologically relevant. Nevertheless, the role of DJ-1 as a protector against oxidative stress has been intensively studied and some of these functions are described below.

DJ-1 does indirectly regulate the transcription of several genes. It has been shown to regulate the activity of the androgen receptor (Takahashi et al., 2001), sterol regulatory element binding protein (Yamaguchi et al., 2012), polypyrimidine tract binding protein-associated splicing factor (PSF) (Zhong et al., 2006), nuclear factor erythroid-2 related factor 2 (Nrf2) (Clements et al., 2006) and p53 (Shinbo et al., 2005). In addition, DJ-1 is shown to positively regulate the expression of superoxide dismutase 3 and glutathione ligase by unknown mechanisms (Nishinaga et al., 2005, Zhou and Freed, 2005). DJ-1 sequesters PSF, which is a corepressor of the tyrosine hydroxylase (TH) gene (Zhong et al., 2006). TH converts tyrosine to L-DOPA, the precursor of dopamine. Contradictory, *Dj-1*^{-/-} mice have normal TH levels (Chen et al., 2005, Goldberg et al., 2005). However, the mouse TH gene lacks a PSF site and therefore it is very likely that the regulation of TH expression in mice differs from the ones in humans (Ishikawa et al., 2010). DJ-1 regulation of p53 and Nrf2 is important for the protection against oxidative stress. Nrf2 is a transcription factor that regulates genes that are relevant for the cell defense against oxidative stress and detoxication. Under basal conditions Nrf2 is kept in the cytosol by kelch-like ECH-associated protein 1 (Keap1). It is shown that DJ-1 upon oxidative stress sequesters Keap1, this allows Nrf2 to translocate to the nucleus and regulate the transcription of its target genes (Clements et al., 2006). p53 is a tumor suppressor that can induce apoptosis under stress conditions. DJ-1 is shown to directly bind to the DNA binding domain of p53 and thus inhibit its transcriptional activity (Fan et al., 2008, Kato et al., 2013).

Fragmented mitochondria have been observed in *Dj-1*^{-/-} mice and cells (Irrcher et al., 2010, Krebiehl et al., 2010). Furthermore, oxidative stress induces DJ-1 translocation to the mitochondria. The twelve most N-terminal amino acids and C106 are shown to be essential for this translocation (Canet-Aviles et al., 2004, Maita et al., 2013). DJ-1 lacks a mitochondrial targeting sequence, but it is possible that it is recruited to the mitochondria by chaperones like mitochondrial heat-shock protein 70 (Li et al., 2005). Interestingly, overexpression of an synthetic mutant DJ-1, which possess an mitochondrial targeting sequence, in a neuroblastoma cell line has been shown to decrease oxidative stress induced apoptosis more efficiently than overexpression of DJ-1^{wt} (Junn et al., 2009). Moreover, DJ-1 is suggested to play a role in the autophagic

degradation of damaged mitochondria, however likely in a parallel pathway to the PTEN-Induced Putative Kinase 1/Parkin mediated autophagic pathway (Thomas et al., 2011).

The phosphoinositide 3-kinase (PI3 K)/Akt pathway is a growth signaling pathway. PI3 K is inhibited by phosphatase and tensin homolog deleted from chromosome 10 (PTEN). DJ-1 can directly bind to PTEN and thereby it can decrease the inhibition caused by PTEN and thus activate the PI3 K/Akt (Kim et al., 2005a, Yang et al., 2005, Kim et al., 2009). In addition, DJ-1 have been shown to protect cells against rotenone and dopamine induced intoxication by positively regulating the extracellular signal regulating kinase (ERK) pathway (Lev et al., 2009, Gao et al., 2012). DJ-1 also regulates the apoptosis signal regulating kinase 1 (ASK1) pathway; this is explained in more detail below.

1.5 ASK1 is a mitogen activated protein kinase kinase kinase

The mitogen activated protein kinase (MAPK) pathways are present in all eukaryotic organisms. They are activated by various physical and biochemical signals and regulate many essential cellular functions such as cell division, survival and apoptosis. The pathways are protein cascades where a MAP kinase kinase kinase (MAP3K) phosphorylates a MAP kinase kinase (MKK), which in its turn phosphorylates a MAPK. MAPK targets are, for example, cytoskeletal proteins, transcription factors and downstream kinases. The current cellular molecular composition and the localization of the MAPK determine which targets are phosphorylated. There are three MAPK subfamilies, the ERKs generally signal cell growth or differentiation, whereas activation of p38 or c-Jun N-terminal kinase (JNK) signaling pathways more often induces apoptosis.

1.5.1 ASK1 is activated in response to stress

ASK1 consists of 1374 amino acids and is conserved in eukaryotes. The protein structure of the whole ASK1 has not been solved, but the protein can be roughly divided into three domains; a globular kinase domain flanked by less structured N- and C-terminal domains (Fig 1.7A) (Tobiume et al., 1997). The N-terminal coil-coiled region (NCC) and the C-terminal coil-coiled region (CCC) are essential for the homooligomerization and activation of ASK1 (Tobiume et al., 2002). ASK1 is a MAP3K, which is activated in response to oxidative stress, endoplasmic reticulum stress,

1 Introduction

calcium overload and inflammatory signals like TNF α and LPS (Fig 1.7 B) (Saitoh et al., 1998, Nishitoh et al., 2002, Takeda et al., 2004). Activation of ASK1 mainly leads to activation of the MKK4/MKK7-JNK and MKK3/MKK6-p38 pathways (Ichijo et al., 1997). Sustained activation of ASK1 induces apoptosis (Ichijo et al., 1997). Notably, ASK1 has been shown to play an important role in many stress related diseases, for example in several forms of cancer, neurodegenerative disorders and vascular diseases (Reviewed in Hayakawa et al., 2012).

The regulation of ASK1 activity is a complex process

Many proteins have been shown to regulate ASK1; the exact regulation of the activity is very complex (Fig 1.7B) (Takeda et al., 2008). Here some of the best known mechanisms are described.

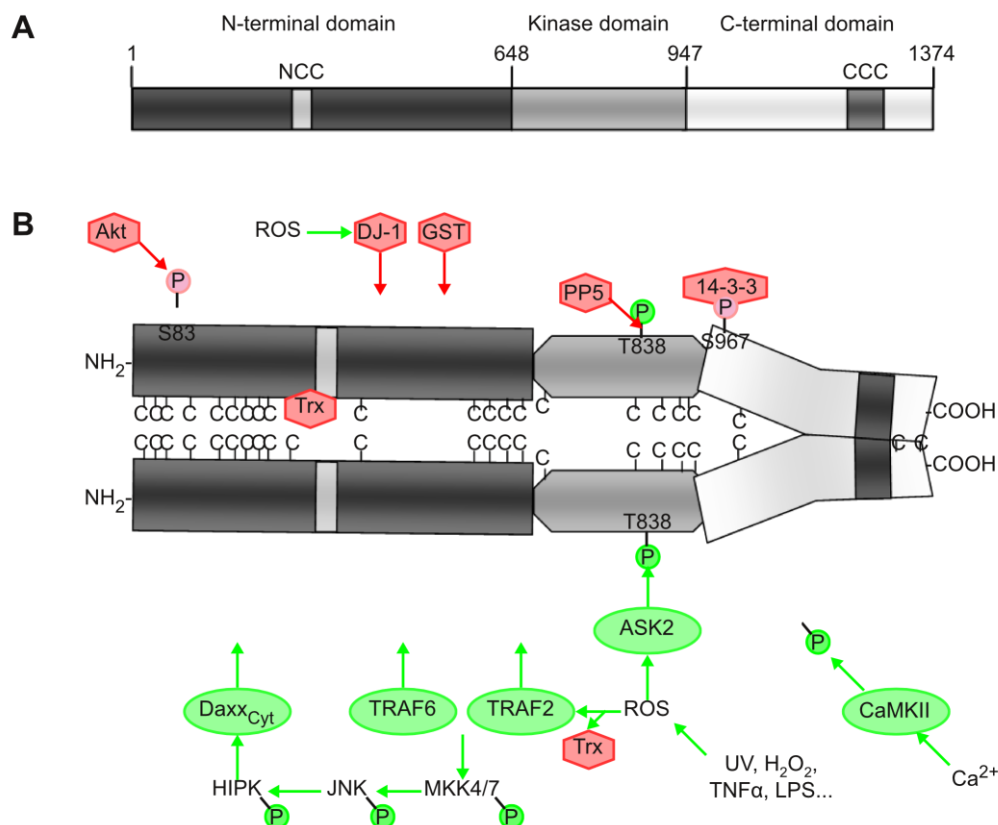


Figure 1.7 Schematic overview of ASK1 and its regulation **A** shows a schematic representation of the ASK1 protein. NCC- N-terminal coiled coil domain, CCC- C-terminal coiled coil domain. **B** shows the regulation of ASK1 activity. Arrows and proteins depicted in green are activating and in red are inhibiting the signalosome activation.

The phosphorylation of T838 (T845 in mouse) in the activation loop of the kinase domain is essential for the activation of ASK1 (Tobiume et al., 2002). Protein phosphatase 5 (PP5) is shown to dephosphorylate T838 and thus inactivate ASK1 in a feedback loop (Fig 1.7B) (Morita et al., 2001). In addition, Akt can deactivate ASK1 by phosphorylating S83 (Fig 1.7B) (Kim et al., 2001). The protein 14-3-3 in its turn binds to and inactivates S967 phosphorylated ASK1. This residue is dephosphorylated in presence of stress (Zhang et al., 1999, Goldman et al., 2004). Moreover, calcium/calmodulin dependent protein kinase type II phosphorylates and activates ASK1 on an unidentified residue in response to increased calcium levels (Fig 1.7B) (Takeda et al., 2004). In addition, other posttranslational modifications, for example ubiquitination (Nagai et al., 2009), have been shown to modify the activity and stability of ASK1.

Under unstressed conditions ASK1 forms oligomers, probably through its CCC region, and thus it exist in higher molecular weight complexes with molecular masses of about 1500 kDa (one ASK1 monomer is about 155 kDa). Notably, negative regulators like thioredoxin (Trx), the first indentified regulator of ASK1, are present in the complex (Saitoh et al., 1998, Noguchi et al., 2005). Under basal conditions Trx forms mixed disulfide bonds with cysteines in the N-terminal domain of ASK1, this inhibits the NCC regions of monomers to interact and form dimers (Fig 1.7B) (Fujino et al., 2007). Especially C250 has been shown to be important for the inhibition of ASK1 by Trx, but also other cysteine residues play a role (Zhang et al., 2004, Nadeau et al., 2009). In presence of oxidative stress Trx is oxidized and released from ASK1. Thus ASK1 activity depends on the redox status of Trx (Saitoh et al., 1998, Liu et al., 2000). When Trx is released, ASK1 forms a higher molecular weight protein complex, the ASK1 signalosome, which molecular weight is around 3000 kDa (Noguchi et al., 2005). TNF receptor associated factor 2 (TRAF2) and TRAF6 are present in this signalosome and they both play important roles in the ROS induced activation of ASK1 (Fig 1.7B) (Nishitoh et al., 1998, Noguchi et al., 2005). ASK2, another protein in the ASK1 family, is shown to be present in the signalosome too. ASK2 is shown to phosphorylate T838 of ASK1 (Fig 1.7B) and activate the JNK pathway. However, ASK2 is not necessary for the activation of ASK1 (Takeda et al., 2007). Thus it is suggested that the presence or absence of ASK2 can determine which pathways are activated after the ASK1 signalosome formation.

1 Introduction

Importantly, DJ-1 is shown to regulate the ASK1 activity. First, DJ-1 was shown to prevent death domain-associated protein (Daxx) from being sequestered to the ASK1 signalosome (Junn et al., 2005). Daxx is normally localized in the nucleus. When ASK1 is activated upon stress it phosphorylates MKK4 and MKK7, these can phosphorylate JNK, which in its turn activates homeodomain-interacting protein kinase 1 (HIPK1). HIPK1 phosphorylates Daxx, which allows Daxx to translocate to the cytosol and therefore to associate with the ASK1 signalosome. This leads to further activation of the signalosome and thus to the activation of apoptosis (Fig 1.7B) (Song and Lee, 2003). DJ-1 inhibits the Daxx translocation by binding it and keeping it in the nucleus (Junn et al., 2005). Second, DJ-1 is shown to covalently bind to the N-terminal domain of ASK1 in an oxidative stress dependent manner and thus inhibit its activation (Fig 1.7B) (Gorner et al., 2007, Waak et al., 2009a, Mo et al., 2010). The binding of DJ-1 to ASK1 was shown to be strictly dependent on C106 of DJ-1 (Waak et al., 2009a). Therefore DJ-1 is able to decrease oxidative stress induced apoptosis by direct regulation of ASK1 activation.

1.6 Objectives

At the beginning of this project two mutations in *DJ-1* were found in Dutch early onset PD patients. These mutations lead to homozygous deletion of the highly conserved P158 and a heterozygous A179T mutation in DJ-1 (Macedo et al., 2009). More recently, an Iranian patient with very early onset PD was designated to have a homozygous mutation, which leads to an A107P point mutation in the DJ-1 protein (Ghazavi et al., 2011). The first aim of this study was to characterize the effects of these three mutations on the protein stability and functions of DJ-1. DJ-1 has many different ways of action to protect the cells. Here the focus was set on the interaction with ASK1 in order to get a better understanding of this regulatory function of DJ-1. Moreover, the role of DJ-1 and ASK1 in a cell culture model of MSA was investigated.

Neuroinflammation plays an important role in the progression of PD. Previously, our group has shown that DJ-1 protects against LPS induced inflammatory responses in primary astrocytes (Waak et al., 2009b). In addition, preliminary experiments suggested that treatment with recombinant α -syn may induce NO production more strongly in *Dj-1*^{-/-} primary astrocytes than in wt astrocytes (Jens Waak dissertation). Moreover, it has been shown *in vivo* that overexpression of α -syn can increase the proinflammatory effect of LPS (Gao et al., 2008). α -syn is predominately found in the cytosol and synapses of neurons, however, a part from the protein is also secreted. More evidence show that the secreted α -syn cause cytotoxic responses and is taken up by surrounding neurons and glial cells (see section 1.3.2). The second aim of this study was to investigate if extracellular α -syn induces inflammatory responses in primary astrocytes and if DJ-1 plays a protective role. We were also interested in characterizing the possible astrocytic α -syn receptor. Furthermore, the ability of astrocytes to internalize extracellular α -syn was investigated. Additionally, the effect on age of onset of motorical symptoms after knock out of *Dj-1* in (Thy1)^h[A30P]SNCA transgenic mice was studied.

2 Material and methods

2.1 Material

2.1.1 Devices

Device (Model)

Agarose gel chamber
AxioImager microscope with ApoTome Imaging system
Autoclave (VX-150)
Bacterial incubator
Blotting Chamber
Burker chamber
Cell incubator (Heracell 240)
Centrifuges
 (Biofuge pico and fresco)
 (Micro 22R)
 (Centrifuge 5810R)
 (Multifuge3 S-R)
 (Evolution Rc)
Chirurgical tools
Developer
Electroporation cuvettes
Electroporation device (MicroPulser)
Film cassettes
Fast protein liquid chromatography device (FPLC)
 (ÄKTA purifier)
French press (EmulsiFlex™-C5)
Gel drying frames
Light cycler
Microtiter plate reader
Micro wave oven
Milli-Q Synthesis
Nanodrop (ND1000)
Pipetboy
Power supply (EV231)
Scanner(Epson Perfection V700 Photo)
SDS-PAGE gel chamber (PerfectBlue Twin S)
Sequencer (ABI 3100 Genetic Analyzer)
Sonicator
Spectrophotometer (Ultrospec 2100 Pro)
Stereo microscope MZ7
Sterile bench (Herasafe)
Stirer (RH basic)
Thermocycler (2720)
Thermomixer (Comfort)
UV-table

Manufacturer

Peqlab (Erlangen, DE)
Carl Zeiss Microimaging GmbH (Jena, DE)
Systemec (Wettenberg, DE)
Binder (Multimed) (Tuttlingen, DE)
Bio-Rad laboratories GmbH (Munich, DE)
Assistent (Sondheim, DE)
Thermo Fisher Hereaus (Hamburg, DE)

Thermo Fisher Hereaus, (Hamburg, DE)
Hettich (Tuttlingen, DE)
Eppendorf (Hamburg, DE)
Thermo Fisher Hereaus, (Hamburg, DE)
Thermo Fisher Sorvall, (Hamburg, DE)
Carl Roth GmbH (Karslsruhe, DE)
Fujifilm (Düsseldorf, DE)
Bio-Rad laboratories GmbH (Munich, DE)
Bio-Rad laboratories GmbH (Munich, DE)
Dr Goos-Suprema GmbH, (Heidelberg, DE)
GE Healthcare (Freiburg, DE)

Avestin Inc (Ottawa, Canada)
Sigma Aldrich Chemie GmbH (Munich, DE)
Roche Applied Science (Mannheim, DE)
Bio-Rad laboratories GmbH (Munich, DE)
Panasonic (Hamburg, DE)
Millipore Corporation (Darmstadt ,DE)
Peqlab (Erlangen, DE)
Integra Bioscience (Fernwald, DE)
Consort (Turnhout, BE)
Epson Corporation
Peqlab (Erlangen, DE)
Applied Biosystems/Ambio (Austin, Tx, USA)
BANDELIN electronic GmbH (Berlin, DE)
Amersham Biosciences GmbH (Munich, DE)
Leica (Solms, DE)
Thermo Fisher Heraeus (Hanau, DE)
IKA (Staufen, DE)
Applied Biosystems (Darmstadt, DE)
Eppendorf (Hamburg, DE)
Vilber Lourmant (Eberhardzell, DE)

2.1.2 Consumables

Consumable

4-20% gradient SDS-PAGE gels
Amersham Hyperfilm ECL High performance
chemiluminescence
Cell culture consumables

Manufacturer

Expedeon Ltd (Cambridgeshire, UK)
GE Healthcare (Freiburg, DE)

BD Biosciences (Heidelberg, DE)
Corning (Kaiserslautern, DE)
Greiner Bio-One GmbH (Frickenhäusen, DE)
Carl Roth GmbH (Karslsruhe, DE)

Coverslips

Disposable pipettes
 FPLC columns
 Glass slides
 Light cycle capillaries
 Microtiter plates
 Nets (Nitex 03-123/44 and 03-210/40)
 Nitrocellulose membrane
 Object glass
 PCR reaction tubes
 Pipette tips

Polypropylene tubes
 Polyvinylidene difluoride (PVDF) membrane
 Reaction tubes

Scalpels
 Syringe filters (0.45 µm)
 Whatman paper

Corning (Kaiserslautern, DE)
 GE Healthcare (Freiburg, DE)
 Langenbrinck (Emmendingen, DE)
 Roche Applied Science (Mannheim, DE)
 Greiner Bio-One GmbH (Frickenhausen, DE)
 Sefar (Munich, DE)
 GE Healthcare (Freiburg, DE)
 Langenbrinck (Emmendingen, DE)
 PeqLab (Erlangen, DE)
 Sarstett (Nürnberg, DE),
 Biozym Scientific (Hessisch Oldendorf, DE)
 Greiner Bio-One GmbH (Frickenhausen, DE)
 Millipore GmbH (Schwalbach, DE)
 Greiner Bio-One GmbH (Frickenhausen, DE)
 Eppendorf AG (Hamburg, DE)
 Braun (Melsungen, DE)
 Thermo Fisher Scientific (Hamburg, DE)
 Schleicher und ScheuLL (Dassel, DE)

2.1.3 Chemicals

Chemical

1,4-Dithiothreitol (DTT)
 2-propanol
 40% Acrylamide/Bis solution 19:1
 4xLDS sample buffer
 Acetic acid (glacial) 100%
 Adenosine triphosphate (ATP)
 γ-³²P ATP
 Agar
 Agarose
 Ammonium persulfate (APS)
 Ampicillin (sodium salt)
 Amplify™
 β-Mercaptoethanol
 Bafilomycin A1
 Bicinchoninic acid (BCA) Protein Assay Kit
 BigDye Terminator v3.1
 Bovine Serum Albumin (BSA)
 Bradford Protein Assay Kit
 Bromphenol blue (sodium salt)
 Calcium chloride
 Chloramphenicol sulfate
 Collagen
 Complete protease inhibitor
 Complete protease inhibitor EDTA-free
 Coomassie Brilliant Blue G-250
 Cycloheximide
 Di-Sodium Hydrogen Phosphate (Na₂HPO₄)
 Dimethyl sulfoxide (DMSO)
 Dulbecco's minimal essential medium (DMEM)
 -high glucose
 DMEM pyruvate free
 DMEM methionine and cysteine free 21013-024
 DNA 1 kb ladder
 DNA loading buffer (6x)
 DNA T4 ligase (1U/µl)
 DNA T4 ligase buffer (10x)
 dNTPs
 EasyTag™ EXPRESS³⁵S Protein Labeling Mix
 Ethanol

Manufacturer

Carl Roth GmbH (Karslsruhe, DE)
 Merck KGaA (Darmstadt, DE)
 Bio-Rad laboratories GmbH (Munich, DE)
 Expedeon Ltd (Cambridgeshire, UK)
 Merck KGaA (Darmstadt, DE)
 Sigma Aldrich Chemie GmbH (Munich, DE)
 Hartman Analytic GmbH (Braunschweig, DE)
 Fluka Analytical (Munich, DE)
 Biozym Scientific (Hessisch Oldendorf DE)
 Sigma Aldrich Chemie GmbH (Munich, DE)
 Sigma Aldrich Chemie GmbH (Munich, DE)
 GE Healthcare (Freiburg, DE)
 Carl Roth GmbH (Karslsruhe, DE)
 Sigma Aldrich Chemie GmbH (Munich, DE)
 Pierce Protein (Bonn, DE)
 Applied Biosystems (Darmstadt, DE)
 Carl Roth GmbH (Karslsruhe, DE)
 Pierce Protein (Bonn, DE)
 Merck KGaA (Darmstadt, DE)
 Merck KGaA (Darmstadt, DE)
 Sigma Aldrich Chemie GmbH (Munich, DE)
 Chemicon (Darmstadt, Germany)
 Roche Applied Science (Mannheim, DE)
 Roche Applied Science (Mannheim, DE)
 Carl Roth GmbH (Karslsruhe, DE)
 AppliChem GmbH (Darmstadt, DE)
 Merck KGaA (Darmstadt, DE)
 Sigma Aldrich Chemie GmbH (Munich, DE)
 Biochrom AG (Berlin DE)

PAA Laboratories GmbH (Pasching, At)
 Invitrogen GmbH (Karslsruhe, DE)
 Fermentas GmbH (St Leon-Rot, DE)
 Fermentas GmbH (St Leon-Rot, DE)
 Fermentas GmbH (St Leon-Rot, DE)
 Fermentas GmbH (St Leon-Rot, DE)
 Fermentas GmbH (St Leon-Rot, DE)
 Perkin Elmer LAS (Rodgau-Jügesheim, DE)
 Merck KGaA (Darmstadt, DE)

2 Material and methods

Ethidium bromide (1% in water)
Ethylene glycol tetraacetic acid (EGTA)
Ethylenediaminetetraacetic acid (EDTA sodium salt)
ExTaq Polymerase Kit
EZview™ Red Anti myc/HA affinity Gel
Fetal bovine serum (FCS)
FuGENE 6 / X-tremeGENE 9
Gentamycin
Glucose
Glycerol
Glycine
GoTaq Polymerase Kit
Griess reagent
Hepes
High Fidelity cDNA Synthesis kit
Hoechst 33342
Hydrochloric acid (HCl)
Hydrogen peroxide (30%)
Imidazol
Immobilon Western HRP Substrate
Isopropyl β-D-1-thiogalactopyranoside (IPTG)
Kanamycinsulfate
Kinase buffer
L-Cysteine
L-Glutamine
L-methionine
Lactose-monohydrate
LPS from Escherichia coli O55:B5
Magnesium chloride (MgCl₂)
Methanol
MG-132
Mowiol/DABCO
Myelin basic protein (MBP)
N,N,N',N'-Tetramethylethyldiamine (TEMED)
Nickel sulfate (NiSO₄)
Non fat milk powder
Nonident P-40 (NP-40)
Normal Goat serum
Paraformaldehyde
PenicillinG/Streptomycin sulfate 100x
Poly-D-lysine
Polynucleotide Kinase Kit
Potassium Chloride (KCl)
Potassium hydroxide
Potassium dihydrogen phosphate (KH₂PO₄)
Precision Plus Protein Standard, prestained
Protein A-agarose
Protein G-agarose
PYROGENT Plus Single Tests 0.06 EU/ml
Q-sepharose
Qiagen Plasmid Midi/Maxi Kit
QIAprep spin MiniPrep Kit
QIAquick gel extraction Kit
QIAprep RNA kit
QIA blood and tissue DNA kit
OptiMEM
Restriction Enzymes and Buffer

Sephadex S-200
Shrimp alkaline phosphatase (SAP)
Sodium azide (NaN₃)

Merck KGaA (Darmstadt, DE)
AppliChem GmbH (Darmstadt, DE)
Sigma Aldrich Chemie GmbH (Munich, DE)
TaKaRa Bio (Saint-Germain-en-Laye, FR)
Sigma Aldrich Chemie GmbH (Munich, DE)
PAA Laboratories GmbH (Pasching, At)
Roche Applied Science (Mannheim, DE)
Invitrogen GmbH (Karslsruhe, DE)
Carl Roth GmbH (Karslsruhe, DE)
AppliChem GmbH (Darmstadt, DE)
Carl Roth GmbH (Karslsruhe, DE)
Promega (Mannheim, DE)
Fluka Analytical (Munich, DE)
Sigma Aldrich Chemie GmbH (Munich, DE)
Roche Applied Science (Mannheim, DE)
Invitrogen GmbH (Karslsruhe, DE)
Merck KGaA (Darmstadt, DE)
Carl Roth GmbH (Karslsruhe, DE)
Merck KGaA (Darmstadt, DE)
Millipore GmbH (Schwalbach, DE)
Peqlab (Erlangen, DE)
Sigma Aldrich Chemie GmbH (Munich, DE)
Cell signaling technology Inc (Frankfurt, DE)
Sigma Aldrich Chemie GmbH (Munich, DE)
Biochrom AG (Berlin DE)
Sigma Aldrich Chemie GmbH (Munich, DE)
Carl Roth GmbH (Karslsruhe, DE)
Sigma Aldrich Chemie GmbH (Munich, DE)
Carl Roth GmbH (Karslsruhe, DE)
Merck KGaA (Darmstadt, DE)
Calbiochem (Darmstadt, DE)
Carl Roth GmbH (Karslsruhe, DE)
Fluka Analytical (Munich, DE)
Merck KGaA (Darmstadt, DE)
Carl Roth GmbH (Karslsruhe, DE)
Sucofin, (Zeven, DE)
United States Biological (Svampscott, USA)
Sigma Aldrich Chemie GmbH (Munich, DE)
Sigma Aldrich Chemie GmbH (Munich, DE)
Biochrom AG (Berlin DE)
Sigma Aldrich Chemie GmbH (Munich, DE)
Promega (Mannheim, DE)
Merck KGaA (Darmstadt, DE)
Carl Roth GmbH (Karslsruhe, DE)
Carl Roth GmbH (Karslsruhe, DE)
Bio-Rad laboratories GmbH (Munich, DE)
Millipore GmbH (Schwalbach, DE)
Millipore GmbH (Schwalbach, DE)
Lonza Group Ltd (Cologne, DE)
GE Healthcare (Freiburg, DE)
Qiagen GmbH (Hilden, DE)
Qiagen GmbH (Hilden, DE)
Qiagen GmbH (Hilden, DE)
Qiagen GmbH (Hilden, DE)
Qiagen GmbH (Hilden, DE)
Invitrogen GmbH (Karslsruhe, DE)
Fermentas GmbH (St Leon-Rot, DE)
New England Biolabs GmbH (Frankfurt, DE)
GE Healthcare (Freiburg, DE)
Fermentas GmbH (St Leon-Rot, DE)
Sigma Aldrich Chemie GmbH (Munich, DE)

Sodium chloride (NaCl)	Merck KGaA (Darmstadt, DE)
Sodium dodecyl sulfate (SDS)	Sigma Aldrich Chemie GmbH (Munich, DE)
Sodium hydroxide (NaOH)	Merck KGaA (Darmstadt, DE)
di-Sodium hydrogen phosphate (Na ₂ HPO ₄)	Carl Roth GmbH (Karslsruhe, DE)
Sodium nitrite (NaNO ₂)	Merck KGaA (Darmstadt, DE)
Sodium pyrophosphate tetrabasic decahydrate (NaPPi)	Sigma Aldrich Chemie GmbH (Munich, DE)
Sodium sulfate (Na ₂ SO ₄)	Carl Roth GmbH (Karslsruhe, DE)
Sodium thiosulfate (Na ₂ S ₂ O ₃)	Carl Roth GmbH (Karslsruhe, DE)
Sucrose	Carl Roth GmbH (Karslsruhe, DE)
Superdex 200 10/300 column	GE Healthcare (Freiburg, DE)
SYBR Green I mini kit	Roche Applied Science (Mannheim, DE)
TLR4 peptide inhibitor set: Viper	Biomol (Imgenex) (San Diego, CA, USA)
Transcriptor High Fidelity cDNA Synthesis kit	Roche Applied Science (Mannheim, DE)
Tris base	Carl Roth GmbH (Karslsruhe, DE)
Triton X-100	AppliChem GmbH (Darmstadt, DE)
Trypsin-EDTA (10x)	Invitrogen GmbH (Karslsruhe, DE)
Tryptone	Carl Roth GmbH (Karslsruhe, DE)
Tween 20	Merck KGaA (Darmstadt, DE)
Western Blocking Reagent Solution	Roche Applied Science (Mannheim, DE)
Yeast extract	AppliChem GmbH (Darmstadt, DE)
Zeocin	Invivogen (La Jolla, CA, USA)

2.1.4 Antibodies

Primary antibodies: α -syn (15G7, Dr. Elisabeth Kremmer, Helmholtz Center, Munich), α -tubulin (SDL.3D10 or T9026, Sigma Aldrich), β -actin (AC15, Sigma Aldrich), β -catenin (C19220, BD Biosciences Pharmingen), β -syn (Syn207, Millipore GmbH), β -tubulin (2-28-33, T5293, Sigma Aldrich), DJ-1 (Stressgen 3E8; Cell Signaling Technology #5933), Flag (affinity purified clone M2, Sigma Aldrich), Glyceraldehyde-3-phosphate dehydrogenase (GAPDH, H86504M, Biodesign International), HA (3F10, Roche Applied Science), iNOS (Sigma Aldrich; #2977 Cell Signaling Technology), JNK (56G8, #9258, Cell Signaling Technology), LC3 (#2775, Cell Signaling Technology), myc (9E10, Sigma Aldrich), p25 α (Kragh et al., 2009), p38 (#9212 Cell Signaling Technology), p65/NF- κ B (#3034, Cell Signaling Technology), peroxidase conjugated anti-HA (3F10, Roche Applied Science), peroxidase conjugated anti-myc (9E10, Roche Applied Science), phospho- α -syn (S129) (EP1536Y, Epitomics/Biomol), phospho-p38 (T180/Y182) (3D7, #9215, Cell Signaling Technology), phospho-JNK (T183/Y185) (#9251, Cell Signaling Technology), V5 (R960-25, Invitrogen GmbH)

Secondary peroxidase conjugated antibodies were purchased from Jackson ImmunoResearch Laboratories and secondary Alexa-Fluor conjugated antibodies were purchased from Invitrogen GmbH.

2.1.5 Electrocompetent bacteria

Luria-Bertani (LB)-media (1.0 % (w/v) Tryptone, 0.5 % (w/v) Yeast extract, 1.0 % (w/v) NaCl) was inoculated with *Escherichia coli* Top10 and cultured over night at

2 Material and methods

37 °C at 200 rpm. Following day 500 ml LB-medium was inoculated with 10 ml over night culture. The bacteria were cultured at 37 °C at 200 rpm until the optical density at 600 nm was 0.7. The culture was cooled down to 4 °C and centrifuged at 4 °C at 3700×g for 10 min. The pellet was washed three times in 500 ml and once in 250, 100 and 50 ml ice cold ddH₂O. The pellet was resuspended in 2 ml 10 % (v/v) glycerol, aliquoted, quick frozen in liquid nitrogen and stored at -80 °C.

2.1.6 Constructs

All pCDNA constructs harbouring ASK1-HA variants and pRK5-Flag-Daxx were kind gifts from Hidenori Ichijo, University of Tokyo, Japan. The pcDNA3.1(-) p25 α zeo(-) vector was a kind gift from Poul Henning Jensen at Århus University, Denmark. pET30a-SCNB was a kind gift from Hilal Lashuel at the Swiss federal institute of technology in Lausanne, Switzerland.

To create the DJ-1^{P158 Δ} point deletion and DJ-1^{A107P} point mutation, pCMV-myc-DJ-1^{wt} (Waak et al., 2009a) was used as template for a two step site specific mutagenesis. The mutagenesis was introduced in the first poly chain reaction (PCR) step, which was made with ExTaq polymerase and following primer pairs; P158 Δ for and pCMV-STOP-NotI rev, A107P for and pCMV-STOP-NotI, P158 Δ rev and pCMV-EcoRI for or A107P rev and pCMV-EcoRI for (Table 2.1). The PCR products were purified using 1.5% agarose gels and QIAquick gel extraction Kit. The two PCR products were used as templates for a second PCR using ExTaq polymerase and pCMV-EcoRI for and pCMV-STOP-NotI rev primers. The PCR product was purified as in previous step, after which pCMV-myc vector (Clontech) and PCR products were incubated with NotI and EcoRI restriction enzymes. The vector was treated with SAP. The samples were purified as in previous steps. The PCR products were ligated over night at 4 °C into the vector using DNA T4 ligase. Following day the ligated products were transformed into electrocompetent *Escherichia coli* Top10. Bacterial colonies were screened for the inserted DNA product and colonies positive for the insert were cultured and DNA was isolated using QIAprep spin MiniPrep Kit.

To create the A179T mutation pCMV-myc-DJ-1^{wt} was used as template and pCMV-EcoRI for and A179T-Stop-NotI rev as primers (Table 2.1). The cloning procedure was done as described above, starting at the second PCR step.

Table 2.1 Mutagenesis primers

Primer	Sequence
P158Δ for P158Δ rev	5'-CCTGATTCTTACAAGCCGGGGGGGGACCAGCTTCG-3' 5'-CGAAGCTGGTCCCCCCCCGGCTTGTAAAGATCAGG-3'
A107P for A107P rev	5'-GCCATCTGTCCAGGTCCTACTG-3' 5'-CAGTAGGACCTGGACAGATGGC-3'
A179T-Stop-NotI rev	5'-AGCGGCCGCCTAGTCTTTAAGAACAAGTGGAGCCTTCACTTGAGTCGCCACCTCCTTGC-3'
pCMV-EcoRI for pCMV-STOP-NotI rev	5'-ACGAATTCGAATGGCTTCCAAAAGAGCTCTGGT-3' 5'-AGCGGCCGCCTAGTCTTTAAGAACAAGTGGAGCC-3'
pCDNA-NcoI forw pCDNA-BamHI-Stop rev	5'-AACCATGGGAATGGCTTCCAAAAGAGCTCTG-3' 5'-CGCGGATCCGATGTCTTTAAGAACAAGTGGAGCC-3'
SNCA-NheI for SNCA-HindIII rev	5'-CATATGGCTAGCATGGATGTATTCATGAAAGGAC-3' 5'-GAGCTCAAGCTTTTAGGCTTCAGGTTCTAGTC-3'

The DJ-1 cDNA was subcloned from pCMV-myc constructs into the *EcoRI/NotI* site of pCMV-HA (Clontech). The pCMV-myc-DJ-1 constructs were used as templates in a PCR with pCDNA-NcoI for and pCDNA-BamHI-Stop rev as primers (Table 2.1) and these PCR products were cloned into the pCDNA3.1-V5/His₆ TOPO vector (Invitrogen GmbH) as described above, starting at the second PCR step.

To create bacterial expression vectors SNCA wt, A30P and S129A were cloned from pCDNA3.1-SNCA (Schell et al., 2009) into *NheI/HindIII* site of pET21a vector (Novagen) using SNCA-NheI for and SNCA-HindIII rev primers (Table 2.1). Cloning was performed as described above starting at the second PCR step.

The nucleic acid sequences of all cloned constructs were confirmed by sequencing using BigDye Terminator v3.1 according to the manufacturer's instructions. Reaction products were analyzed using an ABI 3100 Genetic Analyzer.

DNA used for transfection of cell lines was isolated with Qiagen Plasmid Midi/Maxi Kit.

2.1.7 Preparation of recombinant α -synuclein

DYT medium (1.6 % (w/v) Tryptone, 1 % (w/v) Yeast extract, 0.5 % (w/v) NaCl) supplied with 100 μ g/ml ampicillin was inoculated with *Escherichia Coli* BL21 Rosetta2 (Stratagene) transformed with pET21a-SNCA wt or mutants or pET30a-SCNB. The bacteria were grown at 37 °C at 200 rpm to an optical density between 0.5 and 0.8 at 590 nm. 0.5 mM IPTG was added and the proteins were expressed for 4 to 6 h at 37 °C at 200 rpm. The bacteria were centrifuged at 3500 \times g for 10 min at 4 °C and the cell pellet was stored at -20 °C.

The bacterial pellet was gently diluted in a 10 mM phosphate buffer (pH 7.4) containing 25 mM NaCl and Cømplete protease inhibitor EDTA-free. The cells were lysed in a French press and sonicated three times for 30 s at 50% input. The solutions were incubated for 15 min at 95 °C. The denatured proteins were removed by two

2 Material and methods

time centrifugation at 17.000 ×g at 4 °C for 30 min. The supernatant was applied on a Q-sepharose column (self packed, column volume 50 ml, diameter 23 mm) and eluted with a two column volumes long 25 mM to 1000 mM NaCl gradient in 10 mM phosphate buffer (pH 7.4). The synuclein content in the eluted fractions was monitored by dot blotting. Fractions with strong synuclein signals were desalted on a Sephadex S-200 column (self packed, column volume 180 ml, diameter 16 mm) using a 10 mM phosphate buffer containing 150 mM NaCl, (pH 7.4). The synuclein content in the eluted fractions was monitored by dot blotting. Absence of contaminating proteins was examined by sensitive Coomassie staining (see section 2.4.2). Fractions that were positive for an immunoblot synuclein signal and had only one visible protein band in the Coomassie gel were pooled, aliquoted and stored at -20 °C.

The absorbance at 280 nm was measured and the synuclein concentrations were calculated using the extinction factors $\epsilon_{(280, 0.1\%)}$ 0.354 for α -syn and 0.417 for β -syn (calculated with the ProtParam tool of ExPASy, Swiss Institute of Bioinformatics).

The endotoxin levels were estimated using PYROGENT Plus Single Tests 0.06 EU/ml following the manufacturer's instructions. Three dilutions of the protein stocks were used (1:1, 1:10 and 1:25).

2.2 Animals

2.2.1 Mouse maintenance

Mice were kept under standard conditions with free access to food and water in a cycle of 12 h of light and 12 h of dark. The local animal welfare and ethics committee of the country commission Tübingen approved all experiments and procedures. Number of animals used and their suffering was kept to a minimum.

The genotype of the mice was determined from ear punches, from which whole genome DNA was isolated using the DNeasy -Blood and tissue kit. Genotyping was performed using the primers shown in Table 2.2. Genotyping for *Dj-1* and *Tlr4* was done by PCR. Genotyping for *hSNCA* was done by quantitative PCR.

The homozygous (Thy1)^h[A30P]SNCA transgenic mice of C57BL/6 background were crossbred with *Dj-1*^{-/-} mice with C57BL6/J background (Table 2.2). Homozygous mice were weekly examined from the age of 12 to 24 months. The mice were lifted by the tail and the presence of tail muscle tonus was noticed. Mice with motorical symptoms tend to fail to counter balance movements when lifted by the tail; severely affected mice fail to spread their hind legs. The mice were let to walk around on the grid of the

Table 2.2 Mouse lines and genotyping primers

Promotor/ vector	Transgene/ Target gene	Genotyping primers	Reference
Thy1	human [A30P]SNCA	SNCA rev: 5'-TGTAGGCTCCAAAACCAAGG-3' SNCA rev: 5'-TGTCAGGATCCACAGGCATA-3' actin for: 5'-TATTGGCAACGAGCGG-3' actin rev: 5'-CGGATGTCA ACGTCAC-3'	Kahle et al., 2000
pGT1Lxf.	<i>Dj-1</i>	<i>Dj-1</i> ^{+/+} for 5'-AGGCAGTGGAGAAGTCCATC-3' <i>Dj-1</i> ^{+/+} rev 5'-AACATACAGACCCGGGATGA-3' <i>Dj-1</i> ^{-/-} rev 5'-CGGTACCAGACTCTCCCATC-3'	Pham et al., 2010
pMC1-neo- poly(A)	<i>Tlr4</i>	<i>Tlr4</i> ^{+/+} rev 5'-CGTGTAACCAGCCAGGTTTTGAAGGC-3' <i>Tlr4</i> ^{+/+} for 5'-TGTTGCCCTTCAGTCACAGAGACTCTG-3' <i>Tlr4</i> ^{-/-} rev 5'-TGTTGGGTCGTTTGTTCGGATCCGTCG-3'	Hoshino et al., 1999

cage. Mice with motorical symptoms have a high tendency to miss the catching of the grids and they fall into the ripping of the cage lid.

2.3 Cell culture

2.3.1 Preparation of primary astrocytes

Dj-1^{+/-} (Pham et al., 2010) and *Tlr4*^{+/-} (Hoshino et al., 1999) mice were crossed. Astrocyte-rich primary cultures were prepared as described previously (Hamprecht and Loffler, 1985). Newborn pups were decapitated, and whole brains were removed. The brain from each pup was handled separately. Cells were separated in preparation buffer (137 mM NaCl, 5.4 mM KCl, 0.2 mM KH₂PO₄, 0.2 mM Na₂HPO₄, 1 g/l glucose, 20 g/l sucrose, 50 µg/ml Gentamycin) by mechanically forcing the brains through nets with a mesh width of first 250 µm and second 135 µm. The cells were resuspended in DMEM (Biochrom) supplemented with 10% FCS, 10 U/ml penicillin G and 10 µg/ml streptomycin sulfate. Cells were cultured in 75 cm² cell culture bottles at 37 °C in 5% CO₂ in a humidified atmosphere. Each individual culture was genotyped by PCR of genomic DNA as described above using the tails of the puppies. After one week in culture the flasks containing the astrocytes were shaken at 37 °C at 180 rpm over night. In the morning the cells were washed once with **phosphate buffered saline** (PBS, pH 7.4, 2.2 mM KH₂PO₄, 7.8 mM Na₂HPO₄, 150 mM NaCl) and fresh growth medium was supplied. After one additional week the cells were plated in appropriate cell culture dishes. In order to avoid stress the astrocytes were allowed to normalize for four to seven days and they were supplied with fresh media one or two days before use in experiments. The cells were incubated in growth media unless stated otherwise supplemented with indicated concentrations of LPS or recombinant synuclein for indicated times.

2 Material and methods

2.3.2 Cell line maintenance

Mouse embryonic fibroblasts (MEF) lacking DJ-1 and littermate controls (Gorner et al., 2007) as well as human embryonic kidney (HEK) 293E cells (American Tissue Culture Collection) were cultured in DMEM (Biochrom) containing 10% FCS in humid 37 °C and 5% CO₂. Oligodendroglial cells stably overexpressing human α -syn (OLN AS) (Kragh et al., 2009) were maintained at 37 °C under 5% CO₂ and grown in DMEM (Biochrom) supplemented with 10% FCS, 100 μ g/ml zeocin, 50 units/ml penicillin and 50 μ g/ml streptomycin.

2.3.3 Transfection

FuGENE 6 or X-tremeGENE 9 was used according to the manufacturer's instructions for transient transfections.

In addition, in some experiments calcium phosphate (CaPO₄) transfection was used. Briefly, the DNA was diluted in 250 mM CaCl₂ and dropped onto a equal volume of 2x HeBs (pH 7.2, 274 mM NaCl, 10 mM KCl, 1.4 mM Na₂HPO₄ 15 mM D-glucose, 42 mM HEPES) while swirling the tube. The mixture was incubated 20 min at room temperature and dropped on cells. For one 15 cm plate total amount of 24 μ g of DNA in 1200 μ l of DNA-calcium phosphate mixture was added to cells in 10 ml of growth medium.

2.4 Protein biochemistry

2.4.1 SDS-Polyacrylamide Gel Electrophoresis (SDS-PAGE)

Samples were diluted in **laemmli sample buffer** (62.5 mM Tris-HCl (pH 6.8), 1.5% (w/v) SDS, 8.3 % (v/v) glycerol, 1.5 % (w/v) β -mercaptoethanol, 0.01% bromphenol blue). Samples were boiled at 95 °C for 5 min and centrifuged for 20 s at 16.1 \times g before loading to gels. 7.5 to 15% acrylamide gels were used (resolving gel: pH 8.8, 7.5-15% (w/v) acrylamide 19:1, 0.375 M Tris-HCl, 0.1% (w/v) SDS, 0.01% (w/v) APS, 0.001 % (v/v) TEMED and stacking gel: pH 6.8, 4.6% (w/v) acrylamide 19:1, 0.13 M Tris-HCl, 0.1% (w/v) SDS, 0.01% (w/v) APS, 0.001% (v/v) TEMED). The gels were run at 110 V for 30 min and thereafter for 60 to 90 min at 140 V. The gel running buffer contained 25 mM Tris pH 8.3, 193 mM Glycine and 3.5 mM SDS.

2.4.2 Sensitive coomassie staining

SDS-PAGE gels were heated twice to 100 °C in ddH₂O in a microwave oven to remove the SDS. After which the gels were heated to 100 °C in sensitive coomassie stain (10 % (v/v) EtOH, 30 mM HCl and 0.3 mM Coomassie Brilliant Blue G250) and incubated on a rocker for 10-15 minutes at room temperature. The gels were destained in ddH₂O. Faster destaining was achieved by heating to 100 °C followed by 10-15 min incubation on a rocker.

2.4.3 Immunoblot

The proteins were transferred from the SDS-PAGE gels to either PVDF or a nitrocellulose membrane using wet blotting technology. PVDF membranes were pre-activated 1 min in methanol. Membranes, Whatman paper and sponges were pre-equilibrated in transfer buffer (25 mM Tris, 192 mM glycine, 20% (v/v) methanol). The transfer was done in the 4 °C room for 2 to 2.5 h at 100 V or over night at 20 V. Following transfer, the membrane was incubated in 5% (w/v) milk-tris buffered saline with Tween (TBST: 50 mM Tris-HCl (pH 7.4), 150 mM NaCl, 0.1% (v/v) Tween-20) or in 2-5% (w/v) BSA-TBST for 1 h at room temperature on a rocker in order to reduce unspecific binding of antibodies. The primary antibodies diluted in 5% (v/v) Western Blocking reagent-TBST supplied with 0.02 % (w/v) NaN₃ or in 2-5% (w/v) BSA-TBST were incubated over night at 4 °C on a rocker. The following day the membrane was washed 3-5 times in TBST. Horse radish peroxidase (HRP) tagged secondary antibodies in 5% (w/v) milk-TBST were incubated for 1 h at room temperature on a rocker. The membrane was washed 3-5 times in TBST. The membrane was soaked in Immobilon Western HRP Substrate. Signals were detected using Amersham Hyperfilm™ ECL. The films were scanned and signals were quantified by densitometry using ImageJ software (National Institutes of Health).

If membranes were reprobated they were incubated for 30 min at 56 °C in stripping buffer (2% (w/v) SDS, 100 mM, β-mercaptoethanol, 62.5 mM Tris-HCl (pH 7.6)). After which the membranes were properly washed in TBST prior to the reprobating.

2.4.4 Immunofluorescence staining

Cells were plated on coverslips coated with poly-D-lysine and collagen (astrocytes) or only with poly-D-lysine (MEF, OLN AS). After appropriate treatments the cells were fixed in 4% paraformaldehyde in PBS (section 2.3.1) for 10 min, permeabilized with 1% (v/v) Triton X-100 for 5 min, and blocked in 3% (w/v) BSA in PBS or 10% (v/v) normal goat

2 Material and methods

Table 2.3 Semi quantitative PCR primers

Primer	Sequence for	Sequence rev
m β -actin	5'-CTAAGGCCAACCGTGAA-3'	5'-CCGGAGTCCATCACAAT-3'
hPBGD	5'-TGCCAGAGAAGAGTGTGGTG-3'	5'-TGTTGAGGTTTCCCCGAATA-3'
DJ-1	5'-ACGAATTCGAATGGCTTCCAAAAGAGCTCTGGT-3'	5'-AGCGGCCGCGTCTTTAAGAACAAGTGGAGCC-3'
IL-1 β	5'-CAGGCAGGCAGTATCACTCA-3	5'-AGGCCACAGGTATTTTGTGCG-3'
IL-6	5'-GTTCTCTGGGAAATCGTGGA-3	5'-GGAAATTGGGGTAGGAAGGA-3'
COX2	5'-TCCTCCTGGAACATGGACTC-3'	5'-CCCCAAAGATAGCATCTGGA-3'
TNF α	5'-AGCCCCCAGTCTGTATCCTT-3'	5'-AGCAAAAGAGGAGGCAACAA-3'
1-TLR4	5'-AAATGCCAGGATGATGCCCTC-3'	5'-ATTTACACCTGGATAAATCCAGC
2-TLR4	5'-CTTGAATCCCTGCATAGAGGT-3'	5'-ATTTACACCTGGATAAATCCAGC
3-TLR4	5'-CCCTGCATAGAGGTAGTTCC-3'	5'-CTTGTTAGTCCAGAGAACTTCC
NGF	5'-GCAGTGAGGTGCATAGCGTA-3'	5'-CACTGAGAACTCCCCATGT-3'
iNOS	5'-GTGGTGACAAGCACATTTGG-3'	5'-GGCTGGACTTTTCACTCTGC-3'

serum in PBS solution for 60 min at room temperature. Primary and secondary antibodies were diluted in 1% (w/v) BSA in PBS and incubated for 1 h at room temperature or over night at 4 °C in a humidified chamber. Nuclei were counterstained with 2 μ g/ml Hoechst 33342 in PBS for 10 min at room temperature. After each step in the staining protocol coverslips were washed 3 times in PBS at room temperature. Coverslips were mounted in Mowiol/DABCO solution onto glass slides. Images were taken with AxioImager microscope equipped with ApoTome Imaging system and processed with AxioVision software.

2.4.5 Semi quantitative PCR

Cells were lysed in RLT-RNA lysis buffer at -20 °C. RNA was isolated using the RNeasy Mini kit. cDNA was produced with Transcriptor High Fidelity cDNA Synthesis kit and the cDNA was used as template for a PCR reaction with given primers (Table 2.3). The DNA fragments were separated in 1.5% (w/v) agarose gels containing ethidium bromide. DNA bands were detected with a Vilber Lourmat. Signals were quantified by densitometry using ImageJ software.

2.4.6 Steady state protein levels

MEF *Dj-1*^{+/+}, MEF *Dj-1*^{-/-} and HEK 293E cells were transiently transfected with pCMV-myc-DJ-1 (wt, A179T, P158 Δ o A107P) or pcDNA-DJ-1-V5/His₆ (wt, A179T or P158 Δ) and proteins were expressed 48 h. Cells were lysed in **lysis buffer** (1% (v/v) Triton X-100, 150 mM NaCl, 2 mM EDTA, 10 mM NaPP_i, 50 mM Tris-HCl (pH 7.6) and Cømplete protease inhibitor cocktail). Protein lysates were analyzed by immunoblotting.

2.4.7 Cycloheximide treatment

Dj-1^{-/-} and *Dj-1*^{+/+} MEF cells were seeded in 10 cm cell culture dishes. The following day, cells were transiently transfected with pCMV-myc-DJ-1 constructs. After 24 h the cells from the 10 cm dishes were split to six wells in 6-well-plates. Another day later, 40 µg/ml cycloheximide was added to the cells and incubated for 0-14 h. Cells were lysed in lysis buffer (section 2.4.6) and protein lysates were analyzed by immunoblotting.

2.4.8 Pulse Chase

HEK 293E cells were plated into 14 cm cell culture plates. On the following day, cells were transiently transfected with pCMV-myc-DJ-1 constructs. Eight hours after transfection, the cells were split into six 6 cm dishes. One day later the cells were washed once in warm PBS (section 2.3.1) and starved 1 h in cysteine and methionine free media (DMEM (Invitrogen), 2 mM L-glutamine, 10 U/ml penicillinG, 10 µg/ml streptomycin), after which a 30 min long pulse with 80 µCi/ml EasyTag™ EXPRESS^{35S} Protein Labeling Mix was given. Cells were washed twice and thereafter chased for 0-24 h in chase media (DMEM (PAA), 2 mM L-glutamine, 1 mM L-cysteine, 1 mM L-methionine, 10% (v/v) FCS, 10 U/ml Penicillin and 10 µg/ml Streptomycin). Cells were lysed in lysis buffer (section 2.4.6) and the protein lysates were quick frozen using dry ice and stored at -20 °C until all samples were collected. Equal amounts of protein, determined by BCA protein assay, were immunoprecipitated over night using EZview™ Red Anti myc affinity Gel. Beads were washed three times in lysis buffer and boiled in 6 x Laemmli buffer (section 2.4.1) at 95 °C for 5 min and proteins were separated on a 12.5% SDS-gel. The gel was Coomassie stained and incubated in Amplify™ for 30 min, after which the gel was dried. Radioactive signals were detected on Amersham Hyperfilm™ ECL using approximately 7 days of exposure at -80 °C. Band densities were quantified using the ImageJ software (National Institutes of Health). Band intensities of the different time points were expressed as percentage to the DJ-1 band intensity at time point zero. Half-life times were calculated by curve fitting assuming an exponential decay rate ($x = e^{-kt}$).

2.4.9 Size exclusion chromatography and co-immunoprecipitations

HEK 293E cells were transiently co-transfected with pCMV-myc-DJ-1 and pCMV-HA-DJ-1 constructs or pCDNA3-ASK1-HA. After 48 h expression cells were washed once in pyruvate free DMEM (PAA) containing 5 mM D-glucose and treated or left untreated

2 Material and methods

with 1 mM H₂O₂ for 30 min. For mapping co-immunoprecipitations and gel filtration chromatography HEK 293E cells were transiently co-transfected with pCMV-myc-DJ-1 constructs and pCDNA3-ASK1-HA. After 24 h medium was changed to pyruvate-free DMEM containing 5 mM D-glucose and 16 h later cells were treated or left untreated with 1 mM H₂O₂ for 30 min.

Cells were lysed in **colP buffer** (0.2% (v/v) NP-40, 10 mM KCl, 50 mM NaCl, 1 mM EDTA, 0.5 mM EGTA, 1.5 mM MgCl₂, 10% (v/v) glycerol, 10 mM NaPP_i, 50 mM HEPES (pH 7.5) plus Cømplete protease inhibitor cocktail). Equal amounts of protein were immunoprecipitated for 1 h or 3 h using anti-myc or EZview™ Red Anti HA affinity Gel beads. The beads were washed three times in ColP buffer and boiled in 6x Laemmli (section 2.4.1) buffer at 95 °C for 15 min. Proteins were separated on 12.5% SDS-gels and immunoblotted.

Alternatively, after lysis in colP buffer the lysates were applied on a Superdex 200 10/300 column preequilibrated with running buffer (10 mM KCl, 150 mM NaCl, 1 mM EDTA, 1 mM EGTA, 1.5 mM MgCl₂, 5% (v/v) glycerol, 50 mM HEPES-KOH, (pH 7.5)). The proteins were separated with a 0.45 ml/min flow rate and the eluate was collected in 0.5 ml fractions. Fractions between 7 ml to 20.5 ml elution volume were applied on 10% SDS-gels and Immunoblotting was performed.

2.4.10 Daxx translocation

MEF *Dj-1*^{-/-} cells were plated onto poly-D-lysine coated coverslips. After 24 h cells were transiently co-transfected with pRK5-Flag-Daxx and pCMV-HA-DJ-1 constructs or empty pCMV-HA. The next day medium was changed to pyruvate free DMEM containing 5 mM D-glucose, after 16 h 500 μM H₂O₂ was added for 30 min, controls were left untreated. The cells were fixed and immunostained as described above. Images were made with a 25x objective. The cytosolic versus nuclear localization of Flag-Daxx was quantified from the images; more than 50 cells per sample were analyzed. Following formula were used: $[N(\text{Cytosol})_{+H_2O_2}:N(\text{total})_{+H_2O_2}]:[N(\text{Cytosol})_{-H_2O_2}:N(\text{total})_{-H_2O_2}]$, where N is the amount of scored cells.

2.4.11 OLN AS viability assays

OLN AS cells on poly-D-lysine coated coverslips were transiently co-transfected with pcDNA-p25α and pCMV-HA, pCMV-HA-DJ-1^{wt/A107P} or pcDNA3-ASK1-HA or transfected only with pcDNA3-ASK1-HA. After 16 h of expression cells were fixed and immunostained. Antibodies for β-tubulin, p25α and HA were used. For the

investigation of the activity of DJ-1^{A107P} in figure 3.9 24 h expression time was used. Images were taken with 25x objective. Double transfected cells with retracted versus normal MT were scored in 100-300 cells per condition from the images. Cells with abnormal MT bundles detected by intense tubulin staining close to the nucleus were scored as positive for MT retraction.

2.4.12 *In vitro* immunocomplex kinase assay

OLN AS cells were seeded in 14 cm dishes. Following day cells were transiently co-transfected with pCDNA3.ASK1-HA and pCDNA-p25 α or pCDNA3. Sixteen hours later cells were lysed in colP buffer (section 2.4.9). Equal protein amounts were immunoprecipitated with EZview™ Red Anti HA affinity Gel beads for 2 h rotating at 4 °C. The agarose beads were washed three times in ColP buffer and once in 1x kinase buffer. The beads were incubated for 20 min at 30 °C in 0.2 μ g/ μ l MBP, 0.2 mM ATP, 2 μ Ci γ -³²P-ATP in 40 μ l kinase buffer. The reaction was stopped with 4xLDS sample buffer for 10 min at 70 °C and the proteins were separated by 4-20% gradient SDS-PAGE. The gels were stained in sensitive coomassie staining and dried over night. The radioactive signals were detected on Amersham Hyperfilm™ ECL.

2.4.13 NO assay

Primary astrocyte cultures were treated with indicated concentrations of LPS or indicated synuclein species in OptiMEM supplemented with penicillin G and streptomycin. In some experiments 5 μ M of TLR4 peptide inhibitor or control peptide was added two hours prior to the addition of synuclein and LPS. Medium was collected, and aliquots were mixed with equal amounts of Griess reagent. The samples were incubated protected from light for 15 min, after which the optic absorption at 450 nm was measured. A standard curve made from 0 to 50 μ M sodium nitrite was used as reference. Measurements were normalized against the protein content of the well.

2.4.14 NF- κ B nuclear translocation

Astrocytes were cultured on poly-D-lysine and collagen coated coverslips. Cells were treated with 0.007-3.5 μ M recombinant α -syn or 0.1-1.0 μ g/ml LPS in growth media for six hours. After which the cells were fixed and immunostained for p65/NF- κ B as described above. Images were acquired with 25x objective and nuclei positive for

2 Material and methods

NF- κ B and total nuclei were quantified from the images. 200-400 cells were analyzed per sample.

2.4.15 Uptake of extracellular α -syn

Primary astrocytes were plated in six-well cell culture plates. The cells were incubated with 0.007-3.5 μ M recombinant synuclein, which was added to the growth media. In some experiments 50 or 100 μ M Bafilomycin A1 or 10 μ M MG-132 was added 1 h prior to addition of the recombinant proteins. The cells were treated for 1 to 48 h. In some experiments a 1 h treatment was followed by a recovery time of 0.5-48 h, where the medium was replaced with fresh medium (supplied with inhibitors for samples where inhibitors had been added earlier). The cells were washed twice in cold PBS and lysed in lysis buffer (see section 2.4.6). Samples were analyzed by immunoblotting.

2.4.16 Statistical analyses

Each experiment was performed independently at least three times unless stated otherwise. The statistical analyses were done with JMP 9 software (SAS Institute Inc). Comparisons were analyzed with either Students t-test or one way ANOVA as stated in the figure legends. P-values less than 0.05 were considered as statistically significant.

3 Results

3.1 Characterization of the PD associated DJ-1^{A179T}, DJ-1^{P158Δ} and DJ-1^{A107P} mutants

3.1.1 *The steady state protein levels of DJ-1^{P158Δ} and DJ-1^{A107P} are decreased compared to the protein levels of DJ-1^{wt} and DJ-1^{A179T}*

First the steady state protein levels of the mutants were investigated in order to know if the mutant proteins are present in the cells. Therefore we introduced the mutations into the human DJ-1 sequence and C-terminally V5/His₆-tagged and N-terminally myc-tagged DJ-1^{wt} and mutants were overexpressed for 48 h in HEK 293E cells. DJ-1 proteins were examined by immunoblotting using both DJ-1 and tag specific antibodies (Fig 3.1). Whereas DJ-1^{A179T} showed similar protein levels as DJ-1^{wt}, the DJ-1^{P158Δ} mutant showed significantly decreased protein levels. This was not dependent on the positioning or nature of the tag (Fig 3.1 A). To further confirm that the decreased protein level was not dependent on the used HEK 293E cell line, which expresses endogenous human DJ-1, stability of overexpressed DJ-1 mutants was investigated in MEF *Dj-1*^{+/+} and MEF *Dj-1*^{-/-} cells. Also in these cell lines the protein level of the P158Δ mutant was significantly lower than that of the wt protein and the A179T mutant (Fig 3.1 B). The difference in the protein levels was not due to differential expression of the vectors, since the mRNA levels of the exogenous proteins were shown to be comparable by semi-quantitative PCR (Fig 3.1 D).

Introduction of the inflexible amino acid proline into a protein can be predicted to affect the structural stability of the protein at least in some degree. N-terminally myc-tagged DJ-1^{A107P} mutant was overexpressed in HEK 293E, MEF *Dj-1*^{+/+} and MEF *Dj-1*^{-/-} and the protein expression was examined by immunoblotting. As the P158Δ mutant the A107P mutant showed clearly decreased protein levels in the MEF cells compared to the wt protein (Fig 3.1 C). Interestingly, in HEK 293E cells the protein level of DJ-1^{A107P} was only slightly decreased compared to the DJ-1^{wt} levels. Perhaps are the high levels of endogenous human DJ-1 present in HEK 293E cells able to stabilize the mutant DJ-1.

3 Results

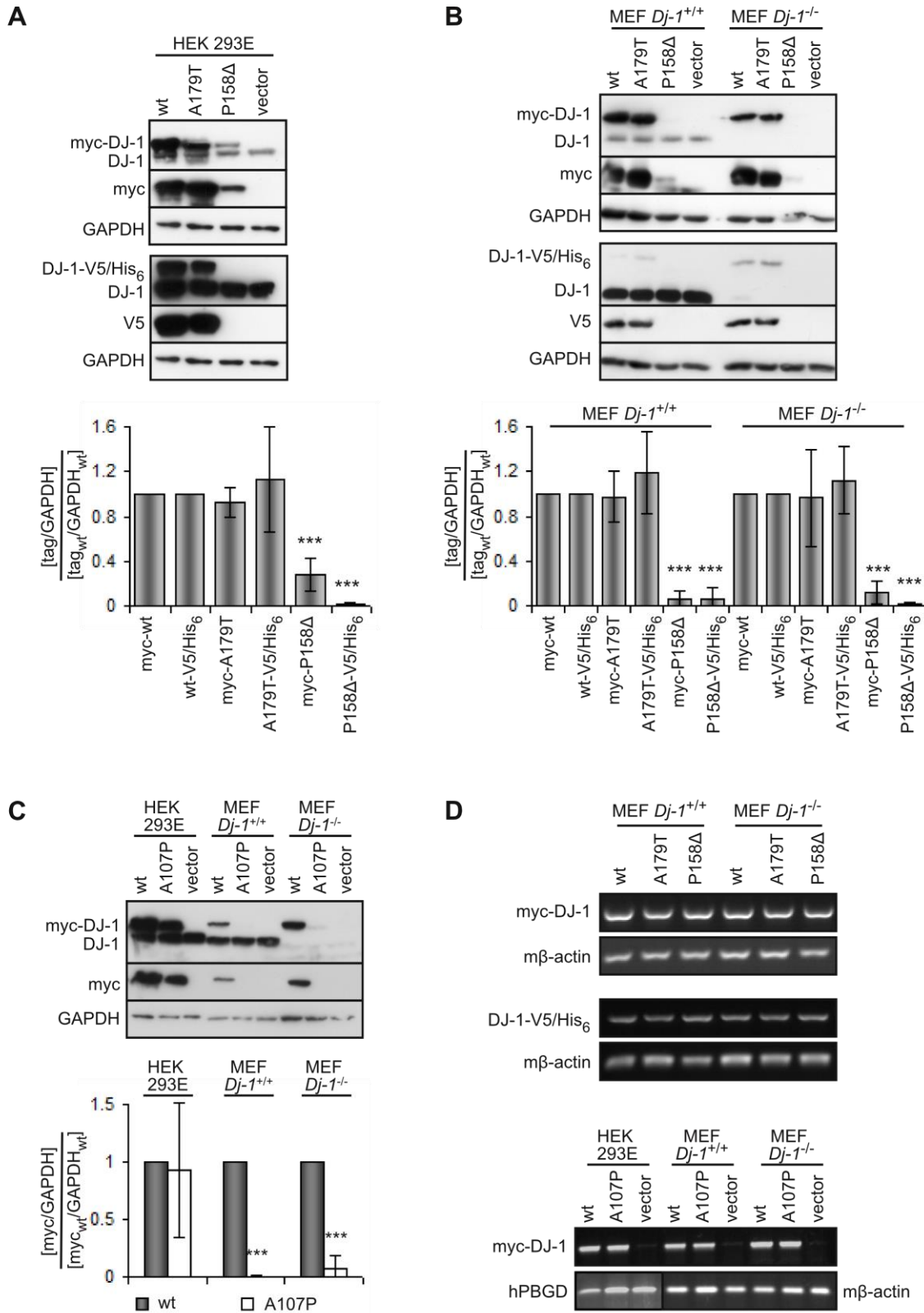


Figure 3.1 DJ-1^{P158Δ} and DJ-1^{A107P} show decreased protein steady state levels compared to DJ-1^{wt} and DJ-1^{A179T}. **A, B, C** N-terminally myc-tagged or C-terminally V5/His₆ tagged DJ-1^{wt} and mutants were overexpressed in HEK 293E, MEF *Dj-1*^{+/+}, MEF *Dj-1*^{-/-} cells for 48 h. The level of expressed protein was examined by immunoblotting with DJ-1 (in A 3E8, in B and C CST #5933) and tag (myc or V5) antibodies. GAPDH serves as a control for equal protein loading. Representative blots are shown in the upper panels. The signals were quantified with ImageJ software and normalized to the DJ-1^{wt} signal (bottom panels). **A.** shows the protein steady state levels of DJ-1^{A179T} and DJ-1^{P158Δ} in HEK 293E cells.

Independent on position and nature of the tag or antibody used the DJ-1^{P158Δ} signal was significantly weaker than the signals of DJ-1^{wt} and DJ-1^{A179T}. **B** shows the steady state levels of DJ-1^{A179T} and DJ-1^{P158Δ} in MEF cells. As in **A**, the signal of DJ-1^{P158Δ} was significantly weaker than the signals from the wt and A179T DJ-1. **C** shows the steady state level of DJ-1^{A107P} in HEK 293E and MEF cells. In MEF cells the signal from DJ-1^{A107P} was significantly weaker than the signal of DJ-1^{wt}. **D** Equal mRNA expression of the constructs was demonstrated by semi-quantitative PCR using primers specific for human DJ-1. Human porphobilinogen deaminase (hPBGD, for HEK 293E cells) or mouse β-actin (for MEF cells) serve as controls for use of equal amounts of cDNA. Error bars denote StDev. N ≥3; ***p < 0.001 (Student's t-test compared to DJ-1^{wt}).

3.1.2 DJ-1^{P158Δ} and DJ-1^{A107P} have decreased protein half-life times compared to DJ-1^{wt} and DJ-1^{A179T}

The DJ-1^{P158Δ} and DJ-1^{A107P} mutants showed decreased steady state protein levels. The accelerated protein decay was monitored by two separate experiments, namely by inhibition of the protein translation with cycloheximide and by a pulse chase assay using different time points (Fig 3.2 and 3.3). The inhibition of protein translation with cycloheximide showed comparable slow protein decay of DJ-1^{wt} and DJ-1^{A179T}, whereas the levels of DJ-1^{P158Δ} decreased rapidly within the examined time frame (Fig 3.2 A, B). DJ-1^{A107P}, on the other hand showed a slow degradation in HEK 293E cells and slightly faster decay than DJ-1^{wt} in MEF *Dj-1*^{-/-} cells. (Fig 3.2 C). This suggests that DJ-1^{A107P} may be slightly more stable when endogenous DJ-1 is present.

In accordance, the pulse chase assay showed a slow protein degradation for DJ-1^{wt} and DJ-1^{A179T} and a significantly faster breakdown of DJ-1^{P158Δ} (Fig 3.3 A). The estimated protein half-life time of DJ-1^{wt} was 24.5 ± 5.4 h and for DJ-1^{A179T} 29.6 ± 6.1 h, these were not significantly different (p>0.8). In comparison the half-life times of the known instable L166P mutant (Macedo et al., 2003, Moore et al., 2003, Gorner et al., 2004) and P158Δ mutant were estimated to be 1.2 ± 0.3 h (p<0.001, compared to wt) and 2.1 ± 0.2h (p<0.001, compared to wt), respectively (Fig 3.3 B).

In conclusion, DJ-1^{wt} and DJ-1^{A179T} had comparable protein half-life times, whereas the half-life time of DJ-1^{P158Δ} was significantly decreased. The protein decay of DJ-1^{A107P} seemed to be slower in the presence of DJ-1^{wt}.

3.1.3 DJ-1^{P158Δ} and DJ-1^{A107P} forms dimers with DJ-1^{wt}, but no homodimers of the mutants were detected

The stability and function of DJ-1 is highly dependent on its ability to form dimers (Moore et al., 2003, Tao and Tong, 2003). To examine the dimerization ability of the DJ-1 mutants, cells were co-transfected with myc- and HA-tagged DJ-1 variants and the myc-tagged DJ-1 was immunoprecipitated. The co-immunoprecipitated HA-tagged DJ-1

3 Results

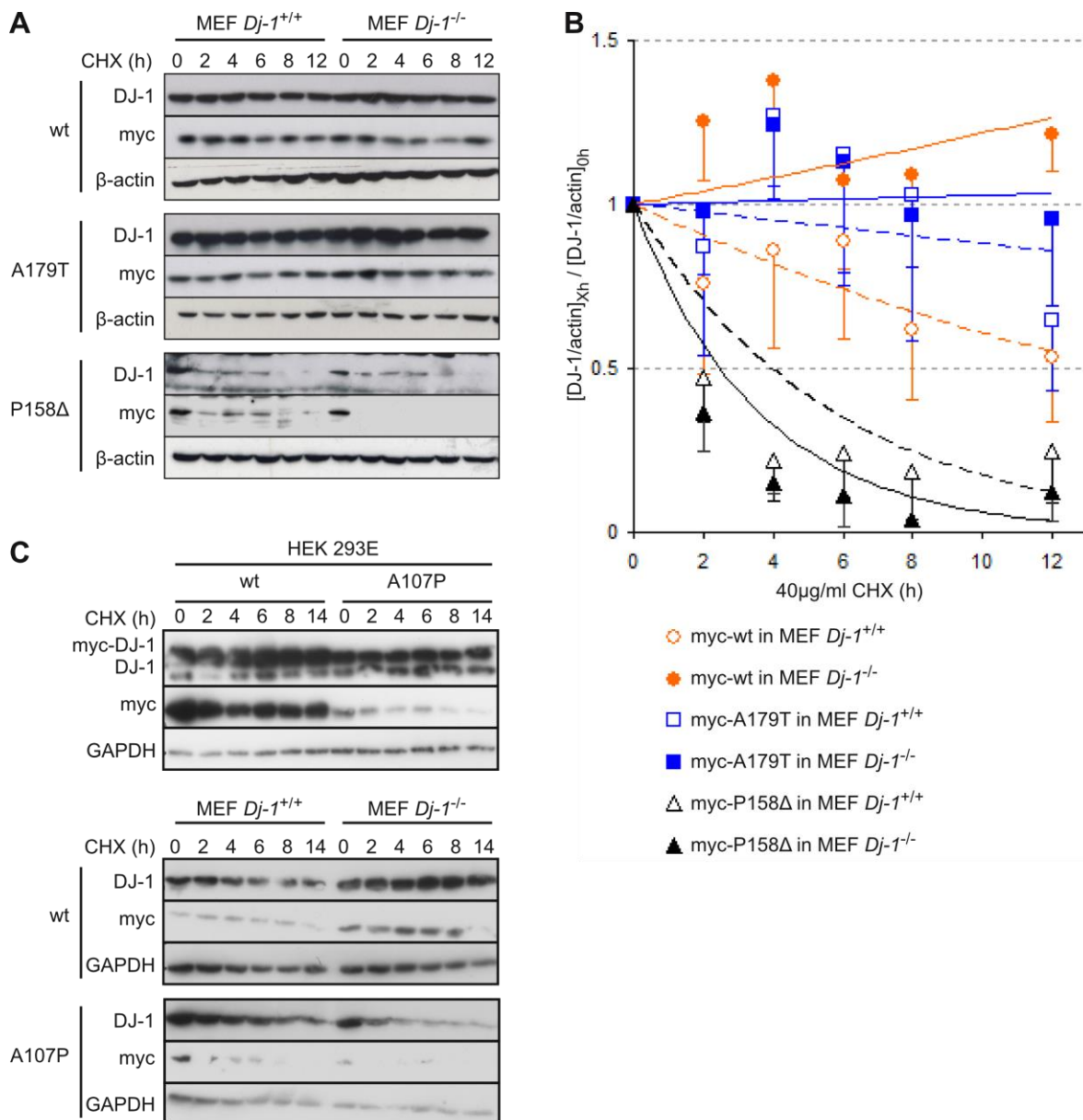


Figure 3.2 Inhibition of protein translation with cycloheximide reveals that DJ-1^{P158Δ} and DJ-1^{A107P} degrade faster than DJ-1^{wt} and DJ-1^{A179T}. **A, B** MEF *Dj-1*^{+/+} and MEF *Dj-1*^{-/-} cells were transiently transfected with myc-DJ-1 variants, after 48 h the cells were treated with 40 μg/ml cycloheximide (CHX) for indicated times. The DJ-1 protein levels were examined by immunoblotting for DJ-1 (3E8) and myc. β-actin serves a control for equal loading. **A** shows representative images from five separate experiments. Whereas the signal from both cell lines and both DJ-1 and myc antibody for DJ-1^{A179T} and DJ-1^{wt} stays equally strong within the time frame, the DJ-1^{P158Δ} signal decreases rapidly. **B** The DJ-1 and β-actin signal intensities in **A** were quantified with ImageJ software and normalized to signal at 0 h. Error bars indicate StDev. **C** HEK 293E, MEF *Dj-1*^{+/+} and MEF *Dj-1*^{-/-} cells were transiently transfected with myc-DJ-1^{wt} or myc-DJ-1^{A107P}. The samples were treated as described for **A**. GAPDH serves a control for equal protein loading. Representative images from five separate experiments are shown. The DJ-1^{wt} signal stays almost equally strong in the investigated time frame. On the other hand the DJ-1^{A107P} signal is not as stable.

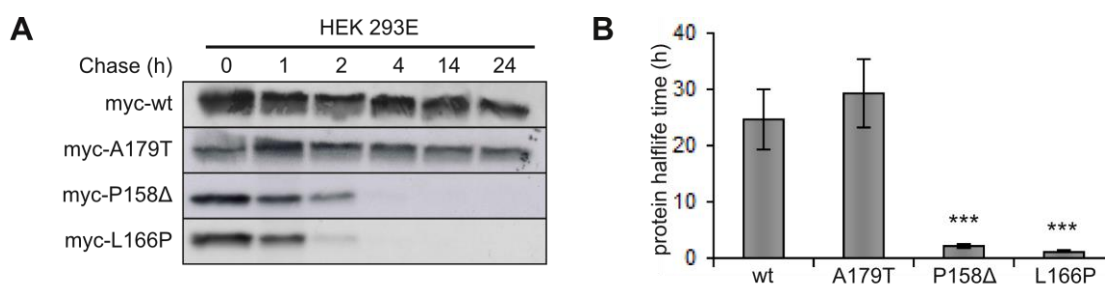


Figure 3.3 The protein half-life time of DJ-1^{P158Δ} is significantly shorter than the half-life times of DJ-1^{wt} and DJ-1^{A179T}. A HEK 293E cells were transiently transfected with myc-DJ-1 variants. Following day the cells were given a 30 min pulse with radioactive methionine and cysteine followed by a 0 to 24 h long recovery time. The myc-DJ-1 proteins were immunoprecipitated with anti-myc-agarose. Immunoprecipitated proteins were separated by SDS-PAGE and the radioactive signals were detected on autoradiography films. The known unstable DJ-1^{L166P} mutant was used for comparison. Shown are representative images from at least six independent experiments. The radioactive signal strength of DJ-1^{P158Δ} and DJ-1^{L166P} decreased faster than the signal strength of DJ-1^{wt} and DJ-1^{A179T}. B The radioactive signals from A were quantified with ImageJ software and the protein half-life times were calculated. Error bars are SEM, ***p ≤ 0.001 (one-way ANOVA, compared to DJ-1^{wt}).

was detected by immunoblotting (Fig 3.4). HA-DJ-1^{A179T} was co-immunoprecipitated with both myc-DJ-1^{A179T} and myc-DJ-1^{wt}. Both HA-DJ-1^{P158Δ} and HA-DJ-1^{A107P} were co-immunoprecipitated to a lesser extent with myc-DJ-1^{wt} and no homodimerization of the mutants could be detected. This suggests that these mutants have a limited ability to form dimers with the stable DJ-1^{wt}, but they are not able to form homodimers. Note that both HA-DJ-1^{P158Δ} and HA-DJ-1^{A107P} show higher protein levels when co-expressed with myc-DJ-1^{wt} compared to when co-expressed with myc-DJ-1^{P158Δ} and myc-DJ-1^{A107P}, respectively (Fig 3.4).

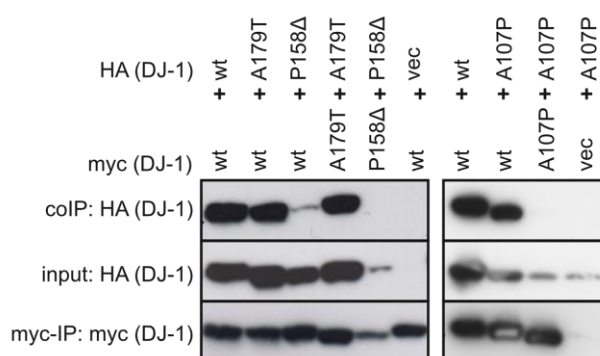


Figure 3.4 The dimerization ability of DJ-1^{P158Δ} and DJ-1^{A107P} is altered. HEK 293E cells were transiently transfected with myc-DJ-1 and HA-DJ-1 mutants in indicated combinations and expressed for 48 h. Equal protein amounts were incubated with anti-myc-agarose beads and immunoprecipitated DJ-1 proteins were detected by immunoblotting for HA and myc. Representative images from three separate experiments are shown. DJ-1^{P158Δ} and DJ-1^{A107P} dimerized with DJ-1^{wt}, but no homodimerization of these two mutants could be detected.

3 Results

3.1.4 DJ-1^{P158Δ} binds to ASK1 also in absence of oxidative stress

DJ-1 is shown to inhibit ASK1 signalosome activation upon oxidative stress through direct binding to ASK1 (Junn et al., 2005, Waak et al., 2009a, Mo et al., 2010). Thus, it was investigated if DJ-1^{A179T}, DJ-1^{P158Δ} and DJ-1^{A107P} bind to ASK1. HEK 293E cells that co-overexpressed ASK1-HA and myc-DJ-1 were stressed with 1 mM H₂O₂ for 30 min. Control cells were left untreated. ASK1-HA was immunoprecipitated and co-immunoprecipitated myc-DJ-1 was detected by immunoblotting. As expected, DJ-1^{wt} and DJ-1^{A179T} co-immunoprecipitated with ASK1 only if H₂O₂ had been applied. Surprisingly, DJ-1^{P158Δ} was co-immunoprecipitated with ASK1 both in presence as well as in absence of H₂O₂ (Fig 3.5 A). Moreover, as previously described, the DJ-1^{M26I} mutant also showed this untypical binding behavior towards ASK1 (Fig 3.5 A) (Waak et al., 2009a). In addition the DJ-1^{A107P} mutant was co-immunoprecipitated with ASK1-HA in absence of oxidative stress. After stress had been applied the co-immunoprecipitation could be further increased (Fig 3.5 D). This suggests a potential functional ability of this mutant towards inhibition of the ASK1 signalosome.

In absence of oxidative stress ASK1 is inactivated by Trx, which covalently binds to cysteine residues in the N-terminal domain (Saitoh et al., 1998). Upon occurrence of oxidative stress Trx is oxidized and the inhibition is released. Previously our group has shown that DJ-1^{wt} can bind to the full length (FL) ASK1 molecule, but not to an ASK1^{ΔN} variant, which is lacking the first 648 N-terminal amino acids of ASK1. In contrast to DJ-1^{wt} the DJ-1^{M26I} mutant was able to bind to the ASK1^{ΔN} variant (Waak et al., 2009a). We therefore investigated if the DJ-1^{P158Δ} and DJ-1^{A107P} possess an abnormal site on ASK1. Thus ASK1^{ΔC} (aa 1-947), which lacks the C-terminal domain, and ASK1^{CT} (aa 945-1374), which lacks the N-terminal and the kinase domain, were applied (Fig 3.5 B). The HA-tagged ASK1 variants were co-overexpressed with myc-DJ-1 in HEK 293E cells. The cells were treated with 1 mM H₂O₂ for 30 min or left untreated and the ASK1-HA variants were immunoprecipitated. Co-immunoprecipitated DJ-1 was detected by immunoblotting. DJ-1^{wt} was co-immunoprecipitated with ASK1^{FL} (amino acids 1-1374) and the truncated ASK1^{ΔC} and ASK1^{CT} variants in an oxidative stress dependent manner (Fig 3.5 C, D). DJ-1^{P158Δ} and DJ-1^{M26I} co-immunoprecipitated as already observed also in absence of oxidative stress with ASK1^{FL}. In contrast to the binding to ASK1^{FL}, both mutants showed an increased binding to both ΔC and CT ASK1 variants when the cells had been treated with H₂O₂ (Fig 3.5 C). DJ-1^{A107P} was co-immunoprecipitated with ASK1^{FL} to a slightly higher extent than DJ-1^{wt} in absence of

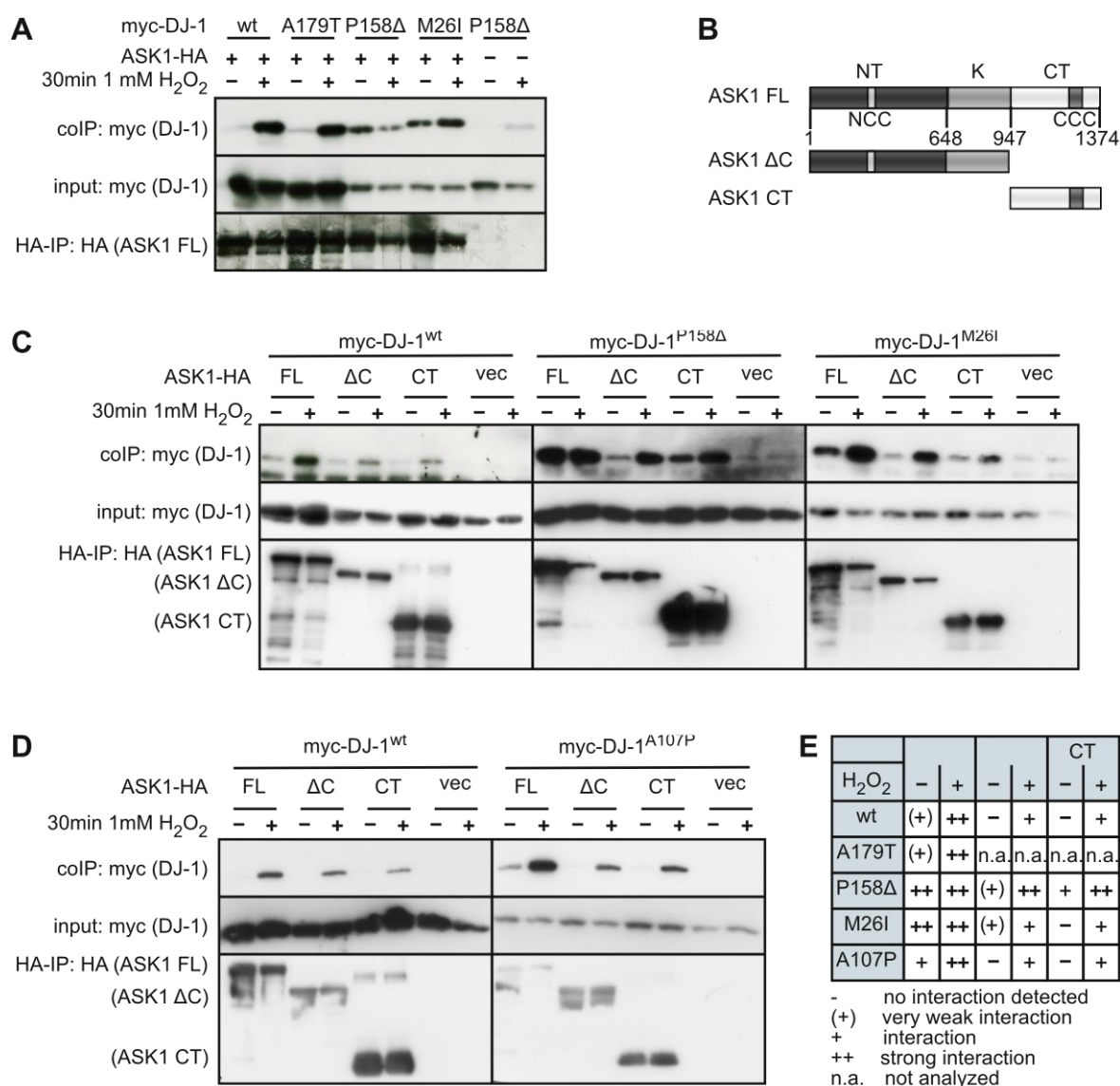


Figure 3.5 DJ-1^{P158Δ} binds also in absence of oxidative stress to ASK1^{FL}, whereas DJ-1^{A107P} seems to behave almost as DJ-1^{wt}. A HEK 293E cells were transiently transfected with ASK1^{FL}-HA and myc-DJ-1 mutants. After two days the cells were treated with 1 mM H₂O₂ for 30 min or were left untreated. Equal amounts of protein were incubated with anti-HA-agarose beads. Co-immunoprecipitated myc-DJ-1 was detected by immunoblotting with anti-myc antibody. DJ-1^{wt} and DJ-1^{A179T} co-immunoprecipitated with ASK1 only in H₂O₂ treated samples, whereas DJ-1^{P158Δ} and DJ-1^{M26I} co-immunoprecipitated with ASK1 both in absence and presence of H₂O₂. B shows a schematic illustration of the used ASK1^{FL}, ASK1^{ΔC} and ASK1^{CT} variants (NT – N-terminal domain, K – kinase domain, CT – C-terminal domain). C DJ-1^{wt} and mutants were co-overexpressed with ASK1-HA variants in HEK 293E cells. The samples were treated as in described in A. DJ-1^{wt} immunoprecipitated with all ASK1 variants in an oxidative stress dependent manner. Also DJ-1^{P158Δ} and DJ-1^{M26I} co-immunoprecipitated with ASK1^{CT} and ASK1^{ΔC} in an oxidative stress dependent manner. D HA-ASK1 variants were co-overexpressed with myc-DJ-1^{wt} or myc-DJ-1^{A107P} in HEK 293E cells. The samples were treated as described for A. DJ-1^{A107P} immunoprecipitated with ASK1^{FL} also in absence of H₂O₂. In the presence of stress DJ-1^{A107P} was able to further increase the interaction. DJ-1^{A107P} behaved as DJ-1^{wt} towards ASK1^{ΔC} and ASK1^{CT}. E The table summarizes the ability of the DJ-1^{wt} and mutants to bind to ASK1^{FL} and variants. All images are representative images from three or more experiments.

3 Results

oxidative stress and behaved as DJ-1^{wt} towards ASK1^{ΔC} and ASK1^{CT} (Fig 3.5 D). The table in Fig 3.5 E summarizes the ability of the DJ-1 mutants to bind to the different ASK1 variants.

In order to confirm the binding behavior of DJ-1^{P158Δ} towards the ASK1 variants, a native co-fractionation assay using size exclusion chromatography was performed (Fig 3.6). The HA-tagged ASK1 variants were co-overexpressed with myc-DJ-1 in HEK 293E cells. The cells were treated with 0.5 mM H₂O₂ for 30 min or left untreated. The cell lysates were applied on a Superdex 200 10/300 column (GE Healthcare). The proteins were separated by size and the eluate was fractionated. The protein content in the fractions was examined by immunoblotting. The UV-absorption curves from the different runs were comparable. The size of myc-DJ-1 is 24 kDa and its dimer is 48 kDa. Therefore DJ-1 elutes in later fractions than ASK1^{FL}, which has the size of around 155 kDa and also exists as a dimer (310 kDa) or larger oligomers (Tobiume et al., 2002). ASK1^{ΔC} is about 107 kDa and ASK1^{CT} about 48 kDa. In control cell lysates that had not been treated with H₂O₂ myc-DJ-1^{wt} eluted in fractions expected for its dimeric form. However, if the cells had been treated with H₂O₂ myc-DJ-1^{wt} eluted also in the earlier fractions where the ASK1-HA variants eluted (Fig 3.6, left panel). In vector transfected cells myc-DJ-1^{wt} did not elute earlier after H₂O₂ treatment. Therefore DJ-1^{wt} is bound to a bigger protein complex only in presence of ASK1 and oxidative stress. On the other hand DJ-1^{P158Δ} eluted in earlier fractions independently of H₂O₂ treatment, but only when an ASK1 variant was present (Fig 3.6, right panel). These findings confirm the previous observation in the coIP-experiments that DJ-1^{P158Δ} is binding constantly to ASK1. Notably, ASK1^{CT} eluted earlier than expected for its monomeric size (Fig 3.6), suggesting a high dimerization and oligomerization ability of this fragment. This is in agreement with assumption that this region is important for the dimerization and oligomerization of the ASK1 protein (Tobiume et al., 2002).

In conclusion, DJ-1^{P158Δ} bound to ASK1 also in absence of oxidative stress. Also DJ-1^{A107P} bound to ASK1 in absence of oxidative stress, but showed a clear increase in the interaction with ASK1 when oxidative stress was present. DJ-1^{A179T} in its turn did not show a different behavior in ASK1 interaction than the wt DJ-1.

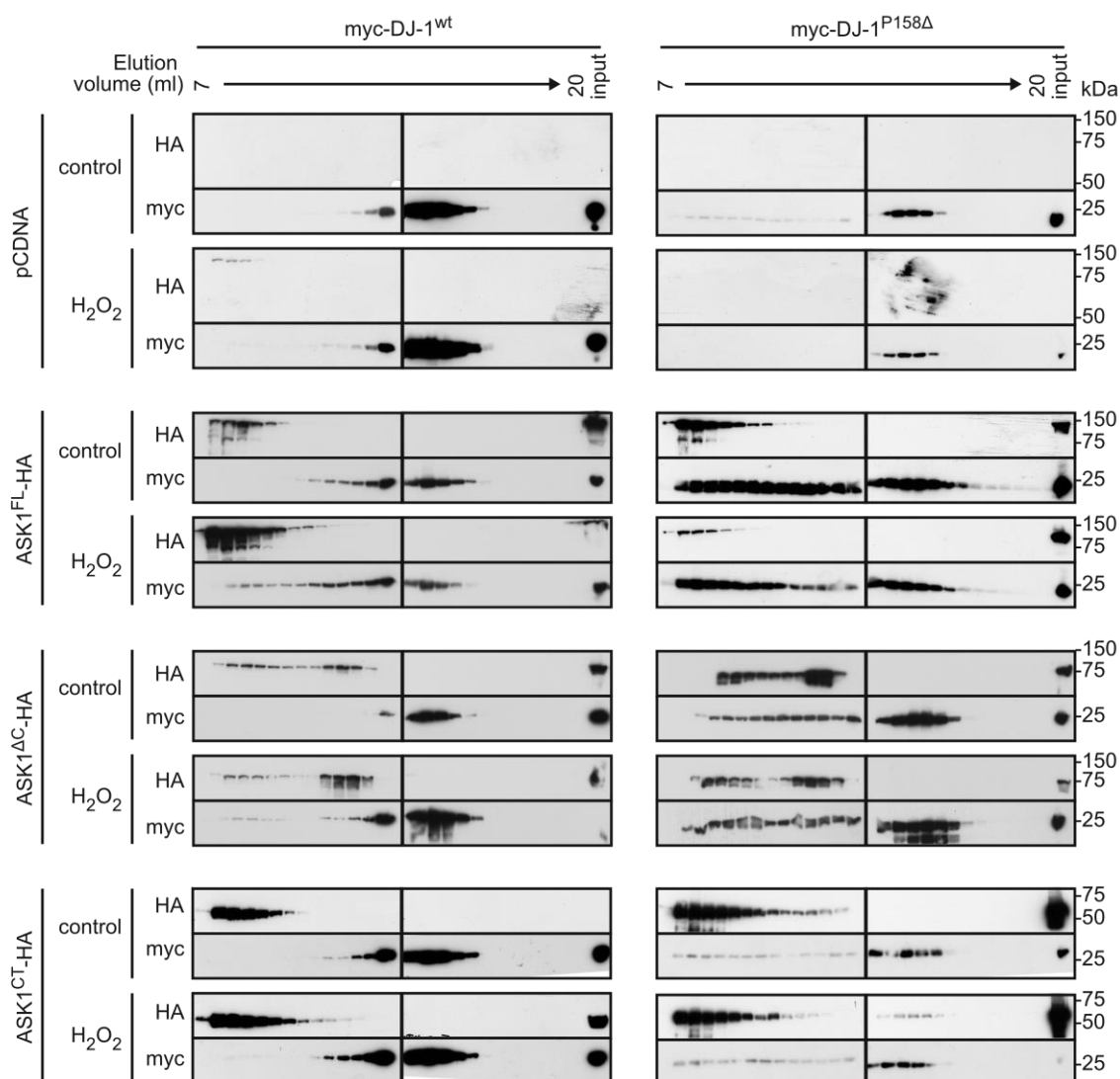


Figure 3.6 Size exclusion chromatography confirmed the binding behavior of DJ-1^{P158Δ} to ASK1. ASK1-HA variants and myc-DJ-1^{wt} or myc-DJ-1^{P158Δ} were co-overexpressed in HEK 293E cells. Cells were treated with 500 μM H₂O₂ for 30 min or left untreated (control). The cells were lysed and the proteins were chromatographically separated by size. The eluate was fractionated in 0.5 ml fractions and the protein content in the fractions was examined by immunoblotting for HA (ASK1) and myc (DJ-1). Shown are representative images from two separate experiments. In absence of H₂O₂ and in absence of ASK1 (upper panels) myc-DJ-1^{wt} (left panel) eluted in later fractions. When ASK1^{FL}, ASK1^{ΔC} or ASK1^{CT} was present DJ-1^{wt} eluted together with larger proteins complexes in earlier fractions. DJ-1^{P158Δ} eluted in earlier fractions also in the absence of H₂O₂, but only if ASK1^{FL}, ASK1^{ΔC} or ASK1^{CT} was present.

3.1.5 DJ-1^{P158Δ} inhibits Daxx nuclear export less efficiently than DJ-1^{wt} and DJ-1^{A179T}

DJ-1 has been shown to directly inhibit the nuclear export of the Daxx, a downstream event after ASK1 activation (Junn et al., 2005, Waak et al., 2009a, Saeed et al., 2010). To investigate if DJ-1^{P158Δ} is able to inhibit Daxx nuclear export, Flag-Daxx and myc-DJ-1 were co-overexpressed in MEF *Dj-1*^{-/-} cells and oxidative stress was applied by treatment with H₂O₂ (Fig 3.7). In absence of stress Flag-Daxx localized to the nucleus in vector transfected samples, but when the cells had been treated with H₂O₂ the distribution of Flag-Daxx was more cytosolic. If Flag-Daxx was co-expressed with

3 Results

DJ-1 a smaller increase in cytosolic Daxx upon oxidative stress was seen. Five times more cDNA of HA-DJ-1^{P158Δ} compared to HA-DJ-1^{wt} and HA-DJ-1^{A179T} was needed to suppress the nuclear export of Daxx, suggesting a weak residual functional ability of the point deletion mutant.

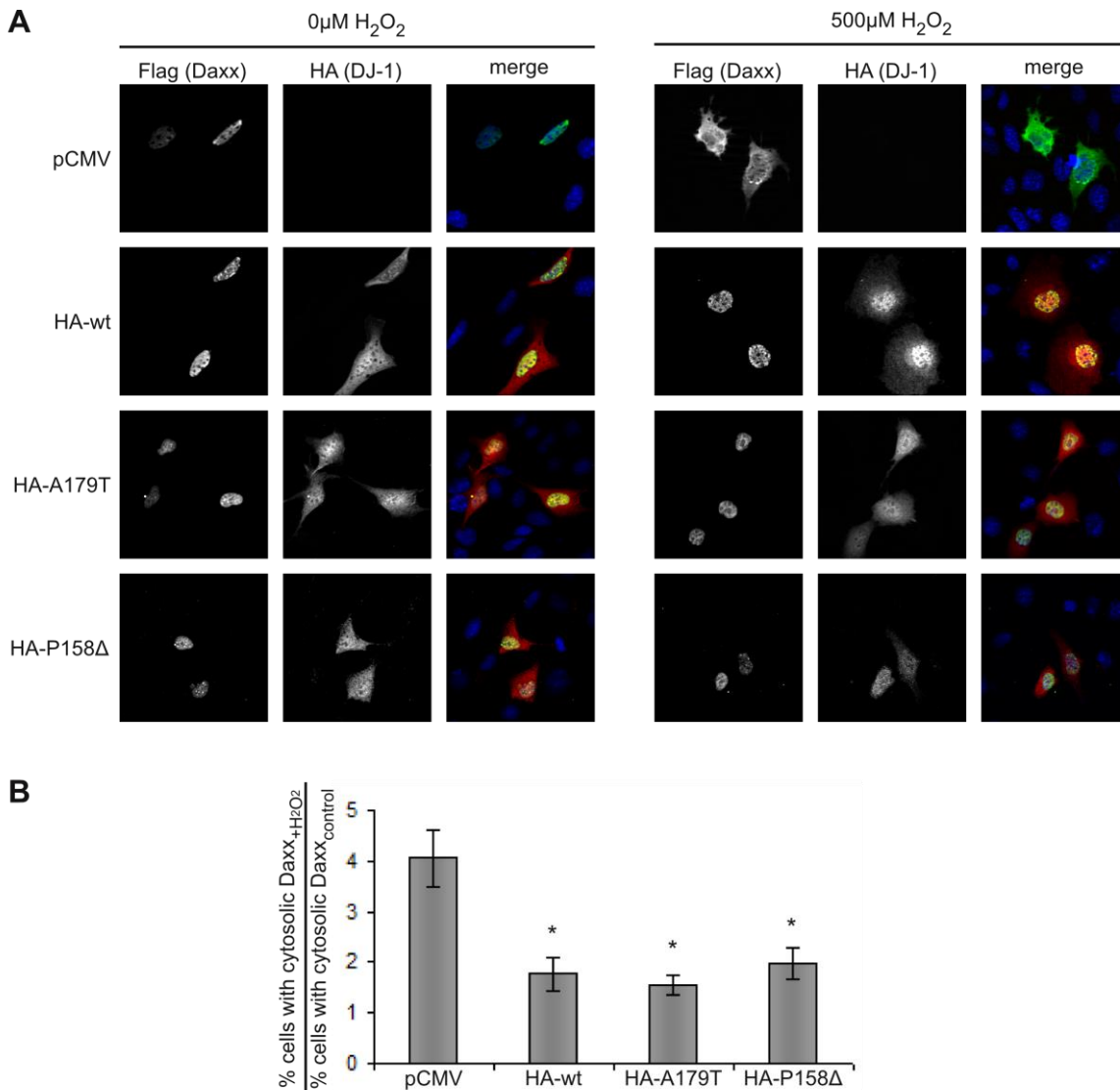


Figure 3.7. Five times more cDNA of DJ-1^{P158Δ} than of DJ-1^{wt} and DJ-1^{A179T} is needed in order to decrease Daxx nuclear translocation upon induction of oxidative stress. **A** MEF *Dj-1*^{-/-} cells were transiently co-transfected with Flag-Daxx and HA-DJ-1^{wt} and mutants. After 48 h the cells were treated with 500 μM H₂O₂ for 30 min or were left untreated. The cells were fixed with paraformaldehyde and immunostained using Flag (to visualize Flag-Daxx) and HA (to visualize HA-DJ-1) specific antibodies. Nuclei were counterstained with Hoechst 33342. Illustrative pictures are shown. Five times more DJ-1^{P158Δ} cDNA had to be used in order to visualize the cells that had been transfected with the unstable mutant. In absence of oxidative stress Flag-Daxx localized mainly to the nucleus and in presence of stress it translocated to the cytosol. Co-overexpression of DJ-1 decreased the translocation of Flag-Daxx. **B** The cytosolic versus nuclear localization of Flag-Daxx in HA-DJ-1 positive cells was quantified from the images; more than 50 cells per sample were used. N≥4, Error bars are StDev, *p<0.05 (one way Anova, compared to pCMV).

3.1.6 DJ-1^{wt}, but not mutants, decrease p25 α dependent MT retraction in an α -syn overexpressing oligodendroglial cell line

Cytoplasmic α -syn and p25 α containing inclusions have been found in oligodendroglial cells of MSA patients (Kovacs et al., 2004, Lindersson et al., 2005, Song et al., 2007). In addition the affected oligodendroglial cells have been shown to have elevated levels of DJ-1 (Neumann et al., 2004). Previously it was shown that when rat oligodendroglial cells, which are stably overexpressing human α -syn (OLN AS), are transfected with p25 α they show a cytotoxic reaction, which can be seen by a retraction of the microtubules (MT) to the perinuclear region (illustrated in Fig 3.9 C) (Kragh et al., 2009). This retraction was dependent on the expression of both α -syn and p25 α , since single transfected cells did not show MT retraction. To investigate if DJ-1 modulates the MT retraction in OLN AS cells our collaboration partners in Aarhus University (Denmark) transiently co-overexpressed p25 α and myc-DJ-1^{wt} or mutants in OLN AS cells. As expected the steady state levels of the overexpressed DJ-1^{M26I}, DJ-1^{P158 Δ} and DJ-1^{L166P} were slightly decreased compared to the overexpressed levels of DJ-1^{wt} and DJ-1^{C106A} (Fig 3.8 A). Interestingly, DJ-1^{wt} was able to decrease the MT retraction in these cells, whereas DJ-1^{C106A}, DJ-1^{M26I}, DJ-1^{L166P} and DJ-1^{P158 Δ} were not able to decrease the MT retraction (Fig 3.8 B).

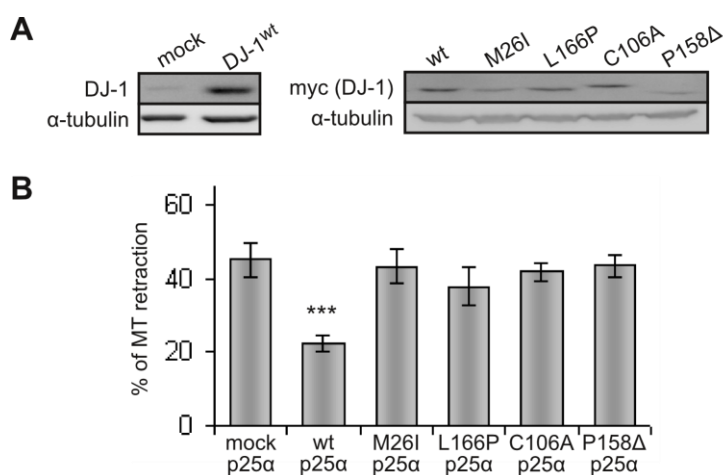


Figure 3.8 DJ-1^{wt}, but not mutant DJ-1, decrease MT retraction induced by co-expression of α -Syn and p25 α in rat oligodendrocytes. **A** OLN AS cells were transiently transfected with myc-DJ-1 or mock plasmid. Immuno blot for DJ-1 (left panel) or myc (right panel) and α -tubulin was performed. Protein levels of overexpressed DJ-1^{M26I} DJ-1^{L166P} and DJ-1^{P158 Δ} were slightly decreased compared to the protein levels of DJ-1^{wt} and DJ-1^{C106A}. **B** OLN AS cells were transiently co-transfected with p25 α and myc-DJ-1. After 24 h the cells were fixed with paraformaldehyde and immunostained with p25 α , DJ-1 and α -tubulin specific antibodies. Nuclei were stained with 4, 6-diamidino-2-phenylindole dihydrochloride (DAPI). MT retraction was scored in 120-200 p25 α and myc-DJ-1 double positive cells per condition localized in five randomly chosen microscopic fields. Error bars indicate StDev, n=4, ***p \leq 0.0001 (Student's t-test, compared to mock).

This experiment was made by Jafar H.A. Shaik in the Department of Biomedicine at the University of Aarhus in Denmark.

3 Results

To investigate if DJ-1^{A107P} was able to decrease the MT retraction in OLN AS cells, we examined the retraction after co-transfection with p25 α and HA-DJ-1^{A107P} (Fig 3.9 A). The steady state protein level of DJ-1^{A107P} in this cell line was slightly decreased compared to DJ-1^{wt} (Fig 3.9 B). We could confirm that DJ-1^{wt} was able to significantly

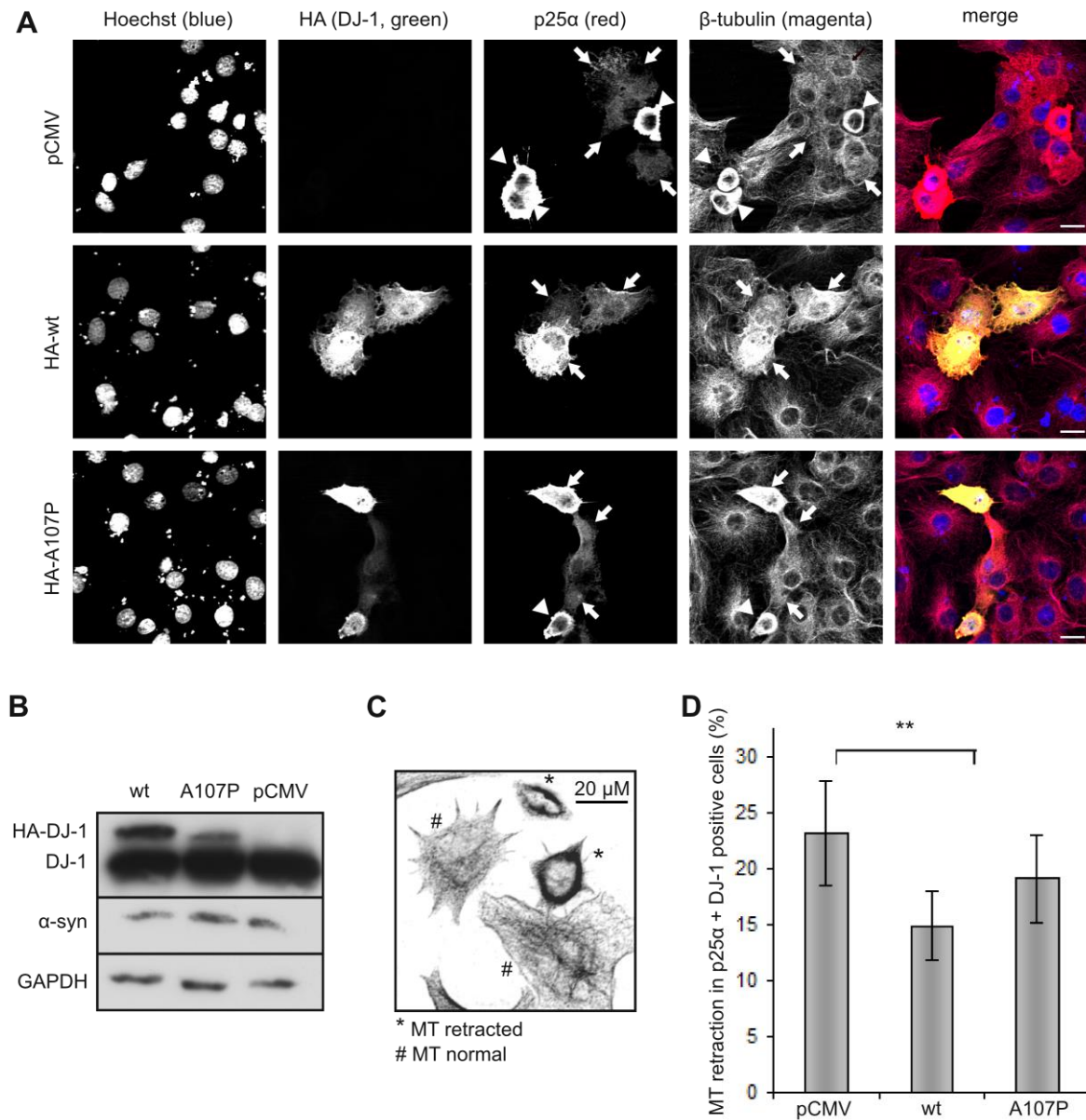


Figure 3.9 DJ-1^{A107P} is to some extent able to decrease the MT retraction after p25 α transfection in OLN AS cells. **A** OLN AS cells were transiently co-transfected with p25 α and HA-DJ-1. After 24 h the cells were fixed with paraformaldehyde and immunostained with antibodies specific for p25 α (red), HA (green) and β -tubulin (magenta). The nuclei were counterstained with Hoechst 33342 (blue). The cells were photographed. Shown are exemplifying images of cells with retracted MT (arrowheads) compared to cells with no MT retraction (arrows) in p25 α and vector or HA-DJ-1 transfected OLN AS cells. **B** The steady state levels of the overexpressed DJ-1 and the α -syn expression in OLN AS cells were examined by immunoblotting using DJ-1 (CST) and α -syn antibodies. GAPDH serves as a control for equal loading. **C** shows an illustrative image of cells with retracted versus normal MT **D**. MT retraction was scored from images. 200-350 p25 α and myc-DJ-1 double positive cells were scored per condition. Error bars indicate StDev, n=7, **p \leq 0.01 (Student's t-test, compared to pCMV). DJ-1^{wt} transfected cells showed significantly less MT retraction compared to pCMV transfected cells. DJ-1^{A107P} showed a tendency to be intermediate in decreasing the MT retraction.

decrease the p25 α dependent MT retraction compared to vector transfected controls. Interestingly, the DJ-1^{A107P} mutant had an intermediate ability to decrease the MT retraction; it was neither significantly performing worse than the DJ-1^{wt} nor significantly better than the vector control (Fig 3.9 D).

3.1.7 ASK1 is involved in p25 α dependent MT retraction in OLN AS cells

Next the conceivable ASK1 involvement in the MT retraction upon p25 α overexpression in the OLN AS cell line was investigated. Our collaborators at H. Lundbeck A/S (Valby, Denmark) transiently transfected OLN AS cells with pCDNA3.1-p25 α and treated the cells with four different ASK1 inhibitors (Fig 3.10 B). They scored the MT retraction and interestingly all ASK1 inhibitors showed a concentration dependent significant decrease in MT retraction in p25 α and α -syn double positive cells (Fig 3.10 A). Moreover, the inhibitors did not change the α -syn levels in the cells (Fig 3.10 C).

Next the effect of exogenously overexpressed ASK1 on the MT retraction in OLN AS cells was examined. Therefore we co-expressed p25 α and ASK1-HA in OLN AS cells. As seen before the positive control HA-DJ-1^{wt} was able to decrease the MT retraction. Interestingly, cells that overexpressed ASK1-HA together with p25 α showed increased MT retraction compared to cells that only overexpressed p25 α (Fig 3.10 D). This is in agreement with the previous assay and indicates that ASK1 is playing a role in the activation of apoptosis when the cellular levels of α -syn and p25 α increase in the oligodendroglial cells.

Furthermore we investigated, using an *in vitro* immunocomplex kinase assay, if ASK1 kinase activity is activated during the MT retraction. Again p25 α and ASK1-HA were co-overexpressed in OLN AS cells. The ASK1-HA in the cell lysates was immunoprecipitated. The ASK1 kinase activation was examined via activation of the phosphorylation of the pseudosubstrate MBP. A slight increase of ASK1 activity in samples with co-overexpressed p25 α compared to samples with only overexpressed ASK1 could be detected, pointing to a p25 α dependent activation of ASK1 (Fig 3.10 E). However, one has to mention that the *in vitro* kinase assay showed an extremely high variability.

3 Results

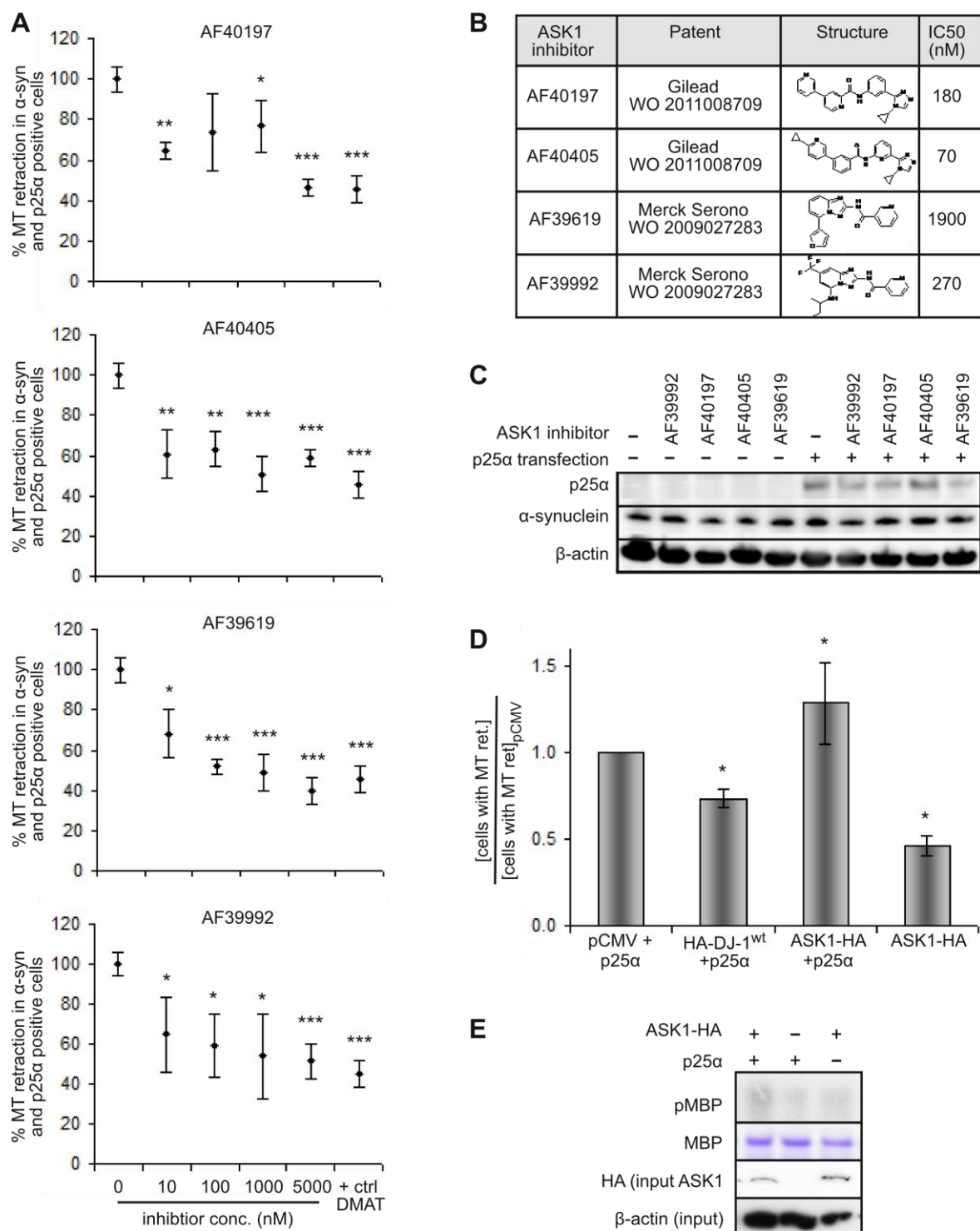


Figure 3.10 Regulation of ASK1 is influencing the MT retraction in p25 α and α -syn expressing OLN cells. A OLN AS cells were transiently transfected with p25 α and four hours later indicated concentrations of ASK1 inhibitors were added. 2-dimethylamino-4,5,6,7-tetrabromo-1H-benzimidazole (DMAT) was used as a positive control inhibitor (Kragh et al., 2009). 24 h after transfection the cells were fixed and immunofluorescence stained for p25 α and α -tubulin. Nuclei were counterstained with Hoechst 33342. Cellomics Array Scanner™ was used for automated quantification of MT retraction in p25 α positive cells. Mean of three wells, Error bars are StDev, approximately 300 cells were counted per condition. * $p < 0.1$, ** $p < 0.01$, *** $p < 0.001$ (Students t-test relative to no inhibitor treated samples). All four ASK1 inhibitors significantly decreased the MT retraction in a concentration dependent manner. **B** The table

gives information about the used ASK1 inhibitors. **C** Lysates of OLN AS cells that had been transiently transfected with p25 α and treated with the ASK1 inhibitors were analysed by immunoblotting using p25 α and α -syn specific antibodies. β -actin serves as a control for equal protein loading. The ASK1 inhibitors did not affect the α -syn and p25 α protein levels in OLN cells. **D** OLN AS cells were transiently co-transfected with ASK1-HA and p25 α , 16 h later the cells were fixed and immunostained with HA, p25 α and β -tubulin specific antibodies. The MT retraction in double transfected cells was scored manually. More than 100 cells per condition were analyzed. Error bars are StDev from four separate experiments, * $p < 0.05$ (Student's t-test compared to vector control). The MT retraction was increased when ASK1 was co-overexpressed with p25 α in OLN AS compared to when p25 α was expressed alone. Overexpression of ASK1 alone did not induce MT retraction. **E** OLN AS cells were transiently co-transfected with p25 α and ASK1-HA or empty vector. 16 h later the cells were lysed and immunoprecipitated using anti-HA-agarose beads. The beads were washed and incubated with MBP and radioactively labeled ATP. The reaction was stopped and the proteins were separated in a 4-20% gradient gel. The gel was stained with the sensitive variant of Coomassie and dried over night. The radioactive signals were detected on autoradiography films. A slightly stronger radioactive signal was seen from MBP when ASK1 and p25 α were co-overexpressed, compared to when ASK1 or p25 α was expressed alone.

Experiments shown in A, B and C were made by Louise Buur Vesterager at H. Lundbeck A/S, department of Neurodegeneration, Valby, Denmark.

3.2 Induction of inflammation by and uptake of extracellular α -syn in primary astrocytes

3.2.1 Quality control of the purified recombinant synuclein proteins

In the experiments described below primary astrocytes were treated with recombinant synuclein. The recombinant human α -syn^{wt}, α -syn^{A30P}, α -syn^{S129A} and β -syn were prepared and the purified protein stocks were tested for possible contaminations (Fig 3.11). Since already low amounts of endotoxin can induce inflammatory responses, the endotoxin levels in all protein samples were estimated (Fig 3.11 A). The α -syn^{wt}, α -syn^{A30P}, and α -syn^{S129A} samples contained less than 0.06, 0.006 and 0.006 ng/ml of endotoxin, respectively. Note that these concentrations were measured for the protein stocks, working dilutions contained lower amounts of endotoxins. Unfortunately the purified β -syn contained high amounts (> 0.15 ng/ml) of endotoxins (Fig 3.11 A).

Contaminating proteins in the synuclein samples were monitored by a sensitive variant of Coomassie SDS-PAGE and mass spectrometry. Only one clear band was detected at the electrophoretic motility expected for α -syn and β -syn in the SDS-PAGE gel (Fig 3.11 B). The proteins were verified to be the expected synuclein by immunoblotting using human α -syn or β -syn specific antibodies (Fig 3.11 C). To exclude contaminating proteins with the same size as synuclein coomassie stained α -syn^{wt} and β -syn protein bands were cut out from the gel and trypsinized. The trypsin cut peptide fragments were analyzed by mass spectrometry by Andreas Maurer in the group of Professor Kalbacher at the Interfaculty Institute of Biochemistry, University of

3 Results

Tübingen. Only peptide fragments corresponding to α -syn or β -syn could be detected (Fig 3.11 D). No C-terminal fragments could be detected even though the whole synuclein proteins should have been expressed. The C-terminus of α - and β -syn is highly acidic, hence it lacks cleavage sites for trypsin and long peptide fragments are hardly recognized in mass spectrometry. However, the epitope of the α -syn antibody is in the C-terminus and the proteins were detected by immunoblotting. Therefore it can be assumed that the protein samples contained the full length synuclein peptides.

In conclusion, the recombinant proteins contained undetectable amounts of contaminating proteins and the α -syn variants contained neglectable levels of endotoxin.

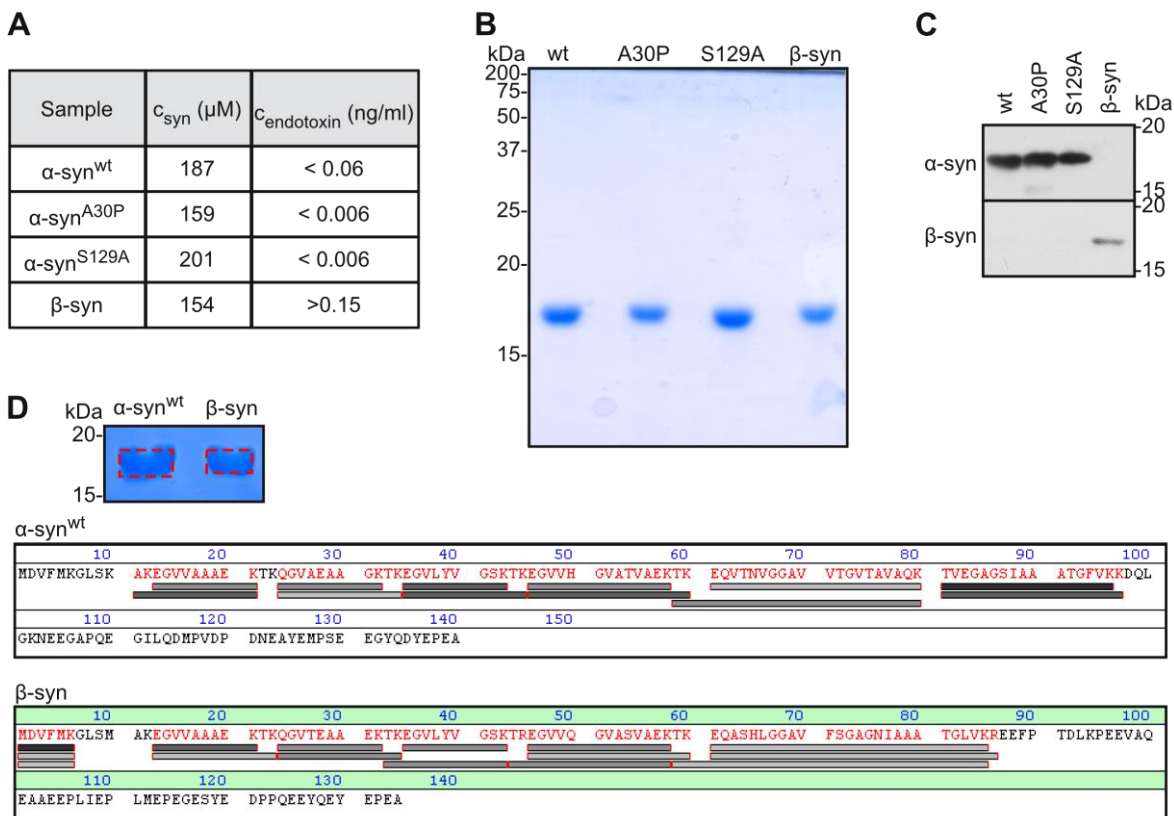


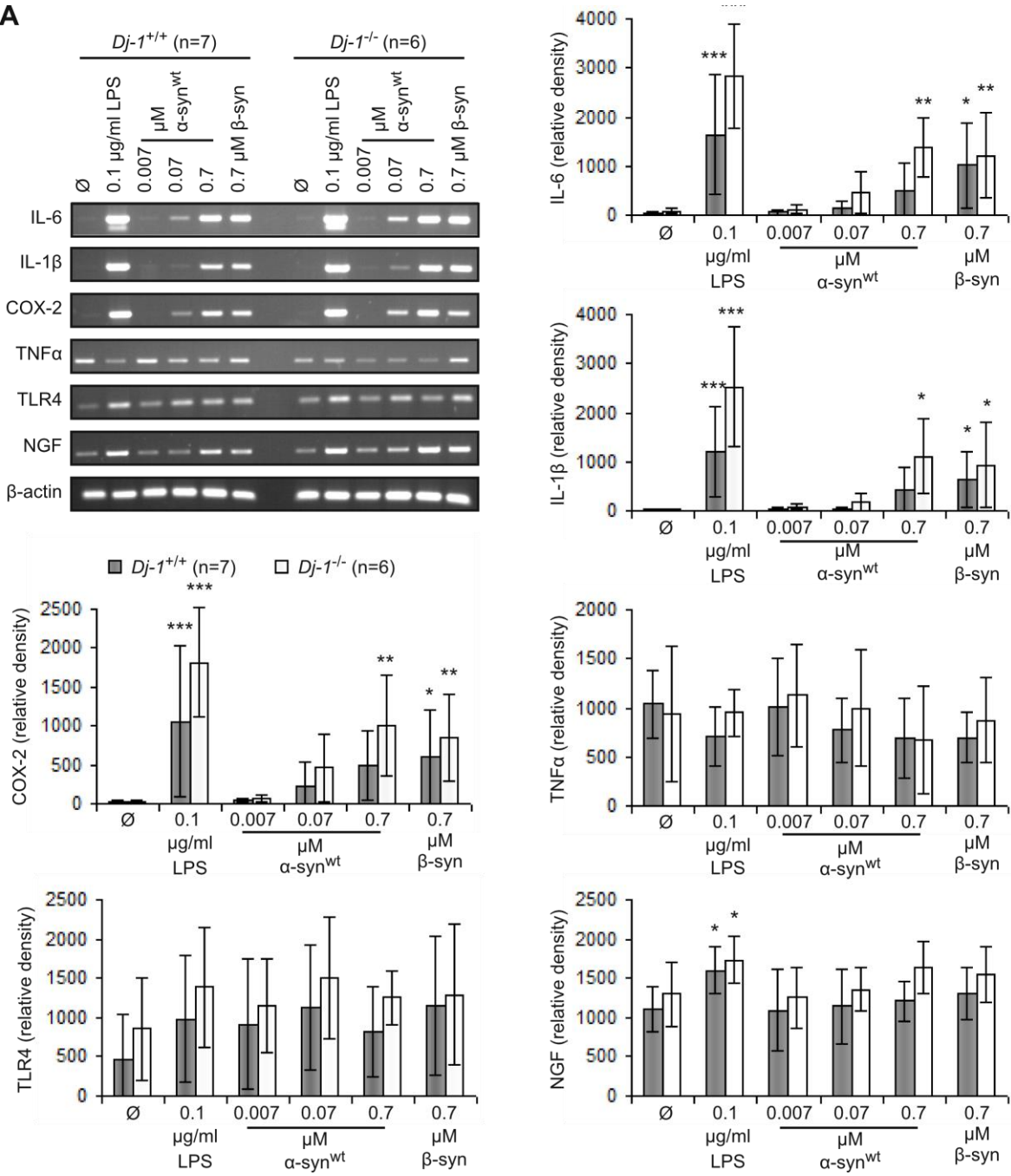
Figure 3.11 Quality control of the purified recombinant synucleins showed that they were absent of other contaminating proteins and contained very low levels of endotoxins. A Endotoxin levels in the purified protein samples were measured with 0.06 EU/ml cut off using three dilutions (1:1, 1:10 and 1:25) of the sample stocks. The table indicates the concentrations of synuclein and endotoxin in the protein stocks. **B** Samples of purified recombinant α -syn and β -syn were tested for purity by a sensitive variant of Coomassie stained SDS-PAGE. Protein bands at the expected electrophoretic motility for α -syn and β -syn were stained and no other bands could be detected. **C** Samples of purified α -syn^{wt}, α -syn^{A30P}, α -syn^{S129A} and β -syn were immunoblotted using antibodies for α -syn and β -syn. The purified proteins were recognized by expected antibodies. **D** Samples that were cut out from the gels (indicated by dashed boxed in the upper panel), the proteins were trypsinized and the peptides were analyzed by mass spectroscopy in professor Kalbacher's group at the Interfaculty Institute of Biochemistry. Only peptide sequences corresponding to α -syn^{wt} and β -syn were detected.

3.2.2 Treatment with recombinant α -syn induces cytokine expression in primary astrocytes

Other groups have shown that extracellular α -syn can induce expression of cytokines in astroglial cells (Klegeris et al., 2006, Lee et al., 2010, Fellner et al., 2013). Therefore, the induction of cytokine expression by extracellular α -syn was investigated. DJ-1 deficient astrocytes were used since our group has previously shown that DJ-1 decreases the cytotoxic response caused by the gram-negative bacterial endotoxin, LPS, in astrocytes (Waak et al., 2009b). Primary astrocytes from littermate *Dj-1^{-/-}* and *Dj-1^{+/+}* mice were treated with 0 to 0.7 μ M recombinant α -syn^{wt}, 0.7 μ M β -syn or 0.1 μ g/ml LPS for 48 h. The mRNA levels of TNF α , IL-1 β , IL-6, COX-2 and nerve growth factor (NGF) was estimated with semi-quantitative PCR. As expected, LPS significantly increased the mRNA levels of IL-6, IL-1 β , COX-2 and NGF ($p < 0.05$, Student's t-test, Fig 3.12 A). The induction of IL-6, IL-1 β and COX-2 mRNA expression was significantly different between *Dj-1^{+/+}* and *Dj-1^{-/-}* cells ($p < 0.05$). Even though LPS is a well known activator of TNF α expression in astrocytes (Chung and Benveniste, 1990), an increase of TNF α mRNA expression by LPS could not be detected here. Interestingly, also α -syn induced expression of IL-6, IL-1 β and COX-2 mRNA in a concentration dependent manner, reaching significant induction when *Dj-1^{-/-}* astrocytes were treated with 0.7 μ M α -syn ($p < 0.05$). The expression of NGF was not significantly affected by α -syn (Fig 3.12 A). Previously extra cellular α -syn has been shown to increase TNF α expression (Lee et al., 2010, Fellner et al., 2013). However, as after LPS treatment, no induction of TNF α expression was seen after α -syn treatment. A mouse model for MSA that overexpresses α -syn has been shown to have higher immunoreactivity for TLR4 in cells with microglial morphology (Stefanova et al., 2007), hence also the TLR4 mRNA changes were measured. However, no changes in TLR4 levels either by LPS or synuclein treatment could be detected (Fig 3.12 A). 0.7 μ M β -syn was able to induce significant increase in IL-6, IL-1 β and COX-2 expression in both wt and *Dj-1* knock out astrocytes ($p < 0.05$), whether this was an effect of the endotoxins in the sample (> 1 pg/ml) or from the β -syn protein itself could not be differentiated. However, 0.5-1.0 ng/ml LPS have been shown to be needed for induction of toxic responses (Gao et al., 2003, Qin et al., 2004).

3 Results

A



B

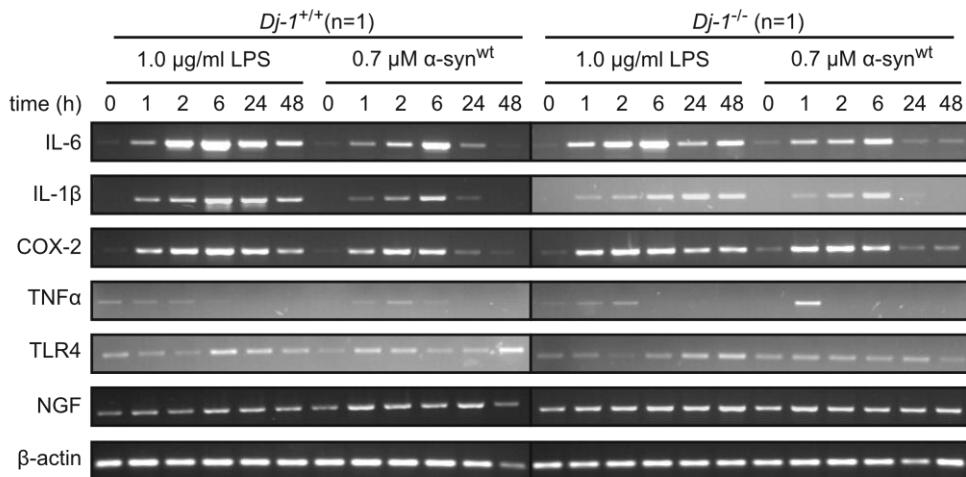


Figure 3.12 Treatment with recombinant α -syn induces expression of COX-2, IL-1 β and IL-6 in primary astrocytes from littermate *Dj-1^{+/+}* and *Dj-1^{-/-}* mice. **A** Primary astrocytes were treated with indicated concentrations of LPS, recombinant α -syn^{wt} or β -syn for 48 h. Expression of mRNA for IL-6, IL-1 β , COX-2, TNF α , TLR4 and NGF was examined in total RNA lysates from the cells by semi-quantitative PCR. Expression of β -actin was used as loading control. Images in the right upper panel are representative. The signals were quantified and normalized to the relative β -actin signal. Error bars indicate StDev. * p <0.05, ** p <0.01. *** p <0.001 (Student's t-test, compared untreated control (\emptyset)). Treatment of the astrocytes with synuclein increased IL-6, IL-1 β and COX-2 mRNA levels in the cells, whereas significant changes in NGF, TLR4 and TNF α levels could not be detected. **B** Primary astrocytes were treated with 1.0 μ g/ml LPS (positive control) or 0.7 μ M recombinant α -syn^{wt} for indicated times. Expression of mRNA was assessed as in A. The induction of IL-6, IL-1 β and COX-2 mRNA expression in astrocytes by treatment with α -syn or LPS increased to a maximum at about six hours.

Next a time course of cytokine mRNA induction in *Dj-1^{-/-}* and *Dj-1^{+/+}* astrocytes after treatment with 1.0 μ g/ml LPS or 0.7 μ M α -syn^{wt} was performed (Fig 3.12 B) This one time experiment could confirm the up-regulation of IL-6, IL-1 β and COX-2 by both the positive control LPS as well as by α -syn^{wt}.

In short, treatment with recombinant α -syn^{wt} induced the mRNA expression of the cytokines IL-6, IL-1 β and COX-2 in primary astrocytes.

3.2.3 Treatment with recombinant α -syn up-regulates the iNOS expression in astrocytes

Treatment with LPS up-regulates the expression of iNOS in astrocytes (Bhat et al., 1998). Therefore, the induction of the expression of iNOS was investigated. Primary astrocytes were treated with 0.1 or 1.0 μ g/ml of the positive control LPS or 0 to 0.7 μ M of recombinant α -syn^{wt} or β -syn. The induction of iNOS expression was examined on mRNA level. Treatment with LPS induced iNOS expression, as expected, in both wt and *Dj-1* knock out astrocytes (Fig 3.13). Treatment with 0.7 μ M recombinant α -syn^{wt} or β -syn induced significant increase in iNOS mRNA levels compared to untreated samples (p <0.05 Student's T-test, Fig 3.13 A, B). Furthermore, the induction of iNOS mRNA expression by LPS and α -syn^{wt} could be confirmed in a one-time time course experiment (Fig 3.13 C). Unfortunately the performance of the iNOS antibody was variable and often it did not show any signal, thus the induction of iNOS on protein levels is not shown. However, one can state that at least on mRNA level treatment with α -syn induced a concentration dependent up-regulation of iNOS expression in primary astrocytes.

3 Results

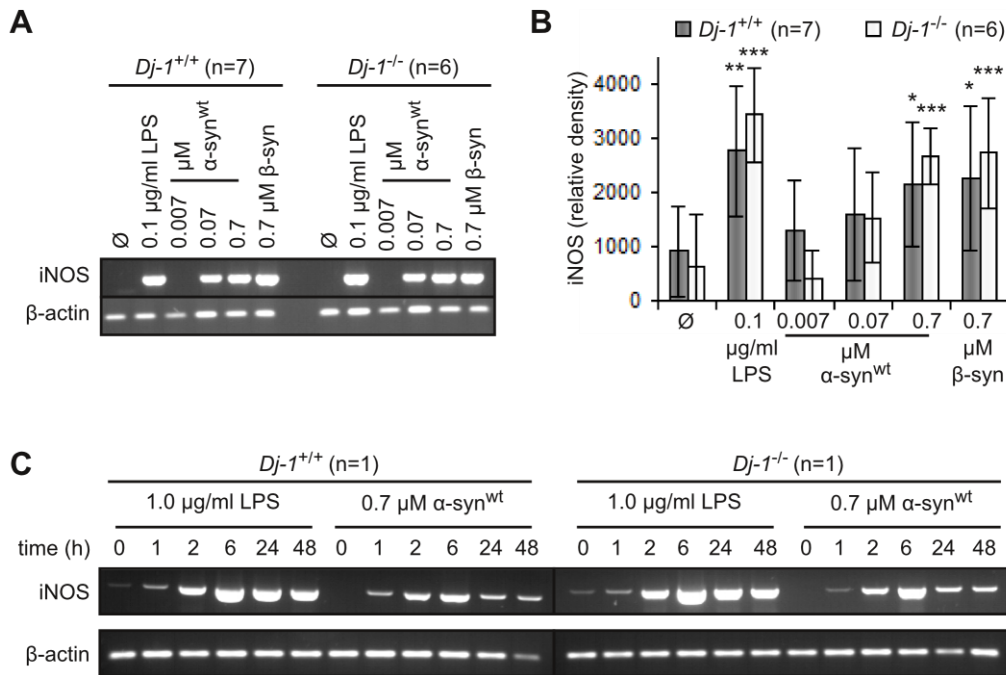


Figure 3.13 Treatment with α -syn induces iNOS mRNA expression in primary astrocytes from littermate *Dj-1^{-/-}* and *Dj-1^{+/+}* mice. A The astrocytes were treated with indicated concentrations of LPS, α -syn^{wt} and β -syn for 48 h. Total RNA was isolated and semi-quantitative PCR using primers specific for iNOS and β -actin was performed. Images are representative. **B** The signals in A were quantified and normalized to β -actin signal. Error bars indicate StDev, * $p < 0.05$, ** $p < 0.01$, *** $p < 0.001$ (Student's t-test compared to untreated control (\emptyset)). Cells that had been treated with synuclein showed induced iNOS mRNA expression in both *Dj-1^{-/-}* and *Dj-1^{+/+}* astrocytes. **C** The astrocytes were treated with 1.0 μ g/ml LPS or 0.7 μ M α -syn^{wt} for indicated times. Semi-quantitative PCR was performed with total RNA lysates. This one time experiment showed that the expression of iNOS protein and mRNA reached its highest levels after 6 h of continuous treatment with α -syn. β -actin serves as control for use of equal cDNA amounts.

3.2.4 Extracellular recombinant α -syn induces a possibly TLR4 dependent astroglial NO production

Since iNOS is directly producing NO, the NO released by the astrocytes into the surrounding media was measured after treatment with LPS or recombinant α -syn^{wt} (Fig 3.14 A). In correlation with the induction of iNOS expression, treatment with LPS induced NO release into the media. Additionally, an α -syn concentration dependent increase in NO release was detected, showing a significant increase already after treatment with only 0.07 μ M α -syn ($p < 0.05$, Fig 3.14 A).

LPS is activating the TLR4 and to some extent TLR2 (Netea et al., 2002). To see if α -syn is activating the TLR4 pathway as well, NO release after inhibition of TLR4 was measured. For this viper, a TLR4 specific peptide inhibitor that arrives from the viral vaccinia protein A46 was used (Lysakova-Devine et al., 2010). Viper or a control peptide was added to *Dj-1^{+/+}* and *Dj-1^{-/-}* astrocytes two hours prior to the addition of LPS or recombinant α -syn^{wt}. The NO release to the media was measured 48 h after LPS and α -syn^{wt} administration (Fig 3.14 B). After TLR4 inhibition the induction of NO

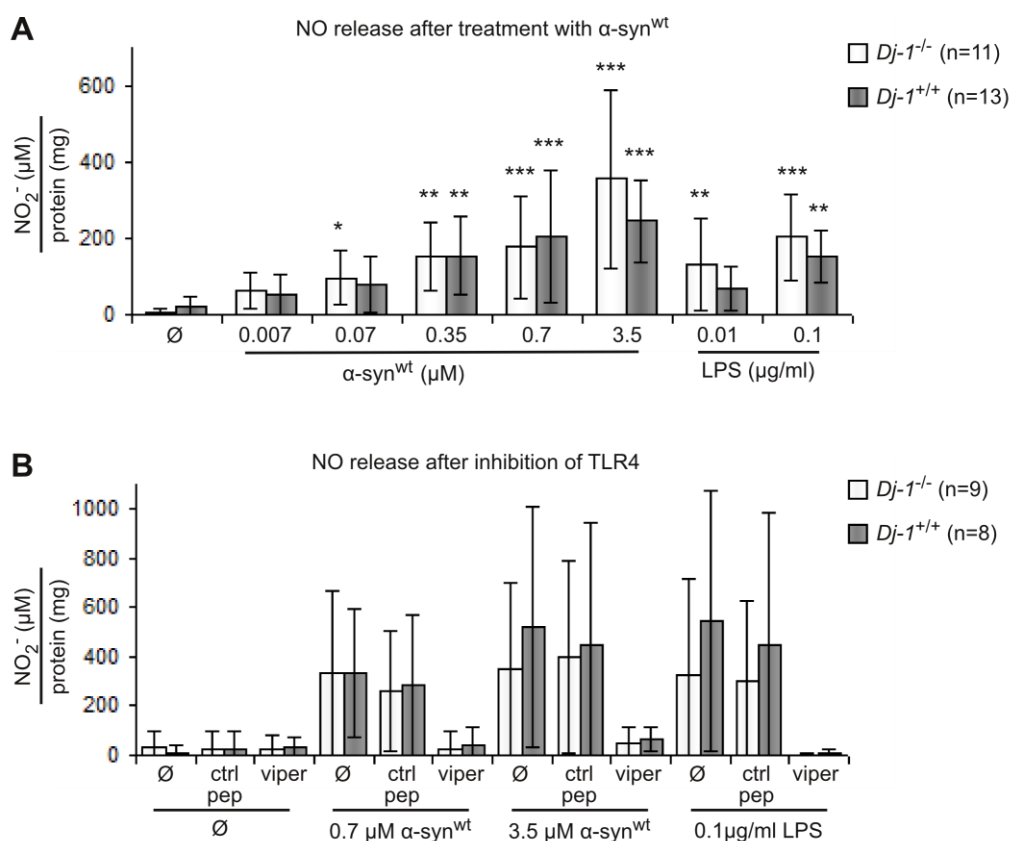


Figure 3.14 Treatment with α -syn induces NO production and release in astrocytes, the induction can be reduced with a TLR4 specific inhibitor. **A** Primary astrocytes from littermate *Dj-1*^{+/+} and *Dj-1*^{-/-} mice were treated for 48 h with indicated concentrations of α -syn^{wt} or LPS. The NO released into the media was measured using Griess reagent. The amount of released NO was normalized to total protein amount in the sample well. Error bars are StDev. * $p < 0.05$, ** $p < 0.01$, *** $p < 0.001$ (Student's t-test compared to untreated control (\emptyset)). As the positive control LPS, the recombinant α -syn induced a concentration dependent NO production in both *Dj-1*^{-/-} and *Dj-1*^{+/+} astrocytes. **B**. Primary astrocytes from littermate *Dj-1*^{+/+} and *Dj-1*^{-/-} mice were treated with 5 μ M of control peptide (ctrl pep) or TLR4 inhibitor peptide (viper) two hours prior to the addition of recombinant α -syn^{wt} or LPS. 48 h later NO released into the media was measured using Griess reagent. Inhibition of TLR4 decreased the α -syn and LPS induced NO production.

release by LPS or α -syn treatment was lower than in samples where the control peptide or no inhibitor was used. This indicates that α -syn can activate the TLR4 receptor.

3.2.5 Induction of cytokine and iNOS expression by α -syn treatment is decreased in *Tlr4*^{-/-} astrocytes

Inhibition of TLR4 with viper decreased the induction of NO release after α -syn treatment. Next the induction of cytokine and iNOS expression by extracellular recombinant synuclein in astrocytes from littermate *Tlr4*^{+/+} and *Tlr4*^{-/-} mice was investigated (Fig 3.15). The mRNA levels of TNF α , COX-2, IL-6, IL-1 β , NGF and iNOS were measured with semi-quantitative PCR (Fig 3.15 A). The induction of COX-2, IL-6,

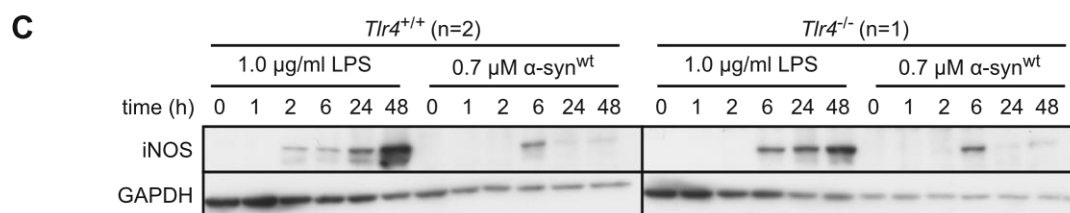
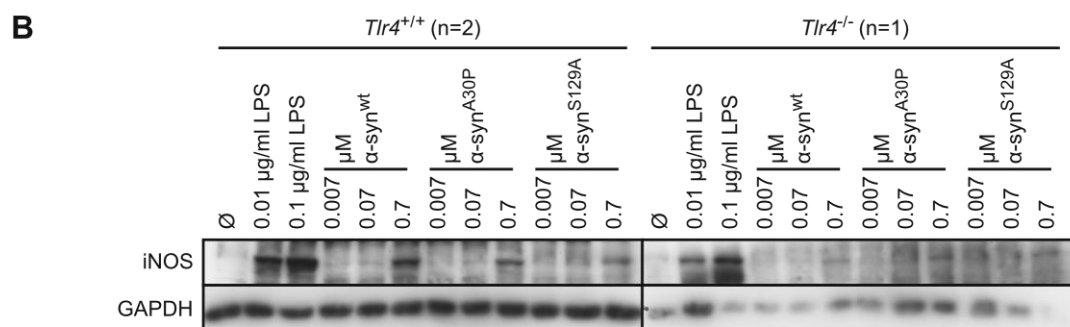
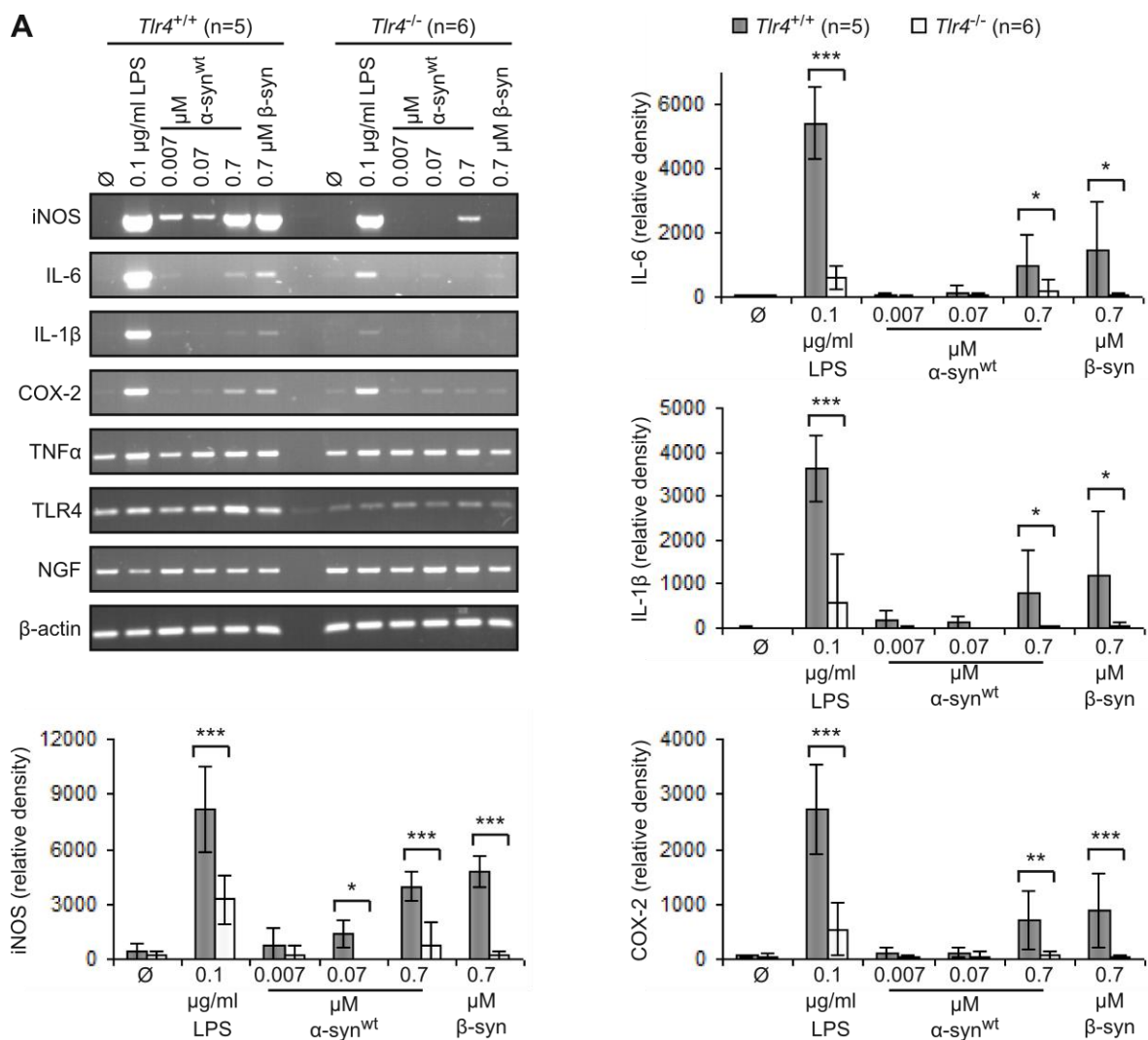
3 Results

IL-1 β and iNOS mRNA expression by α -syn or β -syn treatment was much lower in *Tlr4*^{-/-} than in *Tlr4*^{+/+} astrocytes. As seen above in *Dj-1*^{-/-} and *Dj-1*^{+/+} astrocytes the NGF, TNF α and TLR4 mRNA levels did not significantly change after α -syn treatment. The weak TLR4 signal in *Tlr4*^{-/-} astrocytes (Fig 3.15 A) was seen with astrocytes from every *Tlr4*^{-/-} mouse and with three different pairs of primers. All of these primers bind very early in the 5'-end of the mRNA before the gene disruption insert. This part of the gene may still be transcribed to some extent. The signal was however significantly lower in *Tlr4*^{-/-} than in *Tlr4*^{+/+} astrocytes. Nevertheless, these results indicate that α -syn induce an increase in cytokine expression via the TLR4 signaling pathway.

On protein level, a weaker iNOS signal could be detected in *Tlr4*^{-/-} than in *Tlr4*^{+/+} astrocytes that had been treated with 0.7 μ M α -syn^{wt} or mutants (Fig 3.15 B). However, in a second experiment, where the induction was investigated in a treatment time dependent manner, there was no obvious difference (Fig 3.15 C). Before making any conclusion these experiments need to be repeated because of the biological variance between the primary astrocytic cultures and high variance in the performance of the iNOS antibody (Fig 3.15 B, C).

3.2.6 Induction of p38 and JNK phosphorylation by α -syn treatment is decreased in *Tlr4*^{-/-} astrocytes

The activation of the TLR4 receptor signaling pathway leads to phosphorylation of the MAPK JNK and p38 (Fig 1.2) (Sweet and Hume, 1996). To investigate if extracellular α -syn activates this down stream pathway wt and littermate *Tlr4*^{-/-} astrocytes were treated with LPS and recombinant α -syn for different times (Fig 3.16 A). Alternatively the astrocytes were treated with LPS and recombinant α -syn for one hour and followed by a recovery phase in media that lacked LPS and α -syn (Fig 3.16 B). The phosphorylation of JNK and p38 was investigated by immunoblotting with antibodies recognizing the phosphorylated state of the proteins. Treatment with LPS increased phosphorylation of both JNK and p38 within one hour both in *Tlr4*^{+/+} and *Tlr4*^{-/-} astrocytes (Fig 3.16 A, B). The phosphorylation state of JNK and p38 were still increased after 48 h of LPS treatment. Already one hour treatment with recombinant α -syn increased the phosphorylation of both p38 and JNK in *Tlr4*^{+/+} astrocytes. The induction of phosphorylation of JNK was fast and returned within 24 h to almost basal levels in both cells which had been treated continuously with α -syn as well as in the cells where α -syn had been removed after one hour (Fig 3.16 A, B). The p38 phospho-



3 Results

Figure 3.15 Induction of iNOS and cytokine expression after treatment with recombinant α -syn is greatly reduced in *Tlr4*^{-/-} primary astrocytes. **A.** Primary astrocytes from littermate *Tlr4*^{+/+} and *Tlr4*^{-/-} mice were treated with indicated concentrations of LPS (positive control), recombinant α -syn^{wt} or β -syn for 72 h. Total RNA was isolated from the cells and semi-quantitative PCR was performed with primers specific for iNOS, IL-6, IL-1 β , COX-2, TNF α , TLR4 and NGF. Expression of β -actin mRNA was used as loading control. Representative images are shown (upper left panel). The signals were quantified and normalized to the relative β -actin signal. Error bars indicate StDev. *p<0.05, **p<0.01. ***p<0.001 (Student's t-test compared between *Tlr4*^{+/+} and *Tlr4*^{-/-} astrocytes). Lower mRNA levels of iNOS, IL-6, IL-1 β and COX-2 was detected after treatment with α -syn and LPS in *Tlr4*^{-/-} compared to *Tlr4*^{+/+} astrocytes. \emptyset – untreated control **B** Primary astrocytes were treated with recombinant α -syn^{wt}, α -syn^{A30P}, α -syn^{S129A}, β -syn or LPS (positive control) for 24 h. iNOS expression in protein lysates was examined by immunoblotting. GAPDH serves as control for equal protein loading. Treatment with LPS and synuclein mutants increased iNOS protein levels in *Tlr4*^{+/+}, but not to the same extent in *Tlr4*^{-/-} astrocytes. **C.** Primary astrocytes were treated with 0.7 μ M recombinant α -syn^{wt} and 1.0 μ g/ml of the positive control LPS for indicated times. iNOS levels were detected by immunoblotting. GAPDH serves as control for equal protein loading. An iNOS protein signal was detected both in *Tlr4*^{+/+} and *Tlr4*^{-/-} astrocytes in samples that had been treated for 6 h with α -syn.

rylation, on the other hand, did not return as fast to basal levels. The signal was elevated even after 48 h of continuous α -syn treatment and after 24 h of recovery after one hour α -syn treatment. Interestingly, the induction of the phosphorylation of p38 and JNK by α -syn was very weak in *Tlr4*^{-/-} astrocytes, which indicates that the extracellular α -syn may activate the TLR4 signaling pathway (Fig 3.16 A, B).

3.2.7 NF- κ B nuclear translocation after treatment with α -syn is inhibited in *Tlr4*^{-/-} astrocytes

TLR4 activation also leads to phosphorylation and degradation of I κ B, which is masking the nuclear localization sequence of NF- κ B. The degradation of I κ B makes it possible for the activated NF- κ B to translocate to the nucleus (Fig 1.2). To investigate the possible activation of NF- κ B by extracellular α -syn *Tlr4*^{+/+} and *Tlr4*^{-/-} astrocytes were treated for six hours with different concentrations of LPS or recombinant α -syn^{wt} (Fig 3.17). The nuclear translocation of NF- κ B was detected by immunofluorescence staining with an NF- κ B/p65 specific antibody (Fig 3.17 A). As expected, treatment with LPS induced NF- κ B translocation to the nucleus in *Tlr4*^{+/+} and to a lesser extent in *Tlr4*^{-/-} astrocytes. Notably, also α -syn^{wt} treatment induced NF- κ B translocation in *Tlr4*^{+/+} astrocytes and close to no cells showed NF- κ B positive nuclei in *Tlr4*^{-/-} astrocytes after treatment with α -syn (Fig 3.17 B).

In conclusion the induction of cytokine and iNOS expression, JNK and p38 phosphorylation and NF- κ B nuclear translocation after treatment with recombinant extracellular α -syn seem to be TLR4 receptor dependent.

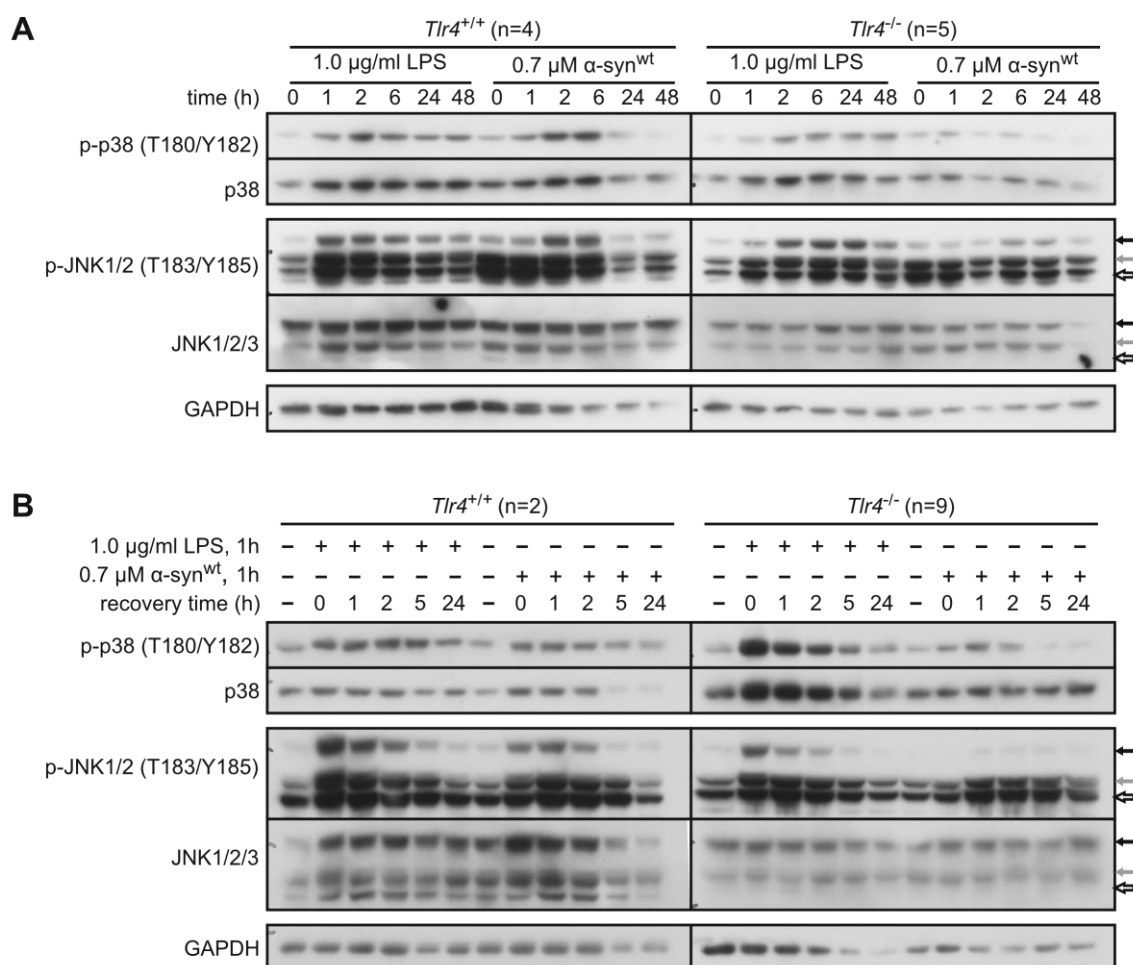


Figure 3.16 Treatment with recombinant α-syn induces p38 and JNK phosphorylation to a lesser extent in *Tlr4^{-/-}* than in *Tlr4^{+/+}* primary astrocytes. **A** Primary astrocytes from littermate *Tlr4^{+/+}* and *Tlr4^{-/-}* mice were treated with LPS (positive control) and recombinant α-syn^{wt} continuously for indicated times. **B** Primary astrocytes from littermate *Tlr4^{+/+}* and *Tlr4^{-/-}* mice were treated one hour with LPS or recombinant α-syn^{wt}, the medium was replaced with fresh growth media and the cells were recovered for indicated times. **A, B** Immediately after lysis the cell lysates were immunoblotted for phosphorylated p38 and JNK. Total p38 and JNK signals and GAPDH serve as controls for equal protein loading. Arrows indicate the corresponding heights in the phosphorylated JNK and total JNK blots. Black arrow is at about 50 kDa, probably corresponds to JNK2α2 and β2 (48 kDa). Grey arrow between 37 and 50 kDa corresponds to JNK1, JNK2 α1 and β1 (44 kDa). Open arrow, may be an unspecific signal from phosphorylated ERK2 (41kDa). Representative images are shown. Both experiments showed TLR4 dependent increase in phosphorylation of p38 and JNK after α-syn treatment. LPS, which also can activate TLR2, showed an induction of phosphorylation of p38 and JNK in both *Tlr4^{+/+}* and *Tlr4^{-/-}* astrocytes.

3.2.8 The recombinant α-syn is taken up by the astrocytes in a TLR4 independent manner and is not phosphorylated in the astrocytes

In recent years many independent groups have shown that α-syn can be transferred between neurons, and is also taken up by microglial and astroglial cells (Steiner et al., 2011). Therefore, the uptake of extracellular α-syn variants into wt, *Tlr4^{-/-}* and *Dj-1^{-/-}* primary mouse astrocytes was investigated. Astrocytes were treated with recombinant

3 Results

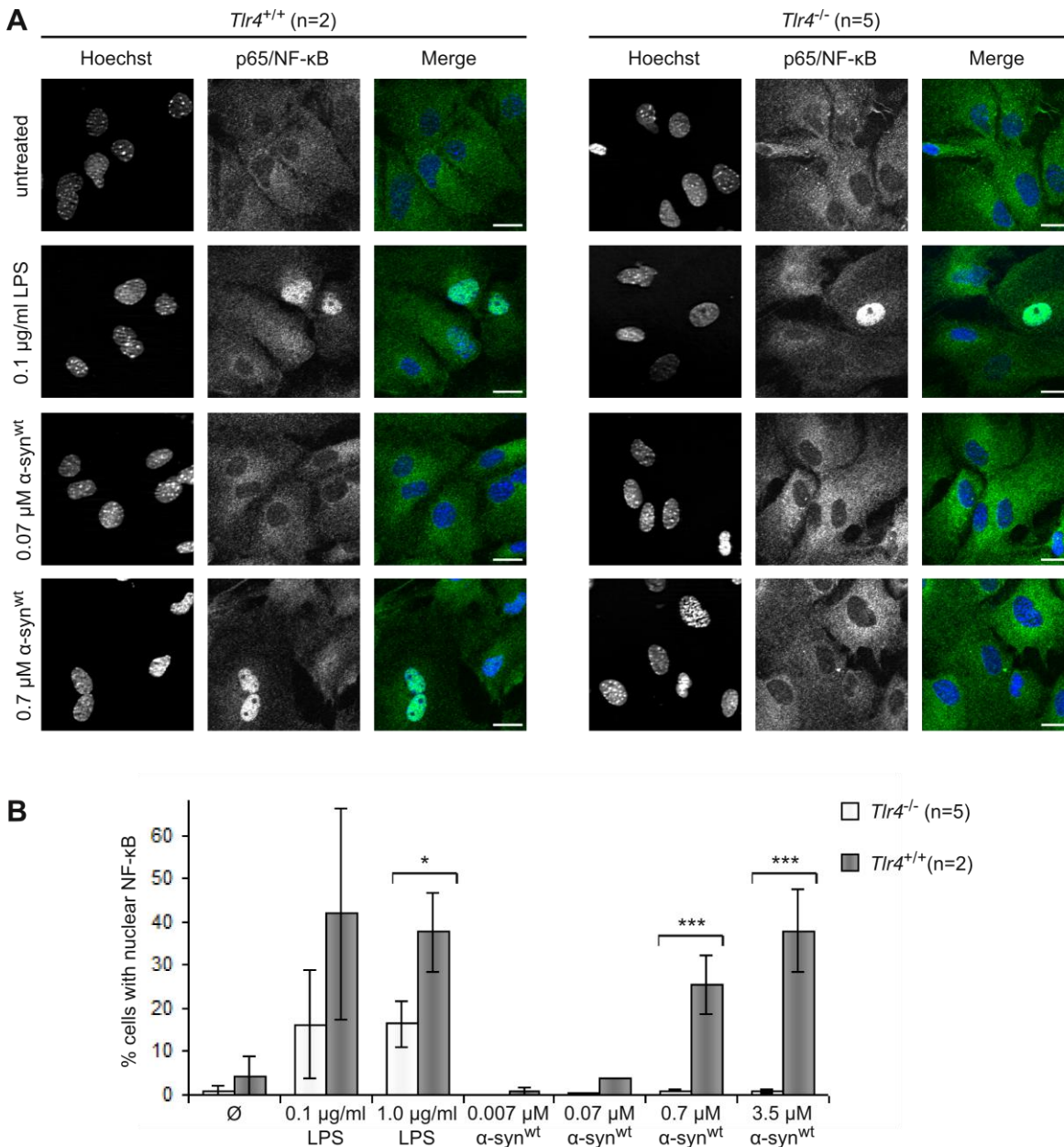


Figure 3.17 Treatment with recombinant α -syn induces NF- κ B nuclear translocation in *Tlr4*^{+/+}, but not in *Tlr4*^{-/-} astrocytes. **A,B Primary astrocytes from littermate *Tlr4*^{+/+} and *Tlr4*^{-/-} mice were treated with indicated concentrations of LPS (positive control) or recombinant α -syn^{wt} for 6 h. The cells were fixed and immunostained for p65/NF- κ B (green). Nuclei were counter stained with Hoechst 33342 (blue). **A** Representative images are shown. Scale bar is 20 μ M. **B**. The nuclear localization of p65/NF- κ B was quantified; 200-400 cells per sample were analyzed. Error bars are StDev, * p <0.05, *** p <0.001 (Student's t-test compared between *Tlr4*^{+/+} and *Tlr4*^{-/-} astrocytes). After treatment with recombinant α -syn more *Tlr4*^{+/+} than *Tlr4*^{-/-} astrocytes had p65/NF- κ B positive nuclei.**

human synucleins for 48 h. Total protein lysates were immunoblotted using an antibody body that is specific for human α -syn, thus detected α -syn signals originated from the applied extracellular recombinant protein (Fig 3.18). Samples that had been treated with 0.07 μ M of α -syn^{wt}, α -syn^{A30P} and α -syn^{S129A} showed a weak monomeric α -syn signal. Treatment with 0.7 or 3.5 μ M α -syn, showed strong signals corresponding

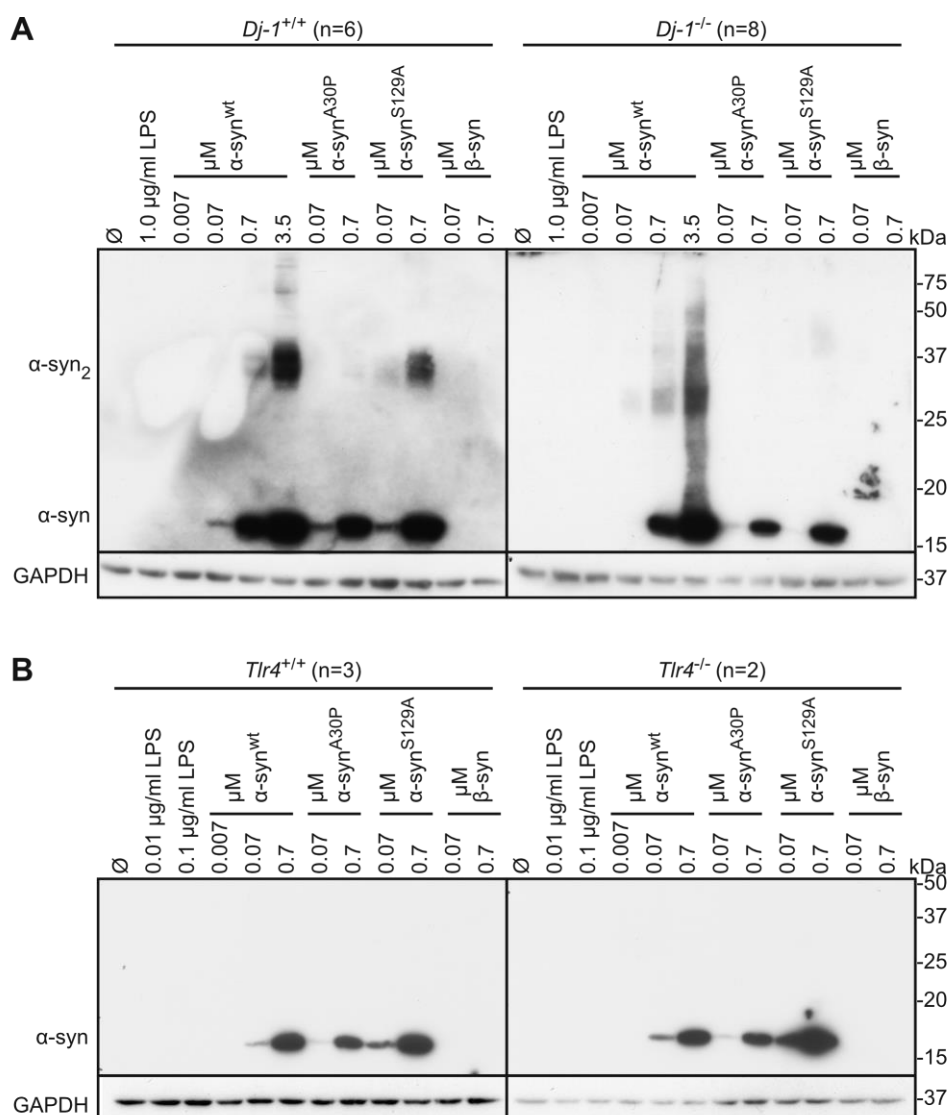


Figure 3.18 Extracellular α -syn is internalized by primary astrocytes in a TLR4 independent manner. A,B Primary astrocytes from littermate *Dj-1^{-/-}* and wt (**A**) or littermate *Tlr4^{-/-}* and wt (**B**) mice were continuously treated for 48 h with indicated concentrations of recombinant human α -syn^{wt}, α -syn^{A30P}, α -syn^{A129A}, β -syn or LPS or left untreated (\emptyset). The cells were washed twice with PBS prior to lysis. The protein lysates were immunoblotted for human α -syn. α -syn₂ – dimeric α -syn. GAPDH serves as control for equal protein loading. Representative images are shown. α -syn was found in all lysates from cells that had been treated with α -syn, indicating that DJ-1 and TLR4 are not influencing the uptake.

to the monomeric, dimeric and higher molecular weight α -syn (Fig 3.18). The α -syn was internalized into wt, *Tlr4^{-/-}* and *Dj-1^{-/-}* astrocytes to a similar extent.

In familial and sporadic PD α -syn is extensively phosphorylated at S129, this phosphorylated α -syn is also found in Lewy bodies (Fujiwara et al., 2002). To see if the internalized α -syn is phosphorylated by the astrocytes, primary astrocytes were treated with recombinant α -syn for 48 h. The protein lysates were immunoblotted using an antibody that is specific for S129 phosphorylated α -syn (Fig 3.19). As seen above, uptaken α -syn could be detected. In addition, a strong signal of phosphorylated α -syn

3 Results

was detected in the positive control, which was a mouse brain lysate from an aged Thy1[A30P]h α -syn mouse, which harbors excessive amounts of phosphorylated α -syn. However, no signal of phosphorylated, internalized α -syn could be detected by the antibody.

In conclusion, primary astrocytes take up recombinant α -syn from the surrounding media in a TLR4 receptor independent manner, but the internalized α -syn is not phosphorylated in the astrocyte.

3.2.9 The internalized extracellular α -syn is possibly degraded via the proteasome in astrocytes

Next, it was examined how fast the uptake of extracellular α -syn under these experimental conditions occurs. Therefore, primary astrocytes were treated continuously with recombinant α -syn^{wt} for different time points and the uptaken α -syn was examined by immunoblotting with the human specific α -syn antibody (Fig 3.20 A). Already after 1 h treatment a strong signal from internalized α -syn could be detected in

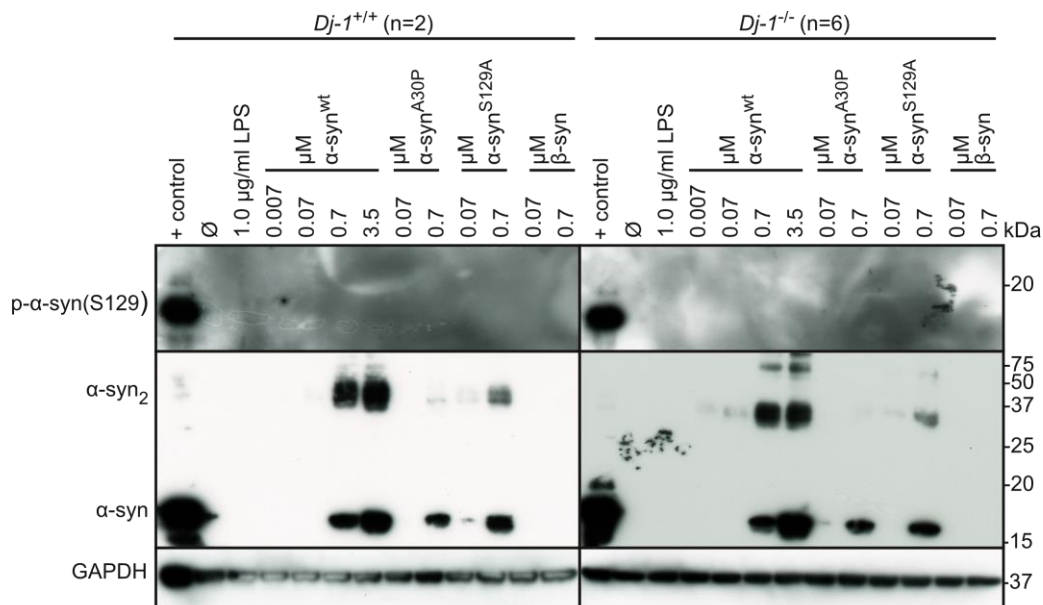


Figure 3.19 The internalized recombinant α -syn is not phosphorylated in the astrocytes. Primary *Dj-1^{-/-}* and wt astrocytes were continuously treated for 48 h with indicated concentrations of recombinant α -syn^{wt}, α -syn^{A30P}, α -syn^{S129A}, β -syn, LPS or left untreated. The cells were washed twice prior to lysis. The protein lysates were immunoblotted for phospho-S129 α -syn and total human α -syn. GAPDH serves as a control for equal protein loading. As a positive control for the phospho- α -syn antibody brain protein lysate from an old Thy1[A30P]h α -syn mouse, which has high amounts of phosphorylated α -syn, was used. α -syn₂ - α -syn dimer. No phosphorylation of the internalized recombinant α -syn could be detected. Representative images are shown.

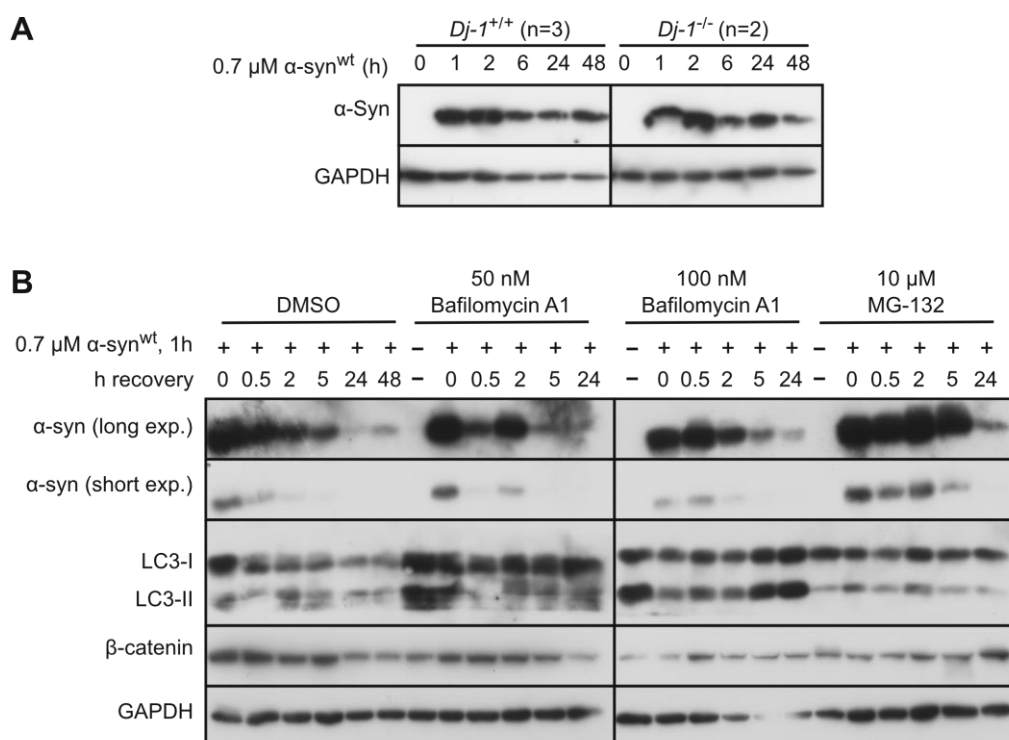


Figure 3.20 The amount of $\alpha\text{-syn}$ taken up by the astrocytes decrease with time, possibly via proteasomal degradation. **A** Primary wt astrocytes were treated continuously with 0.7 μM recombinant human $\alpha\text{-syn}$ for indicated times. Cells were washed twice prior to lysis. The protein lysates were examined by immunoblotting for $\alpha\text{-syn}$. Equal protein loading was shown with GAPDH. The images are representative. Already after one hour treatment, $\alpha\text{-syn}$ was detected in the astrocyte lysates and the $\alpha\text{-syn}$ signal decreased with time. **B** Primary wt astrocytes were treated with 50 or 100 nM of the lysosomal inhibitor Bafilomycin A1, 10 μM of the proteasomal inhibitor MG-132 or DMSO. One hour later 0.7 μM recombinant $\alpha\text{-syn}^{\text{wt}}$ was added and after a further hour the media was replaced with fresh media containing the inhibitors, but no $\alpha\text{-syn}$. The cells were recovered for indicated times after which the cells were washed twice and lysed. The protein lysates were immunoblotted with antibodies specific for human $\alpha\text{-syn}$, LC3 and $\beta\text{-catenin}$. GAPDH serves as a control for equal protein loading. Representative images are shown. MG-132 treated samples showed a slower decrease in internalized $\alpha\text{-syn}$ signal within the investigated time frame in comparison to DMSO and Bafilomycin A1 treated samples.

the astrocytes lysates. Interestingly, the signal strength seemed to decrease with the time of treatment. Therefore, the $\alpha\text{-syn}$ degradation in the astrocytes was investigated more closely. The proteolytic activity of the 26S proteasome was inhibited with MG-132. In addition, the lysosomal function was inhibited with bafilomycin A1, which specifically inhibits vacuolar type H(+)-ATPase and thereby the acidification and the protein degradation in the lysosomes (Bowman et al., 1988, Yoshimori et al., 1991). Primary wt astrocytes were treated with DMSO or inhibitors for one hour prior to the addition of 0.7 μM $\alpha\text{-syn}^{\text{wt}}$. After one hour $\alpha\text{-syn}$ treatment medium was exchanged to fresh media containing DMSO or inhibitors, but no $\alpha\text{-syn}$, and the cells were recovered for up to 24 h. The internalized $\alpha\text{-syn}$ was examined with a human $\alpha\text{-syn}$ specific antibody (Fig 3.20 B). As a control for lysosomal inhibition the increase in cleaved LC3

3 Results

was used and as a control for proteasomal inhibition increase in β -catenin was used. However, the increase in β -catenin was unfortunately less transparent. Nonetheless, in DMSO and Bafilomycin A1 treated samples the α -syn signal declined fast after the removal of α -syn. The signal was clearly weaker already after only 30 min recovery time. Interestingly, the reduction of the α -syn signal was not as fast in MG-132 treated samples. After 5 h recovery the α -syn signal was still detectable, but after 24 h the signal was gone. These results suggest that the α -syn taken up by the astrocytes is degraded fast and it possibly degraded via the proteasome.

3.3 Onset of motorical symptoms in *Dj-1^{-/-}//Thy1h[A30P]SNCA* mice

The Thy1h[A30P]SNCA transgenic mouse line show pathological α -syn in the mid brain, brainstem and spinal cord (Kahle et al., 2000, Kahle et al., 2001, Neumann et al., 2002). This leads to the development of motorical impairments at the age of 16 months (Freichel et al., 2007). The motorical impairments can be detected by a decrease in the muscle tonus of the tail and hind legs and by a reduced coordination. When put on the grid of the cage the affected mice tend to miss the catching of the grid and have problems to rescue the movement. Within weeks after the first symptoms can be detected the mice start to fall to the side and eventually they become immobile. *Dj-1* knock out mice, on the other hand, show no major pathological and motorical abnormalities, but are more sensitive to some stress conditions, for example treatment with the toxin MPTP (Chen et al., 2005, Kim et al., 2005b, Andres-Mateos et al., 2007, Yamaguchi and Shen, 2007).

To investigate if lack of DJ-1 can accelerate the onset of the motorical symptoms in the Thy1h[A30P]hSNCA transgenic mice, *Dj-1^{-/-}* mice (Pham et al., 2010) were crossbred with Thy1h[A30P]hSNCA mice. Between the age of 12 and 24 months the mice were examined once a week by lifting them by the tail to the grid and observing their proficiency to walk on the grid. The age when the first deficits appeared were marked as age of onset (Fig 3.21). Wt mice and *Dj-1^{-/-}* mice did not show any motorical failures before the age of 24 months in this test (not shown). As expected, mice that were homozygous for the human [A30P]SNCA gene (*SNCA^{+/+}*) developed motorical impairments. The mean age of onset for female *Dj-1^{-/-}//SNCA^{+/+}* double transgenic mice was 16.3 months (\pm 2.1, StDev), the youngest individual was 11.0 and the oldest

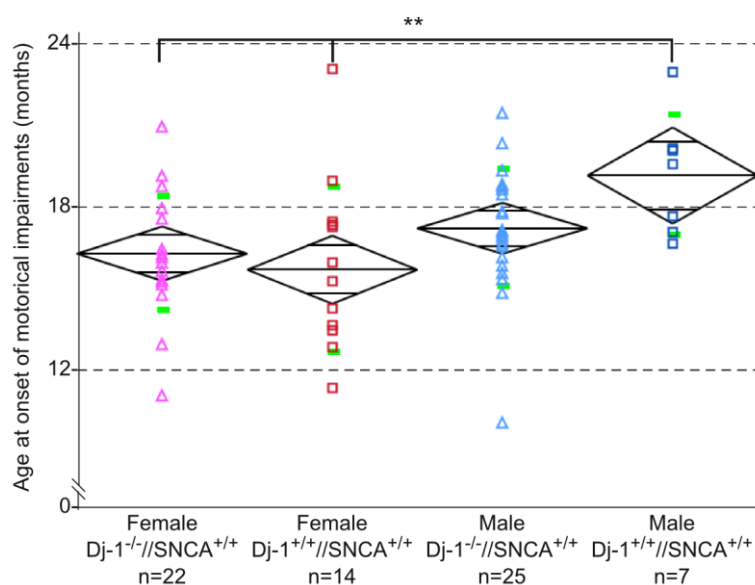


Figure 3.21 Knock out of *Dj-1* does not accelerate the onset of motorical symptoms in Thy1h[A30P]SNCA transgenic mice. Thy1h[A30P]SNCA were crossbred with *Dj-1*^{-/-} mice. Homozygous mice were inspected once a week for decrease in muscle tail tonus and ability to walk on a grid. The age when the first motorical impairments was detected was noted. *Dj-1*^{-/-}//SNCA^{+/+} double transgenic mice did not show earlier age of onset than their gender matched *Dj-1*^{+/+}//SNCA^{+/+} mice. However, the male mice showed later onset than the females mice. Black diamonds show the means of Anova. Green lines show the StDev. **p<0.01 (One-way Anova, male *Dj-1*^{+/+}//SNCA^{+/+} mice compared to female mice).

19.2 months. For female *Dj-1*^{+/+}//SNCA^{+/+} mice the mean age was 15.7 months (± 3.0), the youngest was 11.4 and the oldest was 23.1 months old. Male *Dj-1*^{-/-}//SNCA^{+/+} mice had a tendency to show the first motorical impairments at a higher age than the females (17.3 \pm 2.1 months, youngest 10.1 and oldest 21.5 months). The male *Dj-1*^{+/+}//SNCA^{+/+} mice had even a significantly higher age (21.0 \pm 2.2 months, youngest 16.7 and oldest 23 months, p< 0.01, Student's t-test) than the females at the onset of motorical failure. In conclusion, knock out of *Dj-1* did not change the age of onset of motorical symptoms.

4 Discussion

4.1 P158 and A107 are important for the stability of the DJ-1 dimer

DJ-1 protects cells against oxidative stress and it is upregulated in many forms of cancer. Moreover, mutations that lead to loss of DJ-1 function are associated with PD. Here the effect of three mutants found in three patients with early onset PD was investigated.

4.1.1 A179 to T mutation does not affect the stability and binding behavior of DJ-1

One Dutch patient with early onset PD was identified to be a heterozygous carrier of the A179 to T point mutation (Macedo et al., 2009). This patient had an affected mother. However, DJ-1^{A179T} mutant seem to have similar dimerization ability, stability and binding behavior towards ASK1 as the wt protein (Fig 3.1-3.5, 3.7). A179 is not a conserved residue among DJ-1 homologs (Fig 1.5). It is positioned on the surface of the protein in the C-terminal H- α -helix (Fig 1.6 C). A change of alanine to threonine is not predicted to introduce significant sterical disturbance to the α -helix, but it introduces a potential phosphorylation site at the surface of the protein, which phosphorylation may influence the protein in unknown ways.

The very C-terminal H- α -helix is not present in the other proteases of the Pfp1 family, with which DJ-1 show structural similarity. This α -helix is shown to block the entrance to the putative active site of DJ-1 (Honbou et al., 2003, Tao and Tong, 2003, Wilson et al., 2003). Moreover, the putative catalytical H/C/E triade of DJ-1 is distorted in comparison to the other proteases of the family. Moreover, protease assays made with recombinant full length DJ-1 showed no protease activity (Lee et al., 2003, Wilson et al., 2003, Shendelman et al., 2004). Contradictory, Chen and colleagues suggested that the activation of a protease activity of DJ-1 involves a cleavage of the 15 most C-terminal amino acids, which would remove the whole H- α -helix (Chen et al., 2010). They could show that cells that overexpressed a C-terminal truncated DJ-1 mutant exhibit less cell death in response to rotenone treatment than cells overexpressing full length DJ-1. This suggests that cleavage of the C-terminus from DJ-1 is cytoprotective. They could also detect a cleaved DJ-1 product corresponding to the size of the C-terminal truncated mutant after treatment with low concentrations of H₂O₂ (100 μ M) or rotenone (10 nM) or 1-methyl-4-phenylpyridinium (5 μ M). The signal strength of the cleaved product was about 2 to 5 % of the strength of the full length protein and it

could not be detected with an antibody that recognizes the C-terminus of DJ-1 (Chen et al., 2010). The cleavage site they propose is four amino acids away from A179. Considering that one turn in an α -helix is 3.6 amino acids long means that A179 is placed very close to this cleavage site. Exchange of the hydrophobic alanine to the polar threonine may disturb the proteolytic cleavage and thereby prevent the activation of the protease activity. In contrast to the antibodies used by Chen et al., the antibodies used in this work could not detect a cleaved DJ-1 product after treatment with H_2O_2 (not shown). So we could not confirm this hypothesis. Moreover, recently it was shown that removal of the nine last C-terminal amino acids was enough to increase the proteolytic activity of DJ-1 (Mitsugi et al., 2013). Thus, more work needs to be done in order to identify the possible dysfunction of the DJ-1^{A179T} mutant.

4.1.2 Deletion of P158 and mutation of A107 affect stability and dimerization ability of DJ-1

P158 is positioned in a highly conserved GPGT- β -turn motif adjacent to the C-terminal helix-kink-helix motif (Fig 1.5, 1.6 C). A β -turn involves four amino acids and is a 180 degree turn in a protein, most often connecting the ends of two adjacent segments in an anti-parallel β -sheet. The turn involving P158 connects a β -sheet with an α -helix. The proline in a β -turn is in its *cis*-conformation. It stabilizes the turn, since an opening of a covalent bond is needed to change the conformation. Deletion of the P158 from the turn changes the sequence from GPGT to RGGT, which would make the β -turn more flexible. This can have an effect on the positioning of the helix-kink-helix motif. Interestingly, it has been shown that removal of this C-terminal helix-kink-helix motif or removal of only the two residues that make up the kink between the helices, deteriorates the stability of the protein (Gorner et al., 2007). This suggests that the correct positioning of the C-terminal helix-kink-helix is essential for the stability of DJ-1. In accordance with this hypothesis, our data showed that the protein steady state level of DJ-1^{P158 Δ} was significantly decreased compared to the levels of DJ-1^{wt} and DJ-1^{A179T} (Fig 3.1) and the protein half-life time of the deletion mutant was a twelfth of the half-life time of the wt (Fig 3.3).

Also A107 is a highly conserved residue of DJ-1 (Fig 1.5). It is situated adjacent to C106 in the putative active site pocket (Fig 1.6 B). C106 is oxidized upon activation of DJ-1 and it has been shown to be essential for the activity of the protein (Canet-Aviles et al., 2004, Taira et al., 2004, Meulener et al., 2006, Waak et al., 2009a). C106 is in a strained backbone conformation in a “nucleophilic elbow” (Wilson et al., 2003).

4. Discussion

Replacement of alanine with proline does not change the hydrophobicity, however, because of its ring formation proline is a very inflexible residue. Thus it can introduce sterical restrictions, which can affect the general structure of the DJ-1 protein and/or affect the oxidation of the adjacent C106. In MEF cells the steady state protein levels of DJ-1^{A107P} were clearly reduced compared to the levels of DJ-1^{wt} (Fig 3.1). In HEK 293E cells, on the other hand, the protein levels of the mutant were not as much reduced. Thus it may be possible that the high levels of endogenous human DJ-1 that is present in HEK 293E cells are able to stabilize the mutant.

In solution DJ-1 is a homodimer and P158 lies in the dimerization interface (Honbou et al., 2003, Wilson et al., 2003). In addition, the helix-kink-helix motif is shown to be important for the dimerization (Gorner et al., 2007). We could show in a co-immunoprecipitation experiment that DJ-1^{P158Δ} is able to form dimers with DJ-1^{wt}, but we could not detect any DJ-1^{P158Δ} homodimerization (Fig 3.4). Interestingly, DJ-1^{A107P} behaved exactly the same; it co-immunoprecipitated with DJ-1^{wt}, but no DJ-1^{A107P} homodimerization was detected (Fig 3.4). One need to mention that the input signal of both mutants were essentially stronger when DJ-1^{wt} was co-over expressed. Thus it may be that the signal of homodimerized mutants was under the detection limit of the films, since less starting material was present for the immunoprecipitation. It is possible that the protein degradation system is impaired because of an overload caused by overexpressed stable DJ-1^{wt} protein and that this leads to the increased mutant protein levels. However, another possible explanation to the essentially higher DJ-1^{P158Δ} and DJ-1^{A107P} protein levels could be that overexpressed DJ-1^{wt} forms heterodimers with the mutants and thus stabilizes the mutants. Nevertheless, in case of the DJ-1^{A107P} this strengthens the observations, which were already seen in the steady state protein levels, that presence of DJ-1^{wt} may stabilize the DJ-1^{A107P} mutant (Fig 3.1).

4.1.3 DJ-1^{P158Δ} and DJ-1^{A107P} show an altered binding behavior towards ASK1

In presence of oxidative stress DJ-1 can regulate the activation of the ASK1 signalosome in at least two ways. First, DJ-1 can directly bind Daxx and retain it in the nucleus (Junn et al., 2005). Here DJ-1^{P158Δ} kept Daxx in the nucleus to the same degree as DJ-1^{wt}, however, five times more cDNA for transfection of DJ-1^{P158Δ} was used (Fig 3.7). Second DJ-1 is shown to directly bind ASK1 and inhibit the activation of the ASK1 signalosome (Gorner et al., 2007, Waak et al., 2009a, Mo et al., 2010). Previously our group has shown that the binding is covalent and that the N-terminal

domain of ASK1 and C106 of DJ-1 seem to be involved in the binding (Waak et al., 2009a). In this present work two binding assays were used, firstly co-immunoprecipitations and secondly size exclusion chromatography. Unexpectedly, DJ-1^{P158Δ} was immunoprecipitated with ASK1^{FL} regardless of the presence of oxidative stress (Fig 3.5). A similar binding behavior was previously seen with the DJ-1^{M26I} mutant (Waak et al., 2009a). Regarding the binding to the ASK1 truncated variants (ASK1^{ΔC} and ASK1^{CT}) the DJ-1^{P158Δ} mutant showed a slightly increased interaction when H₂O₂ was applied. This may suggest that DJ-1^{P158Δ} is partly active and may to some extent inhibit the activation of ASK1 signaling pathway.

DJ-1^{A107P} was also immunoprecipitated with ASK1^{FL} in absence of oxidative stress, but the interaction seemed to be stronger in presence of H₂O₂ (Fig 3.5). Moreover, the A107P mutant seemed to bind the truncated variants of ASK1 in an oxidative stress dependent manner. This suggests that this mutant is able to at least bind to ASK1 in an oxidative dependent manner, whether it is also able to decrease the activation of the ASK1 signalosome is still open.

In accordance with the previous findings DJ-1^{wt} co-immunoprecipitated with ASK1^{FL} only in the presence of oxidative stress. DJ-1^{wt} also co-immunoprecipitated in an oxidative stress dependent manner with a truncated variant of ASK1, which lacked the C-terminal domain. Surprisingly, contradictory to the previous study DJ-1^{wt} also co-immunoprecipitated with a truncated variant of ASK1 that lacked the N-terminal domain and kinase domain (Fig 3.5). These results were confirmed with size exclusion chromatography (Fig 3.6). In the previous study an ASK1 truncated variant that lacked only the N-terminal domain was used (Waak et al., 2009a). In addition, in this work the interactions with the truncated variants were weaker than with the ASK1^{FL}. Especially the interaction with ASK1^{CT} was barely detectable in the size exclusion chromatography assay. This may certainly be since deletions of fairly large parts of a protein can interrupt the structure of the remaining domains and thereby influence the protein interactions. Indeed, in a preliminary vector expression test the C-terminal domain alone had higher protein steady state levels than the variant with the C-terminal plus the kinase domain (not shown). That means that more truncated ASK1 was present in our experiments. Nevertheless, it is also possible that DJ-1 has more than one binding site on ASK1. The molar ratio of the interaction between these two proteins is not known. ASK1 possesses 23 cysteine residues, from which three are in the C-terminal domain, five in the kinase domain and fifteen in the N-terminal domain

4. Discussion

(Fig 1.7B). The structure of the whole ASK1 protein is not solved, whether all cysteines are available for interaction with other proteins is rather unlikely. In addition, the coiled coil regions in both N- and C-terminal domains are highly potential protein interaction sites. Thus, there seem to be several possible sites for non-covalent interaction and the suggested covalent C-C binding between DJ-1 and ASK1. Trx is shown to covalently bind to the N-terminal domain of ASK1 under reducing conditions and be released by oxidation under stress (Saitoh et al., 1998). However, later it has been shown that it is possible that Trx binds under unstressed conditions to C250 of ASK1 and in presence of stress it stays bound to the activated ASK1, but to C22 or C30 (Nadeau et al., 2009). C250 has been suggested to be essential for the H₂O₂ induced activation of ASK1 (Nadeau et al., 2009). Thus it is possible that when effector proteins bind to certain sites of ASK1 it influences the activation to a higher extent than when they bind to other sites. Therefore, closer investigation needs to be made in order to trustworthy explain the exact regulation of ASK1 activity by DJ-1.

4.1.4 DJ-1 protection and ASK1 activation in a MSA cell culture model

The molecular mechanisms leading to degeneration of oligodendroglial cells and neurons in MSA patients are largely unclear. However, it is well known that GCIs, which contain the microglial MT polymerizing protein p25 α (also called TPPP) and S129 phosphorylated α -syn are present in diseased brains (Papp et al., 1989, Wakabayashi et al., 1998, Dickson et al., 1999, Lindersson et al., 2005). The formation of GCIs is suggested to start with p25 α accumulation. This is followed by increased α -syn levels and subsequent formation of GCIs by α -syn aggregation (Song et al., 2007). Interestingly, it is shown that p25 α can increase α -syn fibril formation *in vitro* (Lindersson et al., 2005). The oligodendroglial cells with cytoplasmic inclusions have been shown to have elevated DJ-1 levels (Neumann et al., 2004). Therefore, our collaboration partners in Denmark studied the effect of DJ-1 in a MSA cell culture model, namely a rat oligodendroglial cell line that stably expresses human α -syn (OLN AS). Upon transient overexpression of p25 α these cells show morphological impairments, which can be detected by retraction of the MT network to the perinuclear region (Kragh et al., 2009). The retraction has been shown to be dependent on S129- α -syn phosphorylation, α -syn aggregation, caspase activity and was inhibited by DMAT, which is a casein kinase 2 and polo-like kinase inhibitor (Kragh et al., 2009). Notably, cells that co-overexpressed DJ-1^{wt}, but not mutants including DJ-1^{C106A} and DJ-1^{P158 Δ} , showed less MT retraction than vector control transfected cells (Fig 3.8). DJ-1^{A107P}

seemed to have an intermediate ability to protect in this assay (Fig 3.9). This is a novel function for DJ-1 and it implies that DJ-1 may indeed have a protective role in the affected oligodendroglial cells in the MSA brain. Unfortunately, the few genetic studies done in MSA patient cohorts have not yet included *DJ-1*.

Furthermore, decrease of ASK1 activity with chemical inhibitors abated the MT retraction in the OLN AS cells. Correspondingly, overexpression of ASK1 increased the retraction (Fig 3.10). This indicates that ASK1 plays a role in the cytotoxic response in oligodendroglia caused by simultaneous elevated protein levels of α -syn and p25 α . Even though ASK1 is shown to play a role in a variety of diseases (Reviewed in Hayakawa et al., 2012), it has not yet been implied to play a role in MSA. Accordingly, it was shown recently that the cell death caused by co-expression of p25 α and α -syn in OLN cells is FAS dependent (Kragh et al., 2013). FAS (CD95) is a death domain receptor which activates apoptosis through caspase 3 and 8. However, it has also been shown to activate Daxx and subsequently activate ASK1 (Yang et al., 1997). Thus the protective role of DJ-1 may be caused by direct down regulation of ASK1 activity. Though we can not rule out the possible chaperone function of DJ-1, as it has been shown *in vitro* to down regulate α -syn fibril formation either by directly acting as a chaperone or by up regulating heat-shock protein 70 expression (Shendelman et al., 2004, Zhou and Freed, 2005, Batelli et al., 2008, Liu et al., 2008). Thus, the question still remains open how DJ-1 protects against the p25 α and α -syn dependent cell death in oligodendrocytes.

In conclusion, if the genetic linkage of the DJ-1^{A179T} mutation is not coincidental, other functional assays need to be done in order to find its pathophysiological effect. Moreover, the main abnormality of DJ-1^{P158 Δ} and DJ-1^{A107P} seem to be the lack of formation of stable dimers and thus they lack protein stability. Therefore, a possible reason why the patients that hold these homozygous *DJ-1* mutations developed PD may be the decreased protection against cellular stress since only little DJ-1 protein is present (Fig 4.1).

4. Discussion

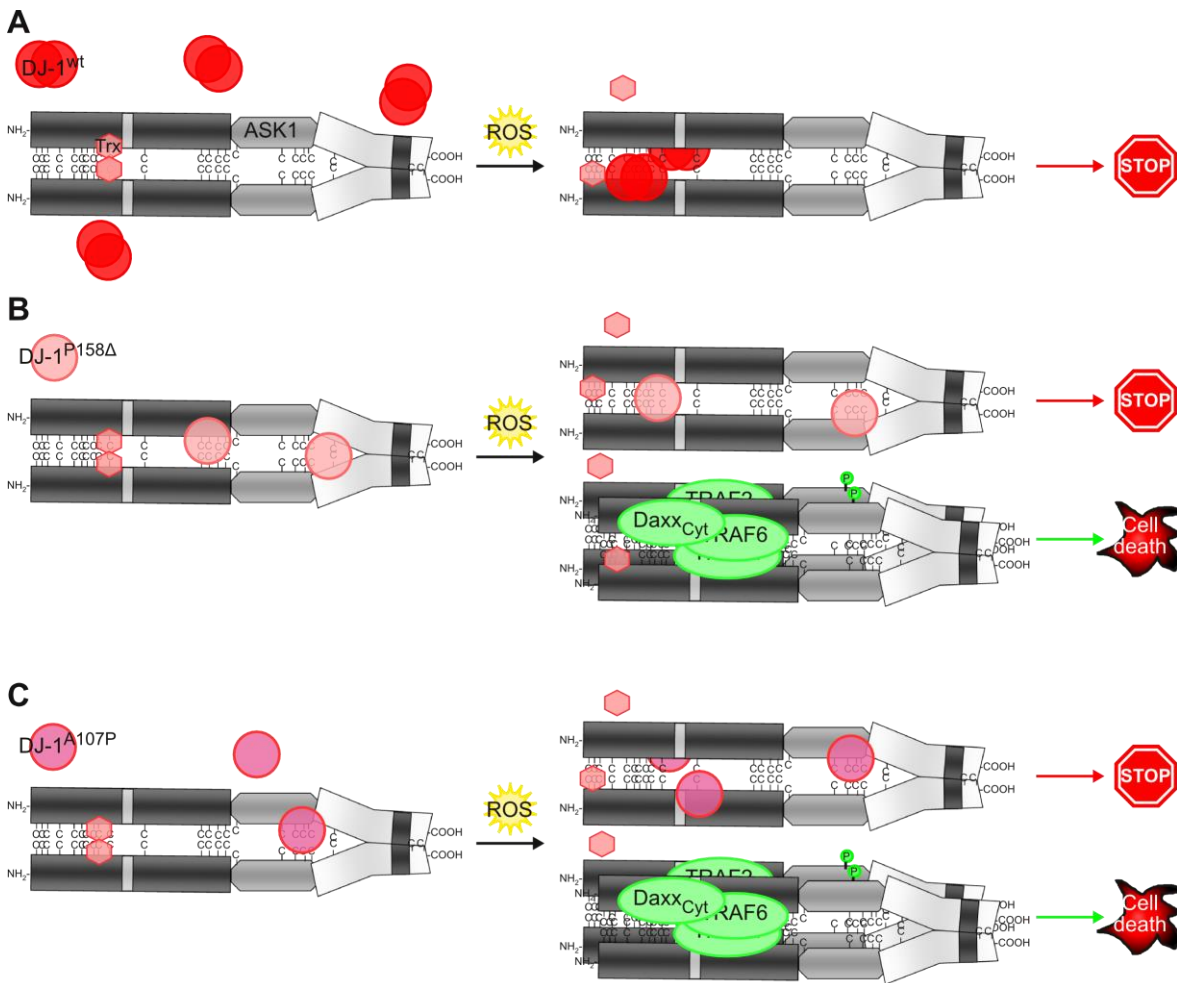


Figure 4.1 Suggested model of mutant DJ-1 regulation of ASK1 signalosome activation. Under unstressed conditions Trx binds covalently to ASK1 and inhibits its activation. **A.** In presence of oxidative stress the Trx suppression is removed, but activated DJ-1^{wt} can bind to and inhibit further activation of ASK1. **B, C** Less DJ-1^{P158Δ} (**B**) and DJ-1^{A107P} (**C**) protein is present. P158Δ mutant and to a lesser extent A107P mutant interact with ASK1 also in absence of stress. In presence of oxidative stress, some mutant protein binds and inhibits further activation of ASK1. However, the inhibition is not strong enough, since less DJ-1 is available, and thus the ASK1 signalosome is activated, which induces apoptosis.

4.2 Elevated secretion of α -syn possibly cumulates the neuronal stress

One of the currently heavily discussed topics within the PD research is if it is possible that α -syn act as an agent that spreads the PD pathology from one brain region to another. More evidence to back up this idea is appearing. However, there are also some vagueness and inexplicabilities in this hypothesis. In this work the role of the astrocytes was investigated. This part of the project has still deficits and some inconsistencies, which makes it wrong to draw conclusions. Nonetheless, it provides suggestions, which may or may not help to explain the physiological progression of the disease.

4.2.1 TLR4 involved activation of inflammation induced by extracellular α -syn

In this work we used a cellular system with mouse primary astrocytes to monitor the effects of extracellularly applied recombinant α -syn. Treatment with α -syn or the positive control LPS induced neuroinflammatory responses in the primary astrocytes, which could be seen by increased phosphorylation of MAPKs, nuclear translocation of NF- κ B, induced expression of COX-2, IL-1 β , IL-6 and iNOS and increased production of NO (Fig 3.12-3.17). These results are in agreement with other studies. An early study showed that treatment with recombinant α -syn induced expression of IL-6 and intercellular adhesion molecule-1 in human astrocytes (Klegeris et al., 2006). More recently, Lee and colleagues found that the cell medium of α -syn overexpressing SH-SY5Y cells can upregulate several genes related to among other neuroinflammation, TLR signaling and apoptosis in primary rat astrocytes. However, in opposite to our model system they could also measure an induction of TNF α expression (Lee et al., 2010).

One of the main goals of this study was to identify a possible astrocytic α -syn receptor. The induction of neuroinflammatory responses by the well known bacterial toxin LPS is mediated by the TLR4 receptor (Poltorak et al., 1998). Interestingly, we saw a reduction in the induction of phosphorylation of MAPKs, cytokine expression and nuclear translocation of NF- κ B after treatment with recombinant α -syn in *Tlr4*^{-/-} primary astrocytes compared to littermate wt astrocytes (Fig 3.15, 3.16 and 3.17). Although these results should be considered preliminary due to high variability they are supported by a recently published study, which showed a TLR4 dependent upregulation of microglial and astroglial neuroinflammatory responses after treatment with recombinant α -syn (Fellner et al., 2013). In that study primary wt and *Tlr4*^{-/-} microglia and astrocytes were treated with recombinant monomeric full length or C-terminally truncated or fibrillized α -syn. They could measure an increase in ROS production and TNF α , IL-6 and CXCL1 secretion after α -syn treatment in wt glial cells, but not in *Tlr4*^{-/-} glial cells. The C-terminally truncated α -syn was especially prone to induce the ROS production and cytokine secretion (Fellner et al., 2013). Thus it seems to be possible that α -syn indeed can activate the TLR4 mediated signaling pathway in astrocytes and microglial cells (Fig 4.2). It is important to notice that the concentrations of recombinant α -syn that was used in this work, but also by others, are several times higher than the estimated physiological levels of extracellular α -syn. The α -syn level has been measured to be 0.01 or 0.035 nM in the interstitial fluid of wt

4. Discussion

or transgenic α -syn overexpressing mice, respectively (Emmanouilidou et al., 2011). The inflammatory responses were seen when we used 0.7 μ M of α -syn, which is a more than 20 000 times higher concentration. Moreover, Fellner and colleagues used 3 μ M of α -syn. However, the local concentration within synapses, which are touched by astrocytic endfeet, could be at least temporarily increased. It would be very interesting to be able to measure the α -syn concentration within the synapses and investigate the effect of physiologically relevant extracellular α -syn concentrations.

4.2.2 DJ-1 as protector against α -syn induced stress

Previously our group has showed that primary astrocytes from wt mice showed less neuroinflammatory responses after treatment with LPS than primary astrocytes from littermate *Dj-1*^{-/-} mice. It was shown that DJ-1 was downregulating the p38 involving pathway. In addition, co-cultured cortical neurons showed increased apoptotic signaling after LPS treatment when cultured with *Dj-1*^{-/-} astrocytes compared to when cultured with wt astrocytes. Moreover, co-cultured *Dj-1*^{-/-} neurons were significantly more apoptotic than co-cultured wt neurons (Waak et al., 2009b). In this work LPS was used as a positive control, but the protective role of DJ-1 was not as strong as in the previous work (Fig 3.12, 3.13, 3.14). *Dj-1*^{+/+} astrocytes showed a slight trend to have decreased LPS induced neuroinflammation compared to *Dj-1*^{-/-} astrocytes. It is possible that the difference is caused by the use of another batch of LPS, differences in ways of handling the cultures or that the mice, and thus the astrocytes made from them, have been affected by several years of inbreeding. Moreover, the results shown in this work are rather inconsistent and variable. Thus it is possible that DJ-1 plays a strong protective role as seen in the previous study.

DJ-1 is shown in cultured cells to decrease α -syn fibril formation and to protect against toxic responses of α -syn (Shendelman et al., 2004, Zhou and Freed, 2005, Batelli et al., 2008). Thus it was hypothesized that absence of DJ-1 *in vivo* would increase the toxic effects of α -syn overexpression and accelerate the onset of phenotypic symptoms. In opposite to our expectations, knockout of *Dj-1* in transgenic human α -syn expressing mice did not accelerate the onset of motorical symptoms (Fig 3.21.). This is in agreement with an earlier study (Ramsey et al., 2010). In that study transgenic mice that express human α -syn^{A53T} under the mouse PrP promoter were used (Giasson et al., 2002). Knockout of *Dj-1* in these mice did not shorten their lifespan. The loss of DJ-1 also did not influence the distribution of the α -syn pathology,

the amount of dopaminergic neurons, dopamine levels nor the activation of glial cells (Ramsey et al., 2010).

In humans the male gender seems to be a risk factor for development of PD (Wooten et al., 2004). Accordingly, gene expression experiments have shown gender differences in gene expression profiles. One of the genes that may be expressed to a higher extent in women is the *DJ-1* gene (Simunovic et al., 2010). In this work the human α -syn^{A30P} transgenic male mice showed a later onset of motorical symptoms than the female mice (Fig 3.21). This is the opposite of what is seen in humans. However, the male group in question was relatively small (n=8). Thus, a bigger group would be preferable before stating a later onset of motorical symptoms for males in the Thy1h[A30P]SNCA transgenic mouse line.

4.2.3 Astrocytes as removers of extracellular α -syn

In addition to α -syn induced activation of neuroinflammation we could detect human α -syn in immunoblots made from cell lysates of mouse primary astrocytes that had been treated with recombinant α -syn. The recombinant α -syn could be detected to a similar extent in wt, *Tlr4*^{-/-} and *Dj-1*^{-/-} astrocytes (Fig 3.18). However, no signal was detected with an antibody that recognizes S129 phosphorylated α -syn (Fig 3.19). This does not exclude possible phosphorylation of other residues, but notably S129 is shown to be selectively phosphorylated in pathological α -syn inclusions (Fujiwara et al., 2002). Moreover, we could show a fast decrease in the internalized α -syn after removal of the recombinant protein from the cell media (Fig 3.20). This would indicate that the astrocytes are able to clear the extracellular α -syn and thereby preventing it from becoming pathological. In agreement with our results Fellner and colleagues did not see any TLR4 dependent astrocytic intake of the recombinant α -syn. They however, showed a TLR4 dependent intake of α -syn into microglial cells (Fellner et al., 2013). Lee and colleagues showed that the astrocytic intake of α -syn secreted from SH-SY5Y cells was dynamin1 dependent. In addition, they saw that most of the internalized α -syn co-localized with the lysosomal marker LAMP2 and treatment with bafilomycin A1 lead to increased accumulation of internalized α -syn (Lee et al., 2010). This would indicate that the internalized α -syn uses the endosomal pathway and is degraded in the lysosomes. This is not in agreement with our results, since treatment with Bafilomycin A1 did not slow down the reduction of the detected signal from internalized α -syn. On the other hand, the inhibition of the proteasome with MG-132 did slow down the reduction (Fig 3.20). Our results would indicate that the internalized

4. Discussion

α -syn is not surrounded by a membrane and is degraded by the proteasome (Fig 4.2). Use of other inhibitors, for example inhibition of clathrin mediated endocytosis, or to use more specific inhibitors, for example the proteasomal inhibitor epoxomicin, may help to clarify the difference in the results. Notable is also the difference in the source of extracellular α -syn. The treatment in this work was primarily done with monomeric, recombinant α -syn. Although, it can not be ruled out that some oligomeric or fibrillar α -syn was present, which usually occurs first after incubation at 37 °C for several days. In the work of Lee and colleagues cell secreted α -syn was used. This α -syn may contain a mixture of oligomeric, fibrillar and monomeric α -syn. In addition it is possible that cell-secreted α -syn is in membrane surrounded exosomes whereas recombinant purified α -syn is not surrounded by a membrane. One should also not forget the eventuality that resecretion caused the decrease in internalized α -syn in both of these assays. Nonetheless, if the internalized α -syn is indeed degraded by the proteasome it needs to be cytosolic. It is possible that α -syn enters the cell by passive diffusion as previously suggested (Ahn et al., 2006, Lee et al., 2008a) and thus it would be directly

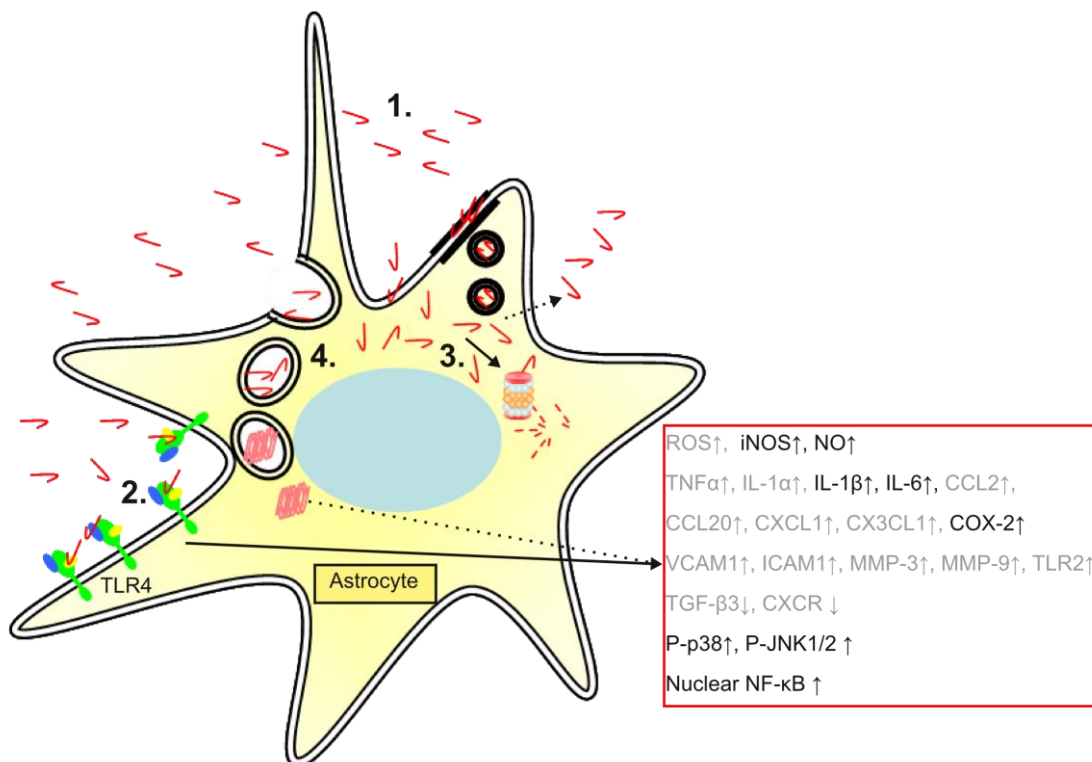


Figure 4.2 Model of how extracellular monomeric α -syn may influence astrocytes. 1. In this work mouse primary astrocytes were treated with recombinant α -syn. 2. We suggest that extracellular α -syn activates the TLR4 signaling pathway. (Proteins and genes that are covered in this work are shown in black and previously shown genes are shown in grey.) 3. In addition, we suggest that α -syn is taken up by the astrocytes and may be degraded by the proteasome or alternatively it is resecreted. 4. Other studies have suggested that α -syn is internalized by astrocytes through endocytosis and that α -syn inclusions induce expression of several genes (dotted arrow).

cytosolic. However, proteins that are taken up by endocytosis are surrounded by a membrane. Interestingly, α -syn was shown recently to be able to exit lysosomes by rupturing the membrane (Freeman et al., 2013). Nevertheless, it seems like astrocytes are able to efficiently sequester and degrade extracellular α -syn.

4.2.4 Transmission of pathogenic α -syn during disease progression

We and others have noticed that α -syn can be taken up by different types of cells. Although most of the α -syn aggregates are found in neurons, Lewy body-like inclusions have been detected in astrocytes in striatum and substantia nigra and in oligodendrocytes in the midbrain of PD patients (Wakabayashi and Takahashi, 1996, Wakabayashi et al., 2000, Braak et al., 2007). Thus one important question remains – is it possible that α -syn pathology spreads from one region to another in a specific pattern? Or is the pathology coincidentally appearing in certain more vulnerable regions? Many of the studies supporting the theory of α -syn transmission are already discussed in more detail in the introduction (section 1.3.2). Briefly α -syn is secreted from neurons, is possibly able to induce neuroinflammatory responses in neighboring cells and is internalized by neighboring cells (Fig 1.4).

The most affected neurons in PD are the G-protein-coupled inward rectifying current potassium channel type 2 expressing dopaminergic neurons in the ventral tier of substantia nigra pars compacta (A9) (Fearnley and Lees, 1991). These neurons project almost exclusively to the dorsolateral putamen. In contrast, the adjacent calbindin positive dopaminergic neurons in the ventral tegmental area (A10), which project to the mesolimbic brain region, are almost spared from PD pathology (Yamada et al., 1990). Accordingly, recent studies support an antrograde axonal spreading and release of α -syn (Angot et al., 2012, Freundt et al., 2012, Luk et al., 2012a, Luk et al., 2012b). In a study by Luk and colleagues brain lysates from old, α -syn^{A53T} expressing symptomatic transgenic mice or synthetic α -syn fibrils were injected to the neocortex or striatum of young α -syn^{A53T} expressing transgenic mice. These mice showed severe α -syn pathology in regions with neuronal connections to the injected area. Regions that were adjacent, but not connected had more spared pathology. Noteworthy, the pure, synthetic α -syn fibrils induced a similar pathology as the brain lysates (Luk et al., 2012b). Moreover, *in vitro* experiments have showed that a transfer of α -syn from the axon to the recipient cells does not depend on a presence of synapses (Freundt et al., 2012). In late 1980's and early 1990's embryonic human midbrains were transplanted into the brain of PD patients. As the patients gradually pass away these

4. Discussion

brains are appearing to autopsy, which has given an opportunity to a long term experiment in humans. The grafted neurons have been shown to strongly innervate the putamen already 18 months after the transplantation. However, no host to graft sprouting was seen (Kordower et al., 1995, Kordower et al., 1996). Ten or more years after the transplantation α -syn inclusions have been found in the relatively young cells within the transplanted embryonic midbrain in PD patient brains (Kordower et al., 2008, Li et al., 2008). This seems to imply that a retrograde spreading of α -syn can take place. This would challenge the theory of an anterograde α -syn spreading, which is also the base of the Braak's staging model (see section 1.3.2). However it would still not argue against the hypothesis that α -syn is a disease spreading agent.

It has been shown *in vitro* that α -syn fibrils accelerate fibrillization, a phenomenon referred to as seeding (Wood et al., 1999). Thus secretion of oligomeric and fibrillar α -syn and uptake of these could theoretically induce fibril formation in the recipient cells, assuming that the recipient cell either express endogenous α -syn or internalize high amounts of exogenous α -syn. It can be questioned if formation of the Lewy-body-like inclusions in the recipient cells is relevant for the spreading of the disease, considering the current view that the oligomeric species are responsible for the cytotoxicity and that aggregation is a cytoprotective action. Interestingly, wt mice injected with α -syn fibrils into the dorsal striatum showed a slow spreading of α -syn aggregation to regions with neuronal connections and degeneration of the sensitive dopaminergic neurons in substantia nigra pars compacta. No dopaminergic cell loss was seen in mice that were injected with monomeric α -syn or in *Snca*^{-/-} mice that were injected with α -syn fibrils, both of which also did not show any α -syn deposits (Luk et al., 2012a). This suggests that the neuronal death was dependent on α -syn aggregation, which was dependent on presence of endogenous α -syn and preformed fibrils.

One argument speaking against the possibility of α -syn acting alone as a disease spreading factor is the fact that α -syn inclusions are found in other diseases as well; both in synucleinopathies as well as in diseases where its inclusions are in minority. The brain areas where the inclusions can be found differ between the diseases and these areas are not always connected with neurons. For example, α -syn inclusions are found in MSA in oligodendroglia and neurons primarily in *substantia nigra* and cerebellum and dementia with Lewy bodies is characterized by diffuse cortical α -syn pathology. Thus the presence of high amounts of other cellular stressors like ROS,

proinflammatory cytokines and NO in the PD brain should be taken into consideration when explaining the progression of α -syn pathology. Interestingly, extensive staining for activated microglial was seen in the area of transplanted embryonic midbrain with Lewy body like inclusions (Kordower et al., 2008, Li et al., 2008). Conversely, in another study no inclusions were seen in grafts in five PD brains 9 to 14 years after the transplantation. In this study the transplanted area also showed only a small number of activated microglia (Mendez et al., 2008). Although these studies include very few patients, this suggests that presence of α -syn accumulation in young neurons comes hand in hand with activated microglia. Accordingly, one can perhaps at least partly explain the formation of α -syn inclusion in the young grafted neurons by the stressful environmental conditions in the PD brain. Of course what comes first, α -syn pathology or activation of microglia, is still open.

In conclusion, in this work the astrocytes were able to internalize the recombinant α -syn and possibly degrade it. Moreover, we suggest that monomeric α -syn possibly induces the neuroinflammatory responses by activating the TLR4 receptor in astrocytes. Accordingly, we and others have shown that elevated levels of extracellular α -syn, no matter if monomeric, oligomeric or fibrillar, can directly activate the micro- and astroglial production of ROS, proinflammatory cytokines and NO. This would enhance the local stress conditions, which in its turn would cumulate the neuronal impairment and α -syn aggregation and thereby α -syn secretion. Thus an accelerating destructive circle of brain damage on the molecular level would be created. A lot of uncertainties in this hypothesis still need to be tackled. However, it seems to be possible that inhibition of TLR4 could slow down the destructive circle and thereby possibly slow down the neurodegeneration in PD. Thus TLR4 could be considered to be a potential therapeutic target.

4.3 Perspectives

Here it was shown that P158 and A107 are important for the dimerization and thus stability of DJ-1 protein. The point mutant DJ-1^{A179T} did not show any differences to DJ-1^{wt} in the assays used. Furthermore, we suggest that recombinant α -syn can induce neuroinflammatory responses in primary astrocytic cultures, possibly by activating TLR4. The primary astrocytes were also internalizing the extracellular recombinant α -syn. There are still many open questions that would be interesting to investigate, from which some are discussed below.

4. Discussion

Both DJ-1^{P158Δ} and DJ-1^{A107P} were able to bind to ASK1. However, whether they were able to also decrease ASK1 activation in the presence of oxidative stress is still not fully clear. Here a better method for measuring ASK1 activity needs to be developed. In this study we use an *in vitro* immunocomplex kinase assay, for which overexpressed ASK1 protein was used. However, overexpression of the apoptosis inducing ASK1 is in general stressful for cells and thus a method for detection of endogenous ASK1 activity would be preferable. Previously, endogenous ASK1 of MEF cells was used (Gorner et al., 2007). However, at least in my hands, even though I used the described protocol, the ASK1 immunoprecipitation did not work. Detection of the phosphorylation state of ASK1 and its targets by specific antibodies can be used as an alternative method. Upon activation ASK1 is phosphorylated on T838 and dephosphorylated on S967 (Tobiume et al., 2002, Goldman et al., 2004). Activated ASK1 phosphorylates the MKK4/MKK7-JNK and MKK3/MKK6-p38 pathways (Ichijo et al., 1997). Thus the activation of ASK1 can be detected by changes in the phosphorylation pattern.

Further it was shown that DJ-1 is able to decrease the cytotoxicity when p25 α and α -syn are simultaneously present in high concentrations. It would be interesting to investigate if the cytoprotective role of DJ-1 is caused by the chaperone activity that inhibits the aggregation of α -syn or by the direct inhibition of ASK1 activation. This would result in a better understanding of the exact mechanism that produces the toxicity when α -syn and p25 α are simultaneously present in the oligodendrocytes. A triple transient transfection with DJ-1, ASK1 and p25 α into OLN cells that are already stably over expressing α -syn proved to be difficult. A method to examine the endogenous ASK1 activity would also here be beneficial.

Generally there is a lack of a reliable assay for the measurement of DJ-1 activity. Many functions and assays have been published, however, a confirmation of these methods by other groups are often missing. Protection against severe cellular stress could be fatal for the organism. Accordingly, DJ-1 protects cells only in presence of low levels of stress and overoxidation of C106 of DJ-1 to SO₃H is even shown to inactivate the protein (Zhou et al., 2006, Hulleman et al., 2007). In addition, DJ-1 is a multifunctional protein. Thus the effect of DJ-1 in one particular pathway can be very low and therefore it can be hard to detect. Nevertheless, development of consistent methods for measurement of DJ-1 functional ability would be helpful.

Mutation in *DJ-1* cause a monogenic form of PD in only very few patients in the world. Accordingly, the DJ-1 mutants, which have been investigated in this work, were

only found in one patient per mutation. One may wonder if it is relevant to put effort on such a rare cause of a disease. However, DJ-1 is involved in many cellular processes, which are dysfunctional in PD. For example, DJ-1 is shown to participate in mitophagy (Thomas et al., 2011) and it protects against oxidative stress. Moreover, considering that the expression of DJ-1 is upregulated in affected oligodendroglial cells in MSA and in reactive astrocytes in PD (Neumann et al., 2004) and that the loss of this protein can cause a very early onset of PD, its function may be indeed very crucial. Thus exploring the failure and function of DJ-1 could shed a light into the progression of synucleinopathies.

Considering the effects of extracellular α -syn on astrocytes there are still many open questions. First of all, the data that is shown here needs to be considered preliminary. Thus confirmation of the experiments is still needed. Simultaneously, in order to decrease the biological variance further optimization of astrocyte preparation, culturing and treatment conditions should be made. Moreover, we used only very high concentrations of α -syn that has been produced in bacteria. It would be interesting to continue to investigate if cell expressed and secreted α -syn can induce the same neuroinflammatory responses in astrocytes and if a similar TLR4 dependent induction is detected. This would give more physiological relevance for our data, since the natural forms of secreted α -syn would be used. That is more physiological proportions of secreted monomeric, oligomeric to aggregated α -syn and free to membrane surrounded exosomal α -syn would be used. Approaches as shown elsewhere for use of cell secreted α -syn could be considered. Moreover, one open question remains if α -syn directly interacts with TLR4 or if it uses an intermediating protein. LPS is recognized by LBP, which transfers LPS to CD14. CD14 facilitates the transfer of LPS to the MD-2/TLR4 receptor complex. An α -syn recognizing extracellular protein may be characterized in an assay where crosslinkers are used.

This work is using *in vitro* methods and confirmation of the physiological relevance should be done also *in vivo*. One can consider the usage of TLR4 inhibitors or *Tlr4* knock out in α -syn overexpressing transgenic animals. If the extracellular α -syn indeed deteriorates the neuronal stress by inducing neuroinflammation through activation of the astrocytic and/or microglial TLR4 signaling pathway, these mice can be expected to show a delayed onset of phenotypic symptoms. Alternatively injection of either recombinant α -syn, or brain lysate from transgenic old mice to *Tlr4*^{-/-} mice could be made. However, this would reflect the physiological conditions to a lesser extent.

4. Discussion

Because of the inconsistency between our and published results more investigation should be made on the exact mechanism of internalization of extracellular α -syn and its concomitant cellular degradation. As mentioned earlier one could use more specific inhibitors than MG-132, for example epoxomicin for proteasomal inhibition. Furthermore, it would be interesting to measure the pace of reduction of applied α -syn in the media by using enzyme-linked immunosorbent assays and whether additional stress, for example addition of H_2O_2 , affects the degradation efficiency. Another puzzling detail is that other studies show intracellular inclusions of internalized α -syn (Lee et al., 2008a, Fellner et al., 2013). In our approaches no α -syn positive astrocytes were detected by immunofluorescence staining (not shown). The lack of positive staining may be due to differences in used α -syn species, genetic background of used cells, assay conditions or used antibodies. Thus optimization of the staining protocol would be helpful. Immunostainings could be used to detect possible co-localization of endosomal proteins with the internalized α -syn. The lack of positive staining may also be caused by an efficient degradation of the internalized α -syn without it becoming pathological, which the lack of S129 phosphorylated α -syn and the rarity of astrocytic inclusions in PD patients also indicate.

These studies could further clarify the importance of TLR4 signaling activation by extracellular α -syn and whether and how astrocytes remove this possibly toxic extracellular protein.

5 Summary

Mutations in the *DJ-1* gene are rare causes of early onset autosomal recessive PD. DJ-1 is a ubiquitously expressed, cytoprotective protein. The most severe PD associated mutations of DJ-1 lead to absence of the protein. In this work three novel PD associated DJ-1 mutants were characterized. In the assays used in this work point mutation of A179 to T did not lead to different protein properties compared to the wt DJ-1 protein. In contrast, point mutation of the conserved A107 to P and point deletion of the conserved P158 lead to decreased dimerization ability, decreased protein steady state levels and an abnormal binding behaviour towards ASK1. In addition, in a cell cultural model of MSA, DJ-1^{A107P} was only partly able and DJ-1^{P158Δ} was not able to reduce the p25α dependent MT retraction in an α-syn overexpressing oligodendroglial cell line, an event where also ASK1 was shown to be involved in. In conclusion, the DJ-1^{P158Δ} and DJ-1^{A107P} mutants may contribute to neurodegeneration by protein destabilization and hence loss of DJ-1 functions.

The pathological hallmark of PD is intracellular inclusions that mainly consist of misfolded α-syn, a protein that is normally localized in synapses and the cell body of neurons. However, part of the cellular α-syn is secreted to the extracellular space. In this work the effect of extracellular α-syn on astrocytes was investigated. A cell culture model where primary mouse astrocytes were treated with recombinant purified α-syn was used. Treatment with α-syn induced inflammatory responses in the astrocytes. This was seen by increased expression of iNOS, COX-2, IL-6 and IL-1β, increased NO production, increased nuclear translocation of NF-κB and increased phosphorylation of JNK and p38. The induction was decreased in *Tlr4*^{-/-} astrocytes, thus indicating that α-syn is activating the TLR4 signaling pathway. Furthermore, the primary astrocytes internalized the recombinant α-syn. After removal of the protein from the cell media a fast decrease in internalized α-syn was observed. This may have been caused by proteasomal degradation. In conclusion, elevated levels of extracellular α-syn can induce astrocytes to produce cytokines and NO in a TLR4 dependent manner and thereby worsen the stress conditions in PD brains. The astrocytes may also be able to sequester and degrade extracellular α-syn.

6 References

References in tables

- Abou-Sleiman PM, Healy DG, Quinn N, Lees AJ, Wood NW (2003). The role of pathogenic DJ-1 mutations in Parkinson's disease. *Ann Neurol.* 54, 283-6.
- Annesi G, Savettieri G, Pugliese P, D'Amelio M, Tarantino P, Ragonese P, La Bella V, Piccoli T, Civitelli D, Annesi F, Fierro B, Piccoli F, Arabia G, Caracciolo M, Cirò Candiano IC, Quattrone A (2005) DJ-1 mutations and parkinsonism-dementia-amyotrophic lateral sclerosis complex. *Ann Neurol.* 2005 ;58(5):803-7.
- Bonifati V, Rizzu P, van Baren MJ, Schaap O, Breedveld GJ, Krieger E, Dekker MC, Squitieri F, Ibanez P, Joosse M, van Dongen JW, Vanacore N, van Swieten JC, Brice A, Meco G, van Duijn CM, Oostra BA, Heutink P.(2003) Mutations in the DJ-1 gene associated with autosomal recessive early-onset parkinsonism. *Science.* 299: 256–259
- Chartier-Harlin MC, Dachsel JC, Vilarinho-Güell C, Lincoln SJ, Leprêtre F, Hulihan MM, Kachergus J, Milnerwood AJ, Tapia L, Song MS, Le Rhun E, Mutez E, and 38 others (2011) Translation initiator EIF4G1 mutations in familial Parkinson disease. *Am. J. Hum. Genet.* 89: 398-406
- Di Fonzo A, Dekker MC, Montagna P, Baruzzi A, Yonova EH, Correia Guedes L, Szczerbinska A, Zhao T, Dubbel-Hulsman LO, Wouters CH, de Graaff E, Oyen WJ, Simons EJ, Breedveld GJ, Oostra BA, Horstink MW, Bonifati V.(2009) FBX07 mutations cause autosomal recessive, early-onset Parkinsonian-pyramidal syndrome. *Neurology.* 71: 240–245.
- Ghazavi F, Fazlali Z, Banihosseini SS, Hosseini SR, Kazemi MH, Shojaee S, Parsa K, Sadeghi H, Sina F, Rohani M, Shahidi GA, Ghaemi N, Ronaghi M, Elahi E (2011). PRKN, DJ-1, and PINK1 screening identifies novel splice site mutation in PRKN and two novel DJ-1 mutations. *Mov Disord.* 26, 80-9.
- Guo JF,Xiao B,Liao B,Zhang XW,Nie LL,Zhang YH,Shen L,Jiang H,Xia K,Pan Q,Yan XX,Tang BS. (2008). Mutation analysis of Parkin, PINK1, DJ-1 and ATP13A2 genes in Chinese patients with autosomal recessive early-onset Parkinsonism. *Mov Disord* 23: 2074–2079.
- Hague S, Rogaeva E, Hernandez D, Gulick C, Singleton A, Hanson M, Johnson J, Weiser R, Gallardo M, Ravina B, Gwinn-Hardy K, Crawley A, St George-Hyslop PH, Lang AE, Heutink P, Bonifati V, Hardy J, Singleton A. (2003). Early-onset Parkinson's disease caused by a compound heterozygous DJ-1 mutation. *Ann. Neurol.* 54, 271–274.
- Hedrich K, Djarmati A, Schäfer N, Hering R, Wellenbrock C, Weiss PH, Hilker R, Vieregge P, Ozelius LJ, Heutink P, Bonifati V, Schwinger E, Lang AE, Noth J, Bressman SB, Pramstaller PP, Riess O, Klein C (2004). DJ-1 (PARK7) mutations are less frequent than Parkin (PARK2) mutations in early-onset Parkinson disease. *Neurology* 62, 389–394.
- Hering R, Strauss KM, Tao X, Bauer A, Voitalla D, Mietz EM, Petrovic S, Bauer P, Schaible W, Müller T, Schöls L, Klein C, Berg D, Meyer PT, Schulz JB, Wollnik B, Tong L, Krüger R, Riess O. (2004). Novel homozygous p.E64D mutation in DJ1 in early onset Parkinson disease (PARK7). *Hum. Mutat.* 24, 321–329
- Hoshino K, Takeuchi O, Kawai T, Sanjo H, Ogawa T, Takeda Y, Takeda K, Akira S (1999) Cutting edge: Toll-like receptor 4 (TLR4)-deficient mice are hyporesponsive to lipopolysaccharide: evidence for TLR4 as the Lps gene product. *J Immunol.* 162(7):3749-52
- Kahle PJ, Neumann M, Ozmen L, Muller V, Jacobsen H, Schindzielorz A, Okochi M, Leimer U, van Der Putten H, Probst A, Kremmer E, Kretschmar HA, Haass C (2000) Subcellular localization of wild-type and Parkinson's disease-associated mutant alpha -synuclein in human and transgenic mouse brain. *J Neurosci* 20:6365-6373
- Kitada T, Asakawa S, Hattori N, Matsumine H, Yamamura Y, Minoshima S, Yokochi M, Mizuno Y, Shimizu N.(1998) Deletion mutation in a novel protein “Parkin” gene causes autosomal recessive juvenile parkinsonism (AR-JP). *Nature.* 392: 605–608.
- Lautier C, Goldwurm S, Dürr A, Giovannone B, Tsiaras WG, Pezzoli G, Brice A, Smith RJ (2008) Mutations in the GIGYF2 (TNRC15) gene at the PARK11 locus in familial Parkinson disease *Am J Hum Genet* 82(4):822-33
- Leroy E, Boyer R, Polymeropoulos MH (1998) Intron-exon structure of ubiquitin C-terminal hydrolase-L1. *DNA Res.* 5: 397-400
- Macedo MG, Verbaan D, Fang Y, van Rooden SM, Visser M, Anar B, Uras A, Groen JL, Rizzu P, van Hilten JJ, Heutink P (2009). Genotypic and phenotypic characteristics of Dutch patients with early onset Parkinson's disease. *Mov. Disord.* 24, 196–203

- Paisan-Ruiz C, Bhatia KP, Li A, Hernandez D, Davis M, Wood NW, Hardy J, Houlden H, Singleton A, Schneider SA (2009) Characterization of PLA2G6 as a locus for dystonia-parkinsonism. *Ann Neurol.* 65: 19–23
- Pham TT, Giesert F, Rothig A, Floss T, Kallnik M, Weindl K, Holter SM, Ahting U, Prokisch H, Becker L, Klopstock T, Hrabe de Angelis M, Beyer K, Gorner K, Kahle PJ, Vogt Weisenhorn DM, Wurst W (2010) DJ-1-deficient mice show less TH-positive neurons in the ventral tegmental area and exhibit non-motoric behavioural impairments. *Genes Brain Behav* 9:305-317.
- Polymeropoulos MH, Lavedan C, Leroy E, Ide SE, Dehejia A, Dutra A, Pike B, Root H, Rubenstein J, Boyer R, Stenroos ES, Chandrasekharappa S, Athanassiadou A, Papapetropoulos T, Johnson WG, Lazzarini AM, Duvoisin RC, Di Iorio G, Golbe LI, Nussbaum RL (1997) Mutation in the α -synuclein gene identified in families with Parkinson's disease. *Science.* 276: 2045–2047
- Ramirez A, Heimbach A, Gründemann J, Stiller B, Hampshire D, Cid LP, Goebel I, Mubaidin AF, Wriekat AL, Roeper J, Al-Din A, Hillmer AM, Karsak M, Liss B, Woods CG, Behrens MI, Kubisch C (2006) Hereditary parkinsonism with dementia is caused by mutations in ATP13A2, encoding a lysosomal type 6 P-type ATPase. *Nat Genet.* 38: 1184–1191.
- Sidransky E, Nalls MA, Aasly JO, Aharon-Peretz J, Annesi G, Barbosa ER, Bar-Shira A, Berg D, Bras J, Brice A, Chen CM, Clark LN, Condroyer C, De Marco EV, Dürr A, Eblan MJ, Fahn S, Farrer MJ, and 41 others (2009) Multicenter analysis of glucocerebrosidase mutations in Parkinson's disease. *N Engl J Med.* 361: 1651–1661
- Singleton AB, Farrer M, Johnson J, Singleton A, Hague S, Kachergus J, Hulihan M, Peuralinna T, Dutra A, Nussbaum R, Lincoln S, Crawley A, Hanson M, Maraganore D, Adler C, Cookson MR, Muentert M, Baptista M, Miller D, Blancato J, Hardy J, Gwinn-Hardy K (2003) α -Synuclein locus triplication causes Parkinson's disease. *Science.* 302: 841.
- Strauss KM, Martins LM, Plun-Favreau H, Marx FP, Kautzmann S, Berg D, Gasser T, Wszolek Z, Müller T, Bornemann A, Wolburg H, Downward J, Riess O, Schulz JB, Krüger R. (2005) Loss of function mutations in the gene encoding Omi/HtrA2 in Parkinson's disease. *Hum. Molec. Genet.* 14: 2099-2111
- Valente EM, Abou-Sleiman PM, Caputo V, Muqit MM, Harvey K, Gispert S, Ali Z, Del Turco D, Bentivoglio AR, Healy DG, Albanese A, Nussbaum R, González-Maldonado R, Deller T, Salvi S, Cortelli P, Gilks WP, Latchman DS, Harvey RJ, Dallapiccola B, Auburger G, Wood NW (2004) Hereditary early-onset Parkinson's disease caused by mutations in PINK1. *Science.* 304: 1158–1160.
- Vilarino-Guell C, Wider C, Ross OA, Dachsel JC, Kachergus JM, Lincoln SJ, Soto-Ortolaza AI, Cobb SA, Wilhoite, GJ, Bacon JA, Behrouz B, Melrose HL, and 21 others (2011) VPS35 mutations in Parkinson disease. *Am. J. Hum. Genet.* 89: 162-167
- Zimprich A, Biskup S, Leitner P, Lichtner P, Farrer M, Lincoln S, Kachergus J, Hulihan M, Uitti RJ, Calne DB, Stoessl AJ, Pfeiffer RF, Patenge N, Carbajal IC, Vieregge P, Asmus F, Müller-Myhsok B, Dickson DW, Meitinger T, Strom TM, Wszolek ZK, Gasser T (2004) Mutations in LRRK2 cause autosomal-dominant parkinsonism with pleomorphic pathology. *Neuron.* 44: 601–607

References in text

- Adamczyk A, Czapski GA, Kazmierczak A, Strosznajder JB (2009) Effect of N-methyl-D-aspartate (NMDA) receptor antagonists on α -synuclein-evoked neuronal nitric oxide synthase activation in the rat brain. *Pharmacol Rep* 61:1078-1085.
- Agnati LF, Guidolin D, Baluska F, Leo G, Barlow PW, Carone C, Genedani S (2010) A new hypothesis of pathogenesis based on the divorce between mitochondria and their host cells: possible relevance for Alzheimer's disease. *Curr Alzheimer Res* 7:307-322.
- Ahn KJ, Paik SR, Chung KC, Kim J (2006) Amino acid sequence motifs and mechanistic features of the membrane translocation of α -synuclein. *J Neurochem* 97:265-279.
- Alberio T, Lopiano L, Fasano M (2012) Cellular models to investigate biochemical pathways in Parkinson's disease. *FEBS J* 279:1146-1155.
- Alvarez-Erviti L, Seow Y, Schapira AH, Gardiner C, Sargent IL, Wood MJ, Cooper JM (2011) Lysosomal dysfunction increases exosome-mediated α -synuclein release and transmission. *Neurobiol Dis* 42:360-367.
- Andres-Mateos E, Perier C, Zhang L, Blanchard-Fillion B, Greco TM, Thomas B, Ko HS, Sasaki M, Ischiropoulos H, Przedborski S, Dawson TM, Dawson VL (2007) DJ-1 gene deletion reveals that DJ-1 is an atypical peroxiredoxin-like peroxidase. *Proc Natl Acad Sci U S A* 104:14807-14812.
- Angot E, Steiner JA, Lema Tome CM, Ekstrom P, Mattsson B, Bjorklund A, Brundin P (2012) α -Synuclein cell-to-cell transfer and seeding in grafted dopaminergic neurons in vivo. *PLoS One* 7:e39465.

6. References

- Bandopadhyay R, Kingsbury AE, Cookson MR, Reid AR, Evans IM, Hope AD, Pittman AM, Lashley T, Canet-Aviles R, Miller DW, McLendon C, Strand C, Leonard AJ, Abou-Sleiman PM, Healy DG, Ariga H, Wood NW, de Silva R, Revesz T, Hardy JA, Lees AJ (2004) The expression of DJ-1 (PARK7) in normal human CNS and idiopathic Parkinson's disease. *Brain* 127:420-430.
- Barbour R, Kling K, Anderson JP, Banducci K, Cole T, Diep L, Fox M, Goldstein JM, Soriano F, Seubert P, Chilcote TJ (2008) Red blood cells are the major source of alpha-synuclein in blood. *Neurodegener Dis* 5:55-59.
- Batelli S, Albani D, Rametta R, Polito L, Prato F, Pesaresi M, Negro A, Forloni G (2008) DJ-1 modulates alpha-synuclein aggregation state in a cellular model of oxidative stress: relevance for Parkinson's disease and involvement of HSP70. *PLoS One* 3:e1884.
- Beraud D, Twomey M, Bloom B, Mittereder A, Ton V, Neitzke K, Chasovskikh S, Mhyre TR, Maguire-Zeiss KA (2011) alpha-Synuclein Alters Toll-Like Receptor Expression. *Front Neurosci* 5:80.
- Bhat NR, Zhang P, Lee JC, Hogan EL (1998) Extracellular signal-regulated kinase and p38 subgroups of mitogen-activated protein kinases regulate inducible nitric oxide synthase and tumor necrosis factor-alpha gene expression in endotoxin-stimulated primary glial cultures. *J Neurosci* 18:1633-1641.
- Biragyn A, Ruffini PA, Leifer CA, Klyushnenkova E, Shakhov A, Chertov O, Shirakawa AK, Farber JM, Segal DM, Oppenheim JJ, Kwak LW (2002) Toll-like receptor 4-dependent activation of dendritic cells by beta-defensin 2. *Science* 298:1025-1029.
- Bjorkblom B, Adilbayeva A, Maple-Grodem J, Piston D, Okvist M, Xu XM, Brede C, Larsen JP, Moller SG (2013) The Parkinson's disease protein DJ-1 binds metals and protects against metal induced cytotoxicity. *J Biol Chem*.
- Bonifati V, Rizzu P, van Baren MJ, Schaap O, Breedveld GJ, Krieger E, Dekker MC, Squitieri F, Ibanez P, Joosse M, van Dongen JW, Vanacore N, van Swieten JC, Brice A, Meco G, van Duijn CM, Oostra BA, Heutink P (2003) Mutations in the DJ-1 gene associated with autosomal recessive early-onset parkinsonism. *Science* 299:256-259.
- Bowman EJ, Siebers A, Altendorf K (1988) Bafilomycins: a class of inhibitors of membrane ATPases from microorganisms, animal cells, and plant cells. *Proc Natl Acad Sci U S A* 85:7972-7976.
- Braak H, Del Tredici K, Rub U, de Vos RA, Jansen Steur EN, Braak E (2003) Staging of brain pathology related to sporadic Parkinson's disease. *Neurobiol Aging* 24:197-211.
- Braak H, Sastre M, Del Tredici K (2007) Development of alpha-synuclein immunoreactive astrocytes in the forebrain parallels stages of intraneuronal pathology in sporadic Parkinson's disease. *Acta Neuropathol* 114:231-241.
- Bretaud S, Allen C, Ingham PW, Bandmann O (2007) p53-dependent neuronal cell death in a DJ-1-deficient zebrafish model of Parkinson's disease. *J Neurochem* 100:1626-1635.
- Brochard V, Combadiere B, Prigent A, Laouar Y, Perrin A, Beray-Berthat V, Bonduelle O, Alvarez-Fischer D, Callebert J, Launay JM, Duyckaerts C, Flavell RA, Hirsch EC, Hunot S (2009) Infiltration of CD4+ lymphocytes into the brain contributes to neurodegeneration in a mouse model of Parkinson disease. *J Clin Invest* 119:182-192.
- Burre J, Sharma M, Tsetsenis T, Buchman V, Etherton MR, Sudhof TC (2010) Alpha-synuclein promotes SNARE-complex assembly in vivo and in vitro. *Science* 329:1663-1667.
- Canet-Aviles RM, Wilson MA, Miller DW, Ahmad R, McLendon C, Bandyopadhyay S, Baptista MJ, Ringe D, Petsko GA, Cookson MR (2004) The Parkinson's disease protein DJ-1 is neuroprotective due to cysteine-sulfinic acid-driven mitochondrial localization. *Proc Natl Acad Sci U S A* 101:9103-9108.
- Chen J, Li L, Chin LS (2010) Parkinson disease protein DJ-1 converts from a zymogen to a protease by carboxyl-terminal cleavage. *Hum Mol Genet* 19:2395-2408.
- Chen L, Cagniard B, Mathews T, Jones S, Koh HC, Ding Y, Carvey PM, Ling Z, Kang UJ, Zhuang X (2005) Age-dependent motor deficits and dopaminergic dysfunction in DJ-1 null mice. *J Biol Chem* 280:21418-21426.
- Chernomordik L, Kozlov MM, Zimmerberg J (1995) Lipids in biological membrane fusion. *J Membr Biol* 146:1-14.
- Chung IY, Benveniste EN (1990) Tumor necrosis factor-alpha production by astrocytes. Induction by lipopolysaccharide, IFN-gamma, and IL-1 beta. *J Immunol* 144:2999-3007.
- Clements CM, McNally RS, Conti BJ, Mak TW, Ting JP (2006) DJ-1, a cancer- and Parkinson's disease-associated protein, stabilizes the antioxidant transcriptional master regulator Nrf2. *Proc Natl Acad Sci U S A* 103:15091-15096.
- Cohlberg JA, Li J, Uversky VN, Fink AL (2002) Heparin and other glycosaminoglycans stimulate the formation of amyloid fibrils from alpha-synuclein in vitro. *Biochemistry* 41:1502-1511.

- Couch Y, Alvarez-Erviti L, Sison NR, Wood MJ, Anthony DC (2011) The acute inflammatory response to intranigral alpha-synuclein differs significantly from intranigral lipopolysaccharide and is exacerbated by peripheral inflammation. *J Neuroinflammation* 8:166.
- Crowther RA, Jakes R, Spillantini MG, Goedert M (1998) Synthetic filaments assembled from C-terminally truncated alpha-synuclein. *FEBS Lett* 436:309-312.
- Danzer KM, Krebs SK, Wolff M, Birk G, Hengeler B (2009) Seeding induced by alpha-synuclein oligomers provides evidence for spreading of alpha-synuclein pathology. *J Neurochem* 111:192-203.
- Danzer KM, Ruf WP, Putcha P, Joyner D, Hashimoto T, Glabe C, Hyman BT, McLean PJ (2011) Heat-shock protein 70 modulates toxic extracellular alpha-synuclein oligomers and rescues trans-synaptic toxicity. *FASEB J* 25:326-336.
- Davidson WS, Jonas A, Clayton DF, George JM (1998) Stabilization of alpha-synuclein secondary structure upon binding to synthetic membranes. *J Biol Chem* 273:9443-9449.
- Desplats P, Lee HJ, Bae EJ, Patrick C, Rockenstein E, Crews L, Spencer B, Masliah E, Lee SJ (2009) Inclusion formation and neuronal cell death through neuron-to-neuron transmission of alpha-synuclein. *Proc Natl Acad Sci U S A* 106:13010-13015.
- Dickson DW, Liu W, Hardy J, Farrer M, Mehta N, Uitti R, Mark M, Zimmerman T, Golbe L, Sage J, Sima A, D'Amato C, Albin R, Gilman S, Yen SH (1999) Widespread alterations of alpha-synuclein in multiple system atrophy. *Am J Pathol* 155:1241-1251.
- Edwards TL, Scott WK, Almonte C, Burt A, Powell EH, Beecham GW, Wang L, Zuchner S, Konidari I, Wang G, Singer C, Nahab F, Scott B, Stajich JM, Pericak-Vance M, Haines J, Vance JM, Martin ER (2010) Genome-wide association study confirms SNPs in SNCA and the MAPT region as common risk factors for Parkinson disease. *Ann Hum Genet* 74:97-109.
- el-Agnaf OM, Irvine GB (2002) Aggregation and neurotoxicity of alpha-synuclein and related peptides. *Biochem Soc Trans* 30:559-565.
- El-Agnaf OM, Salem SA, Paleologou KE, Cooper LJ, Fullwood NJ, Gibson MJ, Curran MD, Court JA, Mann DM, Ikeda S, Cookson MR, Hardy J, Allsop D (2003) Alpha-synuclein implicated in Parkinson's disease is present in extracellular biological fluids, including human plasma. *FASEB J* 17:1945-1947.
- Eldh M, Ekstrom K, Valadi H, Sjostrand M, Olsson B, Jernas M, Lotvall J (2010) Exosomes communicate protective messages during oxidative stress; possible role of exosomal shuttle RNA. *PLoS One* 5:e15353.
- Emmanouilidou E, Elenis D, Papisilekas T, Stranjalis G, Gerozissis K, Ioannou PC, Vekrellis K (2011) Assessment of alpha-synuclein secretion in mouse and human brain parenchyma. *PLoS One* 6:e22225.
- Emmanouilidou E, Melachroinou K, Roumeliotis T, Garbis SD, Ntzouni M, Margaritis LH, Stefanis L, Vekrellis K (2010) Cell-produced alpha-synuclein is secreted in a calcium-dependent manner by exosomes and impacts neuronal survival. *J Neurosci* 30:6838-6851.
- Fan J, Ren H, Jia N, Fei E, Zhou T, Jiang P, Wu M, Wang G (2008) DJ-1 decreases Bax expression through repressing p53 transcriptional activity. *J Biol Chem* 283:4022-4030.
- Farrer M, Kachergus J, Forno L, Lincoln S, Wang DS, Hulihan M, Maraganore D, Gwinn-Hardy K, Wszolek Z, Dickson D, Langston JW (2004) Comparison of kindreds with parkinsonism and alpha-synuclein genomic multiplications. *Ann Neurol* 55:174-179.
- Fearnley JM, Lees AJ (1991) Ageing and Parkinson's disease: substantia nigra regional selectivity. *Brain* 114 (Pt 5):2283-2301.
- Fellner L, Irschick R, Schanda K, Reindl M, Klimaschewski L, Poewe W, Wenning GK, Stefanova N (2013) Toll-like receptor 4 is required for alpha-synuclein dependent activation of microglia and astroglia. *Glia* 61:349-360.
- Fevrier B, Vilette D, Archer F, Loew D, Faigle W, Vidal M, Laude H, Raposo G (2004) Cells release prions in association with exosomes. *Proc Natl Acad Sci U S A* 101:9683-9688.
- Fortin DL, Troyer MD, Nakamura K, Kubo S, Anthony MD, Edwards RH (2004) Lipid rafts mediate the synaptic localization of alpha-synuclein. *J Neurosci* 24:6715-6723.
- Freeman D, Cedillos R, Choyke S, Lukic Z, McGuire K, Marvin S, Burrage AM, Sudholt S, Rana A, O'Connor C, Wiethoff CM, Campbell EM (2013) Alpha-synuclein induces lysosomal rupture and cathepsin dependent reactive oxygen species following endocytosis. *PLoS One* 8:e62143.
- Freichel C, Neumann M, Ballard T, Muller V, Woolley M, Ozmen L, Borroni E, Kretschmar HA, Haass C, Spooen W, Kahle PJ (2007) Age-dependent cognitive decline and amygdala pathology in alpha-synuclein transgenic mice. *Neurobiol Aging* 28:1421-1435.
- Freundt EC, Maynard N, Clancy EK, Roy S, Bousset L, Sourigues Y, Covert M, Melki R, Kirkegaard K, Brahic M (2012) Neuron-to-neuron transmission of alpha-synuclein fibrils through axonal transport. *Ann Neurol* 72:517-524.

6. References

- Fujino G, Noguchi T, Matsuzawa A, Yamauchi S, Saitoh M, Takeda K, Ichijo H (2007) Thioredoxin and TRAF family proteins regulate reactive oxygen species-dependent activation of ASK1 through reciprocal modulation of the N-terminal homophilic interaction of ASK1. *Mol Cell Biol* 27:8152-8163.
- Fujiwara H, Hasegawa M, Dohmae N, Kawashima A, Masliah E, Goldberg MS, Shen J, Takio K, Iwatsubo T (2002) alpha-Synuclein is phosphorylated in synucleinopathy lesions. *Nat Cell Biol* 4:160-164.
- Gao H, Yang W, Qi Z, Lu L, Duan C, Zhao C, Yang H (2012) DJ-1 protects dopaminergic neurons against rotenone-induced apoptosis by enhancing ERK-dependent mitophagy. *J Mol Biol* 423:232-248.
- Gao HM, Hong JS, Zhang W, Liu B (2003) Synergistic dopaminergic neurotoxicity of the pesticide rotenone and inflammogen lipopolysaccharide: relevance to the etiology of Parkinson's disease. *J Neurosci* 23:1228-1236.
- Gao HM, Kotzbauer PT, Uryu K, Leight S, Trojanowski JQ, Lee VM (2008) Neuroinflammation and oxidation/nitration of alpha-synuclein linked to dopaminergic neurodegeneration. *J Neurosci* 28:7687-7698.
- Ghazavi F, Fazlali Z, Banihosseini SS, Hosseini SR, Kazemi MH, Shojaee S, Parsa K, Sadeghi H, Sina F, Rohani M, Shahidi GA, Ghaemi N, Ronaghi M, Elahi E (2011) PRKN, DJ-1, and PINK1 screening identifies novel splice site mutation in PRKN and two novel DJ-1 mutations. *Mov Disord* 26:80-89.
- Giasson BI, Duda JE, Quinn SM, Zhang B, Trojanowski JQ, Lee VM (2002) Neuronal alpha-synucleinopathy with severe movement disorder in mice expressing A53T human alpha-synuclein. *Neuron* 34:521-533.
- Giasson BI, Murray IV, Trojanowski JQ, Lee VM (2001) A hydrophobic stretch of 12 amino acid residues in the middle of alpha-synuclein is essential for filament assembly. *J Biol Chem* 276:2380-2386.
- Goldberg MS, Pisani A, Haburcak M, Vortherms TA, Kitada T, Costa C, Tong Y, Martella G, Tscherter A, Martins A, Bernardi G, Roth BL, Pothos EN, Calabresi P, Shen J (2005) Nigrostriatal dopaminergic deficits and hypokinesia caused by inactivation of the familial Parkinsonism-linked gene DJ-1. *Neuron* 45:489-496.
- Goldman EH, Chen L, Fu H (2004) Activation of apoptosis signal-regulating kinase 1 by reactive oxygen species through dephosphorylation at serine 967 and 14-3-3 dissociation. *J Biol Chem* 279:10442-10449.
- Gorner K, Holtorf E, Odoj S, Nuscher B, Yamamoto A, Regula JT, Beyer K, Haass C, Kahle PJ (2004) Differential effects of Parkinson's disease-associated mutations on stability and folding of DJ-1. *J Biol Chem* 279:6943-6951.
- Gorner K, Holtorf E, Waak J, Pham TT, Vogt-Weisenhorn DM, Wurst W, Haass C, Kahle PJ (2007) Structural determinants of the C-terminal helix-kink-helix motif essential for protein stability and survival promoting activity of DJ-1. *J Biol Chem* 282:13680-13691.
- Gousset K, Schiff E, Langevin C, Marijanovic Z, Caputo A, Browman DT, Chenouard N, de Chaumont F, Martino A, Enninga J, Olivo-Marin JC, Mannel D, Zurzolo C (2009) Prions hijack tunnelling nanotubes for intercellular spread. *Nat Cell Biol* 11:328-336.
- Hamprecht B, Löffler F (1985) Primary glial cultures as a model for studying hormone action. *Methods Enzymol* 109:341-345.
- Hansen C, Angot E, Bergstrom AL, Steiner JA, Pieri L, Paul G, Outeiro TF, Melki R, Kallunki P, Fog K, Li JY, Brundin P (2011) alpha-Synuclein propagates from mouse brain to grafted dopaminergic neurons and seeds aggregation in cultured human cells. *J Clin Invest* 121:715-725.
- Hasegawa T, Konno M, Baba T, Sugeno N, Kikuchi A, Kobayashi M, Miura E, Tanaka N, Tamai K, Furukawa K, Arai H, Mori F, Wakabayashi K, Aoki M, Itoyama Y, Takeda A (2011) The AAA-ATPase VPS4 regulates extracellular secretion and lysosomal targeting of alpha-synuclein. *PLoS One* 6:e29460.
- Hayakawa R, Hayakawa T, Takeda K, Ichijo H (2012) Therapeutic targets in the ASK1-dependent stress signaling pathways. *Proc Jpn Acad Ser B Phys Biol Sci* 88:434-453.
- Hirsch EC, Hunot S (2009) Neuroinflammation in Parkinson's disease: a target for neuroprotection? *Lancet Neurol* 8:382-397.
- Hlavanda E, Kovacs J, Olah J, Orosz F, Medzihradszky KF, Ovadi J (2002) Brain-specific p25 protein binds to tubulin and microtubules and induces aberrant microtubule assemblies at substoichiometric concentrations. *Biochemistry* 41:8657-8664.
- Honbou K, Suzuki NN, Horiuchi M, Niki T, Taira T, Ariga H, Inagaki F (2003) The crystal structure of DJ-1, a protein related to male fertility and Parkinson's disease. *J Biol Chem* 278:31380-31384.
- Hoshino K, Takeuchi O, Kawai T, Sanjo H, Ogawa T, Takeda Y, Takeda K, Akira S (1999) Cutting edge: Toll-like receptor 4 (TLR4)-deficient mice are hyporesponsive to lipopolysaccharide: evidence for TLR4 as the Lps gene product. *J Immunol* 162:3749-3752.

- Hoyer W, Antony T, Cherny D, Heim G, Jovin TM, Subramaniam V (2002) Dependence of alpha-synuclein aggregate morphology on solution conditions. *J Mol Biol* 322:383-393.
- Hulleman JD, Mirzaei H, Guigard E, Taylor KL, Ray SS, Kay CM, Regnier FE, Rochet JC (2007) Destabilization of DJ-1 by familial substitution and oxidative modifications: implications for Parkinson's disease. *Biochemistry* 46:5776-5789.
- Hunot S, Boissiere F, Faucheux B, Brugg B, Mouatt-Prigent A, Agid Y, Hirsch EC (1996) Nitric oxide synthase and neuronal vulnerability in Parkinson's disease. *Neuroscience* 72:355-363.
- Ichijo H, Nishida E, Irie K, ten Dijke P, Saitoh M, Moriguchi T, Takagi M, Matsumoto K, Miyazono K, Gotoh Y (1997) Induction of apoptosis by ASK1, a mammalian MAPKKK that activates SAPK/JNK and p38 signaling pathways. *Science* 275:90-94.
- Irrcher I, Aleyasin H, Seifert EL, Hewitt SJ, Chhabra S, Phillips M, Lutz AK, Rousseaux MW, Bevilacqua L, Jahani-Asl A, Callaghan S, MacLaurin JG, Winklhofer KF, Rizzu P, Rippstein P, Kim RH, Chen CX, Fon EA, Slack RS, Harper ME, McBride HM, Mak TW, Park DS (2010) Loss of the Parkinson's disease-linked gene DJ-1 perturbs mitochondrial dynamics. *Hum Mol Genet* 19:3734-3746.
- Ishikawa S, Taira T, Takahashi-Niki K, Niki T, Ariga H, Iguchi-Ariga SM (2010) Human DJ-1-specific transcriptional activation of tyrosine hydroxylase gene. *J Biol Chem* 285:39718-39731.
- Ito G, Ariga H, Nakagawa Y, Iwatsubo T (2006) Roles of distinct cysteine residues in S-nitrosylation and dimerization of DJ-1. *Biochem Biophys Res Commun* 339:667-672.
- Jang A, Lee HJ, Suk JE, Jung JW, Kim KP, Lee SJ (2010) Non-classical exocytosis of alpha-synuclein is sensitive to folding states and promoted under stress conditions. *J Neurochem* 113:1263-1274.
- Jankovic J (2008) Parkinson's disease: clinical features and diagnosis. *J Neurol Neurosurg Psychiatry* 79:368-376.
- Jo E, McLaurin J, Yip CM, St George-Hyslop P, Fraser PE (2000) alpha-Synuclein membrane interactions and lipid specificity. *J Biol Chem* 275:34328-34334.
- Junn E, Jang WH, Zhao X, Jeong BS, Mouradian MM (2009) Mitochondrial localization of DJ-1 leads to enhanced neuroprotection. *J Neurosci Res* 87:123-129.
- Junn E, Taniguchi H, Jeong BS, Zhao X, Ichijo H, Mouradian MM (2005) Interaction of DJ-1 with Daxx inhibits apoptosis signal-regulating kinase 1 activity and cell death. *Proc Natl Acad Sci U S A* 102:9691-9696.
- Kahle PJ, Neumann M, Ozmen L, Muller V, Jacobsen H, Schindzielorz A, Okochi M, Leimer U, van Der Putten H, Probst A, Kremmer E, Kretschmar HA, Haass C (2000) Subcellular localization of wild-type and Parkinson's disease-associated mutant alpha-synuclein in human and transgenic mouse brain. *J Neurosci* 20:6365-6373.
- Kahle PJ, Neumann M, Ozmen L, Muller V, Odoj S, Okamoto N, Jacobsen H, Iwatsubo T, Trojanowski JQ, Takahashi H, Wakabayashi K, Bogdanovic N, Riederer P, Kretschmar HA, Haass C (2001) Selective insolubility of alpha-synuclein in human Lewy body diseases is recapitulated in a transgenic mouse model. *Am J Pathol* 159:2215-2225.
- Kasai T, Tokuda T, Yamaguchi N, Watanabe Y, Kametani F, Nakagawa M, Mizuno T (2008) Cleavage of normal and pathological forms of alpha-synuclein by neurosin in vitro. *Neurosci Lett* 436:52-56.
- Kato I, Maita H, Takahashi-Niki K, Saito Y, Noguchi N, Iguchi-Ariga SM, Ariga H (2013) Oxidized DJ-1 inhibits p53 by sequestering p53 from promoters in a DNA-binding affinity-dependent manner. *Mol Cell Biol* 33:340-359.
- Kawai T, Akira S (2007) TLR signaling. *Semin Immunol* 19:24-32.
- Kim AH, Khursigara G, Sun X, Franke TF, Chao MV (2001) Akt phosphorylates and negatively regulates apoptosis signal-regulating kinase 1. *Mol Cell Biol* 21:893-901.
- Kim C, Ho DH, Suk JE, You S, Michael S, Kang J, Joong Lee S, Masliah E, Hwang D, Lee HJ, Lee SJ (2013) Neuron-released oligomeric alpha-synuclein is an endogenous agonist of TLR2 for paracrine activation of microglia. *Nat Commun* 4:1562.
- Kim KS, Choi YR, Park JY, Lee JH, Kim DK, Lee SJ, Paik SR, Jou I, Park SM (2012) Proteolytic cleavage of extracellular alpha-synuclein by plasmin: implications for Parkinson disease. *J Biol Chem* 287:24862-24872.
- Kim RH, Peters M, Jang Y, Shi W, Pintilie M, Fletcher GC, DeLuca C, Liepa J, Zhou L, Snow B, Binari RC, Manoukian AS, Bray MR, Liu FF, Tsao MS, Mak TW (2005a) DJ-1, a novel regulator of the tumor suppressor PTEN. *Cancer Cell* 7:263-273.
- Kim RH, Smith PD, Aleyasin H, Hayley S, Mount MP, Pownall S, Wakeham A, You-Ten AJ, Kalia SK, Horne P, Westaway D, Lozano AM, Anisman H, Park DS, Mak TW (2005b) Hypersensitivity of DJ-1-deficient mice to 1-methyl-4-phenyl-1,2,3,6-tetrahydropyridine (MPTP) and oxidative stress. *Proc Natl Acad Sci U S A* 102:5215-5220.
- Kim YC, Kitaura H, Taira T, Iguchi-Ariga SM, Ariga H (2009) Oxidation of DJ-1-dependent cell transformation through direct binding of DJ-1 to PTEN. *Int J Oncol* 35:1331-1341.

6. References

- Kinumi T, Kimata J, Taira T, Ariga H, Niki E (2004) Cysteine-106 of DJ-1 is the most sensitive cysteine residue to hydrogen peroxide-mediated oxidation in vivo in human umbilical vein endothelial cells. *Biochem Biophys Res Commun* 317:722-728.
- Klegeris A, Giasson BI, Zhang H, Maguire J, Pelech S, McGeer PL (2006) Alpha-synuclein and its disease-causing mutants induce ICAM-1 and IL-6 in human astrocytes and astrocytoma cells. *FASEB J* 20:2000-2008.
- Klegeris A, Pelech S, Giasson BI, Maguire J, Zhang H, McGeer EG, McGeer PL (2008) Alpha-synuclein activates stress signaling protein kinases in THP-1 cells and microglia. *Neurobiol Aging* 29:739-752.
- Kolodziejwski PJ, Koo JS, Eissa NT (2004) Regulation of inducible nitric oxide synthase by rapid cellular turnover and cotranslational down-regulation by dimerization inhibitors. *Proc Natl Acad Sci U S A* 101:18141-18146.
- Kordower JH, Chu Y, Hauser RA, Freeman TB, Olanow CW (2008) Lewy body-like pathology in long-term embryonic nigral transplants in Parkinson's disease. *Nat Med* 14:504-506.
- Kordower JH, Freeman TB, Snow BJ, Vingerhoets FJ, Mufson EJ, Sanberg PR, Hauser RA, Smith DA, Nauert GM, Perl DP, et al. (1995) Neuropathological evidence of graft survival and striatal reinnervation after the transplantation of fetal mesencephalic tissue in a patient with Parkinson's disease. *N Engl J Med* 332:1118-1124.
- Kordower JH, Rosenstein JM, Collier TJ, Burke MA, Chen EY, Li JM, Martel L, Levey AE, Mufson EJ, Freeman TB, Olanow CW (1996) Functional fetal nigral grafts in a patient with Parkinson's disease: chemoanatomic, ultrastructural, and metabolic studies. *J Comp Neurol* 370:203-230.
- Kovacs GG, Laszlo L, Kovacs J, Jensen PH, Lindersson E, Botond G, Molnar T, Perczel A, Hudecz F, Mezo G, Erdei A, Tirian L, Lehotzky A, Gelpi E, Budka H, Ovadi J (2004) Natively unfolded tubulin polymerization promoting protein TPPP/p25 is a common marker of alpha-synucleinopathies. *Neurobiol Dis* 17:155-162.
- Kragh CL, Fillon G, Gysbers A, Hansen HD, Neumann M, Richter-Landsberg C, Haass C, Zalc B, Lubetzki C, Gai WP, Halliday GM, Kahle PJ, Jensen PH (2013) FAS-dependent cell death in alpha-synuclein transgenic oligodendrocyte models of multiple system atrophy. *PLoS One* 8:e55243.
- Kragh CL, Lund LB, Febbraro F, Hansen HD, Gai WP, El-Agnaf O, Richter-Landsberg C, Jensen PH (2009) Alpha-synuclein aggregation and Ser-129 phosphorylation-dependent cell death in oligodendroglial cells. *J Biol Chem* 284:10211-10222.
- Krebiehl G, Ruckerbauer S, Burbulla LF, Kieper N, Maurer B, Waak J, Wolburg H, Gizatullina Z, Gellerich FN, Voitalla D, Riess O, Kahle PJ, Proikas-Cezanne T, Kruger R (2010) Reduced basal autophagy and impaired mitochondrial dynamics due to loss of Parkinson's disease-associated protein DJ-1. *PLoS One* 5:e9367.
- Kruger R, Kuhn W, Muller T, Voitalla D, Graeber M, Kosel S, Przuntek H, Eppelen JT, Schols L, Riess O (1998) Ala30Pro mutation in the gene encoding alpha-synuclein in Parkinson's disease. *Nat Genet* 18:106-108.
- Kurt-Jones EA, Popova L, Kwinn L, Haynes LM, Jones LP, Tripp RA, Walsh EE, Freeman MW, Golenbock DT, Anderson LJ, Finberg RW (2000) Pattern recognition receptors TLR4 and CD14 mediate response to respiratory syncytial virus. *Nat Immunol* 1:398-401.
- Lee HJ, Baek SM, Ho DH, Suk JE, Cho ED, Lee SJ (2011) Dopamine promotes formation and secretion of non-fibrillar alpha-synuclein oligomers. *Exp Mol Med* 43:216-222.
- Lee HJ, Patel S, Lee SJ (2005) Intravesicular localization and exocytosis of alpha-synuclein and its aggregates. *J Neurosci* 25:6016-6024.
- Lee HJ, Suk JE, Bae EJ, Lee JH, Paik SR, Lee SJ (2008a) Assembly-dependent endocytosis and clearance of extracellular alpha-synuclein. *Int J Biochem Cell Biol* 40:1835-1849.
- Lee HJ, Suk JE, Bae EJ, Lee SJ (2008b) Clearance and deposition of extracellular alpha-synuclein aggregates in microglia. *Biochem Biophys Res Commun* 372:423-428.
- Lee HJ, Suk JE, Patrick C, Bae EJ, Cho JH, Rho S, Hwang D, Masliah E, Lee SJ (2010) Direct transfer of alpha-synuclein from neuron to astroglia causes inflammatory responses in synucleinopathies. *J Biol Chem* 285:9262-9272.
- Lee JY, Song J, Kwon K, Jang S, Kim C, Baek K, Kim J, Park C (2012) Human DJ-1 and its homologs are novel glyoxalases. *Hum Mol Genet* 21:3215-3225.
- Lee PH, Lee G, Park HJ, Bang OY, Joo IS, Huh K (2006) The plasma alpha-synuclein levels in patients with Parkinson's disease and multiple system atrophy. *J Neural Transm* 113:1435-1439.
- Lee SJ, Kim SJ, Kim IK, Ko J, Jeong CS, Kim GH, Park C, Kang SO, Suh PG, Lee HS, Cha SS (2003) Crystal structures of human DJ-1 and Escherichia coli Hsp31, which share an evolutionarily conserved domain. *J Biol Chem* 278:44552-44559.
- Lev N, Ickowicz D, Barhum Y, Lev S, Melamed E, Offen D (2009) DJ-1 protects against dopamine toxicity. *J Neural Transm* 116:151-160.

- Li HM, Niki T, Taira T, Iguchi-Ariga SM, Ariga H (2005) Association of DJ-1 with chaperones and enhanced association and colocalization with mitochondrial Hsp70 by oxidative stress. *Free Radic Res* 39:1091-1099.
- Li JY, Englund E, Holton JL, Soulet D, Hagell P, Lees AJ, Lashley T, Quinn NP, Rehncrona S, Bjorklund A, Widner H, Revesz T, Lindvall O, Brundin P (2008) Lewy bodies in grafted neurons in subjects with Parkinson's disease suggest host-to-graft disease propagation. *Nat Med* 14:501-503.
- Lindersson E, Lundvig D, Petersen C, Madsen P, Nyengaard JR, Hojrup P, Moos T, Otzen D, Gai WP, Blumbergs PC, Jensen PH (2005) p25alpha Stimulates alpha-synuclein aggregation and is colocalized with aggregated alpha-synuclein in alpha-synucleinopathies. *J Biol Chem* 280:5703-5715.
- Liu F, Nguyen JL, Hulleman JD, Li L, Rochet JC (2008) Mechanisms of DJ-1 neuroprotection in a cellular model of Parkinson's disease. *J Neurochem* 105:2435-2453.
- Liu H, Nishitoh H, Ichijo H, Kyriakis JM (2000) Activation of apoptosis signal-regulating kinase 1 (ASK1) by tumor necrosis factor receptor-associated factor 2 requires prior dissociation of the ASK1 inhibitor thioredoxin. *Mol Cell Biol* 20:2198-2208.
- Lowe R, Pountney DL, Jensen PH, Gai WP, Voelcker NH (2004) Calcium(II) selectively induces alpha-synuclein annular oligomers via interaction with the C-terminal domain. *Protein Sci* 13:3245-3252.
- Lu YC, Yeh WC, Ohashi PS (2008) LPS/TLR4 signal transduction pathway. *Cytokine* 42:145-151.
- Luk KC, Kehm V, Carroll J, Zhang B, O'Brien P, Trojanowski JQ, Lee VM (2012a) Pathological alpha-synuclein transmission initiates Parkinson-like neurodegeneration in nontransgenic mice. *Science* 338:949-953.
- Luk KC, Kehm VM, Zhang B, O'Brien P, Trojanowski JQ, Lee VM (2012b) Intracerebral inoculation of pathological alpha-synuclein initiates a rapidly progressive neurodegenerative alpha-synucleinopathy in mice. *J Exp Med* 209:975-986.
- Luk KC, Song C, O'Brien P, Stieber A, Branch JR, Brunden KR, Trojanowski JQ, Lee VM (2009) Exogenous alpha-synuclein fibrils seed the formation of Lewy body-like intracellular inclusions in cultured cells. *Proc Natl Acad Sci U S A* 106:20051-20056.
- Lysakova-Devine T, Keogh B, Harrington B, Nagpal K, Halle A, Golenbock DT, Monie T, Bowie AG (2010) Viral inhibitory peptide of TLR4, a peptide derived from vaccinia protein A46, specifically inhibits TLR4 by directly targeting MyD88 adaptor-like and TRIF-related adaptor molecule. *J Immunol* 185:4261-4271.
- Macedo MG, Anar B, Bronner IF, Cannella M, Squitieri F, Bonifati V, Hoogeveen A, Heutink P, Rizzu P (2003) The DJ-1L166P mutant protein associated with early onset Parkinson's disease is unstable and forms higher-order protein complexes. *Hum Mol Genet* 12:2807-2816.
- Macedo MG, Verbaan D, Fang Y, van Rooden SM, Visser M, Anar B, Uras A, Groen JL, Rizzu P, van Hilten JJ, Heutink P (2009) Genotypic and phenotypic characteristics of Dutch patients with early onset Parkinson's disease. *Mov Disord* 24:196-203.
- Maita C, Maita H, Iguchi-Ariga SM, Ariga H (2013) Monomer DJ-1 and its N-terminal sequence are necessary for mitochondrial localization of DJ-1 mutants. *PLoS One* 8:e54087.
- Maroteaux L, Campanelli JT, Scheller RH (1988) Synuclein: a neuron-specific protein localized to the nucleus and presynaptic nerve terminal. *J Neurosci* 8:2804-2815.
- Martinez Z, Zhu M, Han S, Fink AL (2007) GM1 specifically interacts with alpha-synuclein and inhibits fibrillation. *Biochemistry* 46:1868-1877.
- Mata IF, Shi M, Agarwal P, Chung KA, Edwards KL, Factor SA, Galasko DR, Ghingina C, Griffith A, Higgins DS, Kay DM, Kim H, Leverenz JB, Quinn JF, Roberts JW, Samii A, Snapinn KW, Tsuang DW, Yearout D, Zhang J, Payami H, Zabetian CP (2010) SNCA variant associated with Parkinson disease and plasma alpha-synuclein level. *Arch Neurol* 67:1350-1356.
- McGeer PL, Itagaki S, Boyes BE, McGeer EG (1988) Reactive microglia are positive for HLA-DR in the substantia nigra of Parkinson's and Alzheimer's disease brains. *Neurology* 38:1285-1291.
- Mendez I, Vinuela A, Astradsson A, Mukhida K, Hallett P, Robertson H, Tierney T, Holness R, Dagher A, Trojanowski JQ, Isacson O (2008) Dopamine neurons implanted into people with Parkinson's disease survive without pathology for 14 years. *Nat Med* 14:507-509.
- Meulener M, Whitworth AJ, Armstrong-Gold CE, Rizzu P, Heutink P, Wes PD, Pallanck LJ, Bonini NM (2005) *Drosophila* DJ-1 mutants are selectively sensitive to environmental toxins associated with Parkinson's disease. *Curr Biol* 15:1572-1577.
- Meulener MC, Xu K, Thomson L, Ischiropoulos H, Bonini NM (2006) Mutational analysis of DJ-1 in *Drosophila* implicates functional inactivation by oxidative damage and aging. *Proc Natl Acad Sci U S A* 103:12517-12522.

6. References

- Mitsugi H, Niki T, Takahashi-Niki K, Tanimura K, Yoshizawa-Kumagaye K, Tsunemi M, Iguchi-Ariga SM, Ariga H (2013) Identification of the recognition sequence and target proteins for DJ-1 protease. *FEBS Lett* 587:2493-2499.
- Mo JS, Jung J, Yoon JH, Hong JA, Kim MY, Ann EJ, Seo MS, Choi YH, Park HS (2010) DJ-1 modulates the p38 mitogen-activated protein kinase pathway through physical interaction with apoptosis signal-regulating kinase 1. *J Cell Biochem* 110:229-237.
- Moore DJ, Zhang L, Dawson TM, Dawson VL (2003) A missense mutation (L166P) in DJ-1, linked to familial Parkinson's disease, confers reduced protein stability and impairs homo-oligomerization. *J Neurochem* 87:1558-1567.
- Morita K, Saitoh M, Tobiume K, Matsuura H, Enomoto S, Nishitoh H, Ichijo H (2001) Negative feedback regulation of ASK1 by protein phosphatase 5 (PP5) in response to oxidative stress. *EMBO J* 20:6028-6036.
- Murray IV, Giasson BI, Quinn SM, Koppaka V, Axelsen PH, Ischiropoulos H, Trojanowski JQ, Lee VM (2003) Role of alpha-synuclein carboxy-terminus on fibril formation in vitro. *Biochemistry* 42:8530-8540.
- Nadeau PJ, Charette SJ, Landry J (2009) REDOX reaction at ASK1-Cys250 is essential for activation of JNK and induction of apoptosis. *Mol Biol Cell* 20:3628-3637.
- Nagai H, Noguchi T, Homma K, Katagiri K, Takeda K, Matsuzawa A, Ichijo H (2009) Ubiquitin-like sequence in ASK1 plays critical roles in the recognition and stabilization by USP9X and oxidative stress-induced cell death. *Mol Cell* 36:805-818.
- Nagakubo D, Taira T, Kitaura H, Ikeda M, Tamai K, Iguchi-Ariga SM, Ariga H (1997) DJ-1, a novel oncogene which transforms mouse NIH3T3 cells in cooperation with ras. *Biochem Biophys Res Commun* 231:509-513.
- Nakamura T, Tu S, Akhtar MW, Sunico CR, Okamoto S, Lipton SA (2013) Aberrant protein s-nitrosylation in neurodegenerative diseases. *Neuron* 78:596-614.
- Narhi L, Wood SJ, Steavenson S, Jiang Y, Wu GM, Anafi D, Kaufman SA, Martin F, Sitney K, Denis P, Louis JC, Wypych J, Biere AL, Citron M (1999) Both familial Parkinson's disease mutations accelerate alpha-synuclein aggregation. *J Biol Chem* 274:9843-9846.
- Netea MG, van Deuren M, Kullberg BJ, Cavailon JM, Van der Meer JW (2002) Does the shape of lipid A determine the interaction of LPS with Toll-like receptors? *Trends Immunol* 23:135-139.
- Neumann M, Kahle PJ, Giasson BI, Ozmen L, Borroni E, Spooen W, Muller V, Odoj S, Fujiwara H, Hasegawa M, Iwatsubo T, Trojanowski JQ, Kretschmar HA, Haass C (2002) Misfolded proteinase K-resistant hyperphosphorylated alpha-synuclein in aged transgenic mice with locomotor deterioration and in human alpha-synucleinopathies. *J Clin Invest* 110:1429-1439.
- Neumann M, Muller V, Gorner K, Kretschmar HA, Haass C, Kahle PJ (2004) Pathological properties of the Parkinson's disease-associated protein DJ-1 in alpha-synucleinopathies and tauopathies: relevance for multiple system atrophy and Pick's disease. *Acta Neuropathol* 107:489-496.
- Nishinaga H, Takahashi-Niki K, Taira T, Andreadis A, Iguchi-Ariga SM, Ariga H (2005) Expression profiles of genes in DJ-1-knockdown and L 166 P DJ-1 mutant cells. *Neurosci Lett* 390:54-59.
- Nishitoh H, Matsuzawa A, Tobiume K, Saegusa K, Takeda K, Inoue K, Hori S, Kakizuka A, Ichijo H (2002) ASK1 is essential for endoplasmic reticulum stress-induced neuronal cell death triggered by expanded polyglutamine repeats. *Genes Dev* 16:1345-1355.
- Nishitoh H, Saitoh M, Mochida Y, Takeda K, Nakano H, Rothe M, Miyazono K, Ichijo H (1998) ASK1 is essential for JNK/SAPK activation by TRAF2. *Mol Cell* 2:389-395.
- Noguchi T, Takeda K, Matsuzawa A, Saegusa K, Nakano H, Gohda J, Inoue J, Ichijo H (2005) Recruitment of tumor necrosis factor receptor-associated factor family proteins to apoptosis signal-regulating kinase 1 signalosome is essential for oxidative stress-induced cell death. *J Biol Chem* 280:37033-37040.
- Nonaka T, Watanabe ST, Iwatsubo T, Hasegawa M (2010) Seeded aggregation and toxicity of [alpha]-synuclein and tau: cellular models of neurodegenerative diseases. *J Biol Chem* 285:34885-34898.
- Ohashi K, Burkart V, Flohe S, Kolb H (2000) Cutting edge: heat shock protein 60 is a putative endogenous ligand of the toll-like receptor-4 complex. *J Immunol* 164:558-561.
- Papp MI, Kahn JE, Lantos PL (1989) Glial cytoplasmic inclusions in the CNS of patients with multiple system atrophy (striatonigral degeneration, olivopontocerebellar atrophy and Shy-Drager syndrome). *J Neurol Sci* 94:79-100.
- Park J, Kim SY, Cha GH, Lee SB, Kim S, Chung J (2005) Drosophila DJ-1 mutants show oxidative stress-sensitive locomotive dysfunction. *Gene* 361:133-139.
- Park JY, Kim KS, Lee SB, Ryu JS, Chung KC, Choo YK, Jou I, Kim J, Park SM (2009) On the mechanism of internalization of alpha-synuclein into microglia: roles of ganglioside GM1 and lipid raft. *J Neurochem* 110:400-411.

- Parkinson J (2002) An essay on the shaking palsy. 1817. *J Neuropsychiatry Clin Neurosci* 14:223-236; discussion 222.
- Perlmutter JD, Braun AR, Sachs JN (2009) Curvature dynamics of alpha-synuclein familial Parkinson disease mutants: molecular simulations of the micelle- and bilayer-bound forms. *J Biol Chem* 284:7177-7189.
- Pham TT, Giesert F, Rothig A, Floss T, Kallnik M, Weindl K, Holter SM, Ahting U, Prokisch H, Becker L, Klopstock T, Hrabe de Angelis M, Beyer K, Gorner K, Kahle PJ, Vogt Weisenhorn DM, Wurst W (2010) DJ-1-deficient mice show less TH-positive neurons in the ventral tegmental area and exhibit non-motoric behavioural impairments. *Genes Brain Behav* 9:305-317.
- Phillis JW, Horrocks LA, Farooqui AA (2006) Cyclooxygenases, lipoygenases, and epoxygenases in CNS: their role and involvement in neurological disorders. *Brain Res Rev* 52:201-243.
- Poltorak A, He X, Smirnova I, Liu MY, Van Huffel C, Du X, Birdwell D, Alejos E, Silva M, Galanos C, Freudenberg M, Ricciardi-Castagnoli P, Layton B, Beutler B (1998) Defective LPS signaling in C3H/HeJ and C57BL/10ScCr mice: mutations in Tlr4 gene. *Science* 282:2085-2088.
- Polymeropoulos MH, Lavedan C, Leroy E, Ide SE, Dehejia A, Dutra A, Pike B, Root H, Rubenstein J, Boyer R, Stenroos ES, Chandrasekharappa S, Athanassiadou A, Papapetropoulos T, Johnson WG, Lazzarini AM, Duvoisin RC, Di Iorio G, Golbe LI, Nussbaum RL (1997) Mutation in the alpha-synuclein gene identified in families with Parkinson's disease. *Science* 276:2045-2047.
- Qin L, Liu Y, Wang T, Wei SJ, Block ML, Wilson B, Liu B, Hong JS (2004) NADPH oxidase mediates lipopolysaccharide-induced neurotoxicity and proinflammatory gene expression in activated microglia. *J Biol Chem* 279:1415-1421.
- Rahman-Roblick R, Hellman U, Becker S, Bader FG, Auer G, Wiman KG, Roblick UJ (2008) Proteomic identification of p53-dependent protein phosphorylation. *Oncogene* 27:4854-4859.
- Rajendran L, Honscho M, Zahn TR, Keller P, Geiger KD, Verkade P, Simons K (2006) Alzheimer's disease beta-amyloid peptides are released in association with exosomes. *Proc Natl Acad Sci U S A* 103:11172-11177.
- Ramsey CP, Tsika E, Ischiropoulos H, Giasson BI (2010) DJ-1 deficient mice demonstrate similar vulnerability to pathogenic Ala53Thr human alpha-syn toxicity. *Hum Mol Genet* 19:1425-1437.
- Rassa JC, Meyers JL, Zhang Y, Kudravalli R, Ross SR (2002) Murine retroviruses activate B cells via interaction with toll-like receptor 4. *Proc Natl Acad Sci U S A* 99:2281-2286.
- Recchia A, Debetto P, Negro A, Guidolin D, Skaper SD, Giusti P (2004) Alpha-synuclein and Parkinson's disease. *FASEB J* 18:617-626.
- Rizzu P, Hinkle DA, Zhukareva V, Bonifati V, Severijnen LA, Martinez D, Ravid R, Kamphorst W, Eberwine JH, Lee VM, Trojanowski JQ, Heutink P (2004) DJ-1 colocalizes with tau inclusions: a link between parkinsonism and dementia. *Ann Neurol* 55:113-118.
- Rousseaux MW, Marcogliese PC, Qu D, Hewitt SJ, Seang S, Kim RH, Slack RS, Schlossmacher MG, Lagace DC, Mak TW, Park DS (2012) Progressive dopaminergic cell loss with unilateral-to-bilateral progression in a genetic model of Parkinson disease. *Proc Natl Acad Sci U S A* 109:15918-15923.
- Saeed U, Ray A, Valli RK, Kumar AM, Ravindranath V (2010) DJ-1 loss by glutaredoxin but not glutathione depletion triggers Daxx translocation and cell death. *Antioxid Redox Signal* 13:127-144.
- Saitoh M, Nishitoh H, Fujii M, Takeda K, Tobiume K, Sawada Y, Kawabata M, Miyazono K, Ichijo H (1998) Mammalian thioredoxin is a direct inhibitor of apoptosis signal-regulating kinase (ASK) 1. *EMBO J* 17:2596-2606.
- Satake W, Nakabayashi Y, Mizuta I, Hirota Y, Ito C, Kubo M, Kawaguchi T, Tsunoda T, Watanabe M, Takeda A, Tomiyama H, Nakashima K, Hasegawa K, Obata F, Yoshikawa T, Kawakami H, Sakoda S, Yamamoto M, Hattori N, Murata M, Nakamura Y, Toda T (2009) Genome-wide association study identifies common variants at four loci as genetic risk factors for Parkinson's disease. *Nat Genet* 41:1303-1307.
- Schell H, Hasegawa T, Neumann M, Kahle PJ (2009) Nuclear and neuritic distribution of serine-129 phosphorylated alpha-synuclein in transgenic mice. *Neuroscience* 160:796-804.
- Shendelman S, Jonason A, Martinat C, Leete T, Abeliovich A (2004) DJ-1 is a redox-dependent molecular chaperone that inhibits alpha-synuclein aggregate formation. *PLoS Biol* 2:e362.
- Shinbo Y, Niki T, Taira T, Ooe H, Takahashi-Niki K, Maita C, Seino C, Iguchi-Arigo SM, Ariga H (2006) Proper SUMO-1 conjugation is essential to DJ-1 to exert its full activities. *Cell Death Differ* 13:96-108.
- Shinbo Y, Taira T, Niki T, Iguchi-Arigo SM, Ariga H (2005) DJ-1 restores p53 transcription activity inhibited by Topors/p53BP3. *Int J Oncol* 26:641-648.
- Shults CW, Rockenstein E, Crews L, Adame A, Mante M, Larrea G, Hashimoto M, Song D, Iwatsubo T, Tsuboi K, Masliah E (2005) Neurological and neurodegenerative alterations in a transgenic

6. References

- mouse model expressing human alpha-synuclein under oligodendrocyte promoter: implications for multiple system atrophy. *J Neurosci* 25:10689-10699.
- Simon-Sanchez J, Schulte C, Bras JM, Sharma M, Gibbs JR, Berg D, Paisan-Ruiz C, Lichtner P, Scholz SW, Hernandez DG, Kruger R, Federoff M, Klein C, Goate A, Perlmutter J, Bonin M, Nalls MA, Illig T, Gieger C, Houlden H, Steffens M, Okun MS, Racette BA, Cookson MR, Foote KD, Fernandez HH, Traynor BJ, Schreiber S, Arepalli S, Zonozi R, Gwinn K, van der Brug M, Lopez G, Chanock SJ, Schatzkin A, Park Y, Hollenbeck A, Gao J, Huang X, Wood NW, Lorenz D, Deuschl G, Chen H, Riess O, Hardy JA, Singleton AB, Gasser T (2009) Genome-wide association study reveals genetic risk underlying Parkinson's disease. *Nat Genet* 41:1308-1312.
- Simunovic F, Yi M, Wang Y, Stephens R, Sonntag KC (2010) Evidence for gender-specific transcriptional profiles of nigral dopamine neurons in Parkinson disease. *PLoS One* 5:e8856.
- Singleton AB, Farrer M, Johnson J, Singleton A, Hague S, Kachergus J, Hulihan M, Peuralinna T, Dutra A, Nussbaum R, Lincoln S, Crawley A, Hanson M, Maraganore D, Adler C, Cookson MR, Muentner M, Baptista M, Miller D, Blancato J, Hardy J, Gwinn-Hardy K (2003) alpha-Synuclein locus triplication causes Parkinson's disease. *Science* 302:841.
- Snyder H, Mensah K, Theisler C, Lee J, Matouschek A, Wolozin B (2003) Aggregated and monomeric alpha-synuclein bind to the S6' proteasomal protein and inhibit proteasomal function. *J Biol Chem* 278:11753-11759.
- Song JJ, Lee YJ (2003) Role of the ASK1-SEK1-JNK1-HIPK1 signal in Daxx trafficking and ASK1 oligomerization. *J Biol Chem* 278:47245-47252.
- Song YJ, Lundvig DM, Huang Y, Gai WP, Blumbergs PC, Hojrup P, Otzen D, Halliday GM, Jensen PH (2007) p25alpha relocates in oligodendroglia from myelin to cytoplasmic inclusions in multiple system atrophy. *Am J Pathol* 171:1291-1303.
- Spillantini MG, Schmidt ML, Lee VM, Trojanowski JQ, Jakes R, Goedert M (1997) Alpha-synuclein in Lewy bodies. *Nature* 388:839-840.
- Stefanis L, Larsen KE, Rideout HJ, Sulzer D, Greene LA (2001) Expression of A53T mutant but not wild-type alpha-synuclein in PC12 cells induces alterations of the ubiquitin-dependent degradation system, loss of dopamine release, and autophagic cell death. *J Neurosci* 21:9549-9560.
- Stefanova N, Reindl M, Neumann M, Kahle PJ, Poewe W, Wenning GK (2007) Microglial activation mediates neurodegeneration related to oligodendroglial alpha-synucleinopathy: implications for multiple system atrophy. *Mov Disord* 22:2196-2203.
- Steiner JA, Angot E, Brundin P (2011) A deadly spread: cellular mechanisms of alpha-synuclein transfer. *Cell Death Differ* 18:1425-1433.
- Stuehr DJ (1999) Mammalian nitric oxide synthases. *Biochim Biophys Acta* 1411:217-230.
- Su X, Maguire-Zeiss KA, Giuliano R, Prifti L, Venkatesh K, Federoff HJ (2008) Synuclein activates microglia in a model of Parkinson's disease. *Neurobiol Aging* 29:1690-1701.
- Sung JY, Kim J, Paik SR, Park JH, Ahn YS, Chung KC (2001) Induction of neuronal cell death by Rab5A-dependent endocytosis of alpha-synuclein. *J Biol Chem* 276:27441-27448.
- Sung JY, Park SM, Lee CH, Um JW, Lee HJ, Kim J, Oh YJ, Lee ST, Paik SR, Chung KC (2005) Proteolytic cleavage of extracellular secreted {alpha}-synuclein via matrix metalloproteinases. *J Biol Chem* 280:25216-25224.
- Sweet MJ, Hume DA (1996) Endotoxin signal transduction in macrophages. *J Leukoc Biol* 60:8-26.
- Taira T, Saito Y, Niki T, Iguchi-Ariga SM, Takahashi K, Ariga H (2004) DJ-1 has a role in antioxidative stress to prevent cell death. *EMBO Rep* 5:213-218.
- Takahashi K, Taira T, Niki T, Seino C, Iguchi-Ariga SM, Ariga H (2001) DJ-1 positively regulates the androgen receptor by impairing the binding of PIASx alpha to the receptor. *J Biol Chem* 276:37556-37563.
- Takahashi M, Tomizawa K, Fujita SC, Sato K, Uchida T, Imahori K (1993) A brain-specific protein p25 is localized and associated with oligodendrocytes, neuropil, and fiber-like structures of the CA3 hippocampal region in the rat brain. *J Neurochem* 60:228-235.
- Takahashi T, Yamashita H, Nakamura T, Nagano Y, Nakamura S (2002) Tyrosine 125 of alpha-synuclein plays a critical role for dimerization following oxidative stress. *Brain Res* 938:73-80.
- Takeda K, Matsuzawa A, Nishitoh H, Tobiume K, Kishida S, Ninomiya-Tsuji J, Matsumoto K, Ichijo H (2004) Involvement of ASK1 in Ca²⁺-induced p38 MAP kinase activation. *EMBO Rep* 5:161-166.
- Takeda K, Noguchi T, Naguro I, Ichijo H (2008) Apoptosis signal-regulating kinase 1 in stress and immune response. *Annu Rev Pharmacol Toxicol* 48:199-225.
- Takeda K, Shimozono R, Noguchi T, Umeda T, Morimoto Y, Naguro I, Tobiume K, Saitoh M, Matsuzawa A, Ichijo H (2007) Apoptosis signal-regulating kinase (ASK) 2 functions as a mitogen-activated protein kinase kinase kinase in a heteromeric complex with ASK1. *J Biol Chem* 282:7522-7531.

6. References

- Tanaka S, Takehashi M, Matoh N, Iida S, Suzuki T, Futaki S, Hamada H, Masliah E, Sugiura Y, Ueda K (2002) Generation of reactive oxygen species and activation of NF-kappaB by non-Abeta component of Alzheimer's disease amyloid. *J Neurochem* 82:305-315.
- Tao X, Tong L (2003) Crystal structure of human DJ-1, a protein associated with early onset Parkinson's disease. *J Biol Chem* 278:31372-31379.
- Tatebe H, Watanabe Y, Kasai T, Mizuno T, Nakagawa M, Tanaka M, Tokuda T (2010) Extracellular neurosin degrades alpha-synuclein in cultured cells. *Neurosci Res* 67:341-346.
- Termeer C, Benedix F, Sleeman J, Fieber C, Voith U, Ahrens T, Miyake K, Freudenberg M, Galanos C, Simon JC (2002) Oligosaccharides of Hyaluronan activate dendritic cells via toll-like receptor 4. *J Exp Med* 195:99-111.
- Thomas KJ, McCoy MK, Blackinton J, Beilina A, van der Brug M, Sandebring A, Miller D, Maric D, Cedazo-Minguez A, Cookson MR (2011) DJ-1 acts in parallel to the PINK1/parkin pathway to control mitochondrial function and autophagy. *Hum Mol Genet* 20:40-50.
- Tirian L, Hlavanda E, Olah J, Horvath I, Orosz F, Szabo B, Kovacs J, Szabad J, Ovadi J (2003) TPPP/p25 promotes tubulin assemblies and blocks mitotic spindle formation. *Proc Natl Acad Sci U S A* 100:13976-13981.
- Tobiume K, Inage T, Takeda K, Enomoto S, Miyazono K, Ichijo H (1997) Molecular cloning and characterization of the mouse apoptosis signal-regulating kinase 1. *Biochem Biophys Res Commun* 239:905-910.
- Tobiume K, Saitoh M, Ichijo H (2002) Activation of apoptosis signal-regulating kinase 1 by the stress-induced activating phosphorylation of pre-formed oligomer. *J Cell Physiol* 191:95-104.
- Tokuda T, Salem SA, Allsop D, Mizuno T, Nakagawa M, Qureshi MM, Locascio JJ, Schlossmacher MG, El-Agnaf OM (2006) Decreased alpha-synuclein in cerebrospinal fluid of aged individuals and subjects with Parkinson's disease. *Biochem Biophys Res Commun* 349:162-166.
- Ubhi K, Low P, Masliah E (2011) Multiple system atrophy: a clinical and neuropathological perspective. *Trends Neurosci* 34:581-590.
- Ulmer TS, Bax A (2005) Comparison of structure and dynamics of micelle-bound human alpha-synuclein and Parkinson disease variants. *J Biol Chem* 280:43179-43187.
- Vella LJ, Sharples RA, Lawson VA, Masters CL, Cappai R, Hill AF (2007) Packaging of prions into exosomes is associated with a novel pathway of PrP processing. *J Pathol* 211:582-590.
- Waak J, Weber SS, Gorner K, Schall C, Ichijo H, Stehle T, Kahle PJ (2009a) Oxidizable residues mediating protein stability and cytoprotective interaction of DJ-1 with apoptosis signal-regulating kinase 1. *J Biol Chem* 284:14245-14257.
- Waak J, Weber SS, Waldenmaier A, Gorner K, Alunni-Fabbroni M, Schell H, Vogt-Weisenhorn D, Pham TT, Reumers V, Baekelandt V, Wurst W, Kahle PJ (2009b) Regulation of astrocyte inflammatory responses by the Parkinson's disease-associated gene DJ-1. *FASEB J* 23:2478-2489.
- Wakabayashi K, Hayashi S, Yoshimoto M, Kudo H, Takahashi H (2000) NACP/alpha-synuclein-positive filamentous inclusions in astrocytes and oligodendrocytes of Parkinson's disease brains. *Acta Neuropathol* 99:14-20.
- Wakabayashi K, Takahashi H (1996) Gallyas-positive, tau-negative glial inclusions in Parkinson's disease midbrain. *Neurosci Lett* 217:133-136.
- Wakabayashi K, Tanji K, Mori F, Takahashi H (2007) The Lewy body in Parkinson's disease: molecules implicated in the formation and degradation of alpha-synuclein aggregates. *Neuropathology* 27:494-506.
- Wakabayashi K, Yoshimoto M, Tsuji S, Takahashi H (1998) Alpha-synuclein immunoreactivity in glial cytoplasmic inclusions in multiple system atrophy. *Neurosci Lett* 249:180-182.
- Waxman EA, Giasson BI (2010) A novel, high-efficiency cellular model of fibrillar alpha-synuclein inclusions and the examination of mutations that inhibit amyloid formation. *J Neurochem* 113:374-388.
- Welch JE, Barbee RR, Roberts NL, Suarez JD, Klinefelter GR (1998) SP22: a novel fertility protein from a highly conserved gene family. *J Androl* 19:385-393.
- Wilson MA, Collins JL, Hod Y, Ringe D, Petsko GA (2003) The 1.1-A resolution crystal structure of DJ-1, the protein mutated in autosomal recessive early onset Parkinson's disease. *Proc Natl Acad Sci U S A* 100:9256-9261.
- Witt AC, Lakshminarasimhan M, Remington BC, Hasim S, Pozharski E, Wilson MA (2008) Cysteine pKa depression by a protonated glutamic acid in human DJ-1. *Biochemistry* 47:7430-7440.
- Wood SJ, Wypych J, Steavenson S, Louis JC, Citron M, Biere AL (1999) alpha-synuclein fibrillogenesis is nucleation-dependent. Implications for the pathogenesis of Parkinson's disease. *J Biol Chem* 274:19509-19512.
- Wooten GF, Currie LJ, Bovbjerg VE, Lee JK, Patrie J (2004) Are men at greater risk for Parkinson's disease than women? *J Neurol Neurosurg Psychiatry* 75:637-639.

6. References

- Yamada T, McGeer PL, Baimbridge KG, McGeer EG (1990) Relative sparing in Parkinson's disease of substantia nigra dopamine neurons containing calbindin-D28K. *Brain Res* 526:303-307.
- Yamaguchi H, Shen J (2007) Absence of dopaminergic neuronal degeneration and oxidative damage in aged DJ-1-deficient mice. *Mol Neurodegener* 2:10.
- Yamaguchi S, Yamane T, Takahashi-Niki K, Kato I, Niki T, Goldberg MS, Shen J, Ishimoto K, Doi T, Iguchi-Ariga SM, Ariga H (2012) Transcriptional activation of low-density lipoprotein receptor gene by DJ-1 and effect of DJ-1 on cholesterol homeostasis. *PLoS One* 7:e38144.
- Yanagida T, Tsushima J, Kitamura Y, Yanagisawa D, Takata K, Shibaike T, Yamamoto A, Taniguchi T, Yasui H, Taira T, Morikawa S, Inubushi T, Tooyama I, Ariga H (2009) Oxidative stress induction of DJ-1 protein in reactive astrocytes scavenges free radicals and reduces cell injury. *Oxid Med Cell Longev* 2:36-42.
- Yang X, Khosravi-Far R, Chang HY, Baltimore D (1997) Daxx, a novel Fas-binding protein that activates JNK and apoptosis. *Cell* 89:1067-1076.
- Yang Y, Gehrke S, Haque ME, Imai Y, Kosek J, Yang L, Beal MF, Nishimura I, Wakamatsu K, Ito S, Takahashi R, Lu B (2005) Inactivation of *Drosophila* DJ-1 leads to impairments of oxidative stress response and phosphatidylinositol 3-kinase/Akt signaling. *Proc Natl Acad Sci U S A* 102:13670-13675.
- Yoshimori T, Yamamoto A, Moriyama Y, Futai M, Tashiro Y (1991) Bafilomycin A1, a specific inhibitor of vacuolar-type H(+)-ATPase, inhibits acidification and protein degradation in lysosomes of cultured cells. *J Biol Chem* 266:17707-17712.
- Zhang L, Chen J, Fu H (1999) Suppression of apoptosis signal-regulating kinase 1-induced cell death by 14-3-3 proteins. *Proc Natl Acad Sci U S A* 96:8511-8515.
- Zhang L, Shimoji M, Thomas B, Moore DJ, Yu SW, Marupudi NI, Torp R, Torgner IA, Ottersen OP, Dawson TM, Dawson VL (2005a) Mitochondrial localization of the Parkinson's disease related protein DJ-1: implications for pathogenesis. *Hum Mol Genet* 14:2063-2073.
- Zhang R, Al-Lamki R, Bai L, Streb JW, Miano JM, Bradley J, Min W (2004) Thioredoxin-2 inhibits mitochondria-located ASK1-mediated apoptosis in a JNK-independent manner. *Circ Res* 94:1483-1491.
- Zhang W, Dallas S, Zhang D, Guo JP, Pang H, Wilson B, Miller DS, Chen B, McGeer PL, Hong JS, Zhang J (2007) Microglial PHOX and Mac-1 are essential to the enhanced dopaminergic neurodegeneration elicited by A30P and A53T mutant alpha-synuclein. *Glia* 55:1178-1188.
- Zhang W, Wang T, Pei Z, Miller DS, Wu X, Block ML, Wilson B, Zhou Y, Hong JS, Zhang J (2005b) Aggregated alpha-synuclein activates microglia: a process leading to disease progression in Parkinson's disease. *FASEB J* 19:533-542.
- Zhong N, Kim CY, Rizzu P, Geula C, Porter DR, Pothos EN, Squitieri F, Heutink P, Xu J (2006) DJ-1 transcriptionally up-regulates the human tyrosine hydroxylase by inhibiting the sumoylation of pyrimidine tract-binding protein-associated splicing factor. *J Biol Chem* 281:20940-20948.
- Zhou W, Freed CR (2005) DJ-1 up-regulates glutathione synthesis during oxidative stress and inhibits A53T alpha-synuclein toxicity. *J Biol Chem* 280:43150-43158.
- Zhou W, Zhu M, Wilson MA, Petsko GA, Fink AL (2006) The oxidation state of DJ-1 regulates its chaperone activity toward alpha-synuclein. *J Mol Biol* 356:1036-1048.

7 Acknowledgments

I want to thank my supervisor **Philipp Kahle** for his help and guidance, for the opportunity to work in his laboratory and on this project and for not giving up on me.

I also want to thank my advisory board members, Prof. **Thilo Stehle** and Prof. **Olaf Rieß**, for taking time for me and for their advice. A special thank to Prof. Stehle for letting me do some of my experiments with equipment in his laboratory.

The financial support I got from the **German National Genome Research Network**.

I can't be grateful enough to **Stephanie Weber**, who was working for and with me during 1.5 years of this project. No one can ask for a more efficient and trustful assistant. I honestly can't say a bad word about her. I also thank **Cindy Boden**, who did a lot of genotyping and bedding of brains for me and helped me in the animal facility when I needed it. These two wonderful assistants saved me a lot of time. I also thank the **animal caretakers** in the animal facility for their big help with my mice.

I thank Prof. **Poul Henning Jensen**, **Karina Fog**, **Louise Buur Vesteragar** and **Jafar Shaik** for the collaboration, sharing their data with us and their help with writing the manuscript.

I'm grateful to **Kerstin Reiss** in Prof. Stehle's group for her advice, guidance and time. I learned a lot about protein purification and chromatography from her.

I want to thank **all my colleagues** during my graduation time; they made the days at work fun and I deeply appreciate their patient with me and all the help I got from them. I specially thank **Heinrich**, **Sven** and **Fabienne** for always being open to help and guidance me whenever I needed it and **Sven** for taking time to carefully read and comment my thesis. **Sven**, **Heinrich** and **Friederike** also get special thanks for all the co-complaining discussions we had, they helped me a lot.

I thank my present and former **flat mates** and **my friends** and **relatives** in Finland for their support. From which I especially mention **Justine**, **Hanne** and **Ville**, whose unlimited support have been priceless for me. I can't thank them enough! At this point I also need to thank Facebook and Skype for decreasing my home sickness and metal bands for making music that made me stand up and fight when I at least felt like it.

Last, but certainly not least, I thank from the bottom of my heart **my mum**, **my dad** and **my sisters, Pia and Nilla**. For encouraging and listening me, their endless support, for all their visits to Germany and for just being who they are. I would never have come this far without them.

Parts of this work have been published in:

Publication:

Rannikko EH, Vesterager LB, Shaik JH, Weber SS, Cornejo Castro EM, Fog K, Jensen PH, Kahle PJ. „Loss of DJ-1 protein stability and cytoprotective function by Parkinson's disease-associated proline-158 deletion" *J Neurochem.* 2012 Dec 14 doi:10.1111/jnc.12126. [Epub ahead of print]

-*EH Rannikko* contributed with the experimental design, performance and analysis of the data in figures 2, 3, 4, 5, 6 and 8d, put together all figures and wrote the manuscript.

-*LB Vesterager* contributed with the experimental design, performance and analysis of the data in figure 8 (a-c), generated the OLN AS7 cell line and edited the manuscript.

-*JH Shaik* contributed with experimental design, performance and analysis of the data in figure 7.

-*SS Weber* contributed with technical assistance in the experimental performance of the data in figures 2, 3, 4, 5, 6 and 8d.

-*EM Cornejo Castro* cloned pCMV-myc-DJ-1^{P158Δ} and pCMV-myc-DJ-1^{A179T}.

-*K Fog* supervised LB Vesterager and edited the manuscript.

-*PH Jensen* supervised JH Shaik and edited the manuscript.

- *PJ Kahle* supervised EH Rannikko, conceived and coordinated the study and wrote the manuscript.

I herewith agree with the statements to the contributions to the co-authorships

Tübingen, 15.10.2013
Location, Date



Prof. Dr. Philipp Kahle

Antrag auf Zulassung zum Promotionsverfahren – Studiengang zelluläre und molekulare Neurowissenschaften

Declaration of co-authorship

Publication:

Rannikko EH, Vesterager LB, Shaik JH, Weber SS, Cornejo Castro EM, Fog K, Jensen PH, Kahle PJ. „Loss of DJ-1 protein stability and cytoprotective function by Parkinson's disease-associated proline-158 deletion” *J Neurochem.* 2012 Dec 14
doi:10.1111/jnc.12126. [Epub ahead of print]

- *EH Rannikko* contributed with the experimental design, performance and analysis of the data in figures 2, 3, 4, 5, 6 and 8d, put together all figures and wrote the manuscript.
- *LB Vesterager* contributed with the experimental design, performance and analysis of the data in figure 8 (a-c), generated the OLN AS7 cell line and edited the manuscript.
- *JH Shaik* contributed with experimental design, performance and analysis of the data in figure 7.
- *SS Weber* contributed with technical assistance in the experimental performance of the data in figures 2, 3, 4, 5, 6 and 8d.
- *EM Cornejo Castro* cloned pCMV-myc-DJ-1^{P158Δ} and pCMV-myc-DJ-1^{A179T}.
- *K Fog* supervised LB Vesterager and edited the manuscript.
- *PH Jensen* supervised JH Shaik and edited the manuscript.
- *PJ Kahle* supervised EH Rannikko, conceived and coordinated the study and wrote the manuscript.

I herewith agree with the statements to the contributions to the co-authorships. Moreover I agree that the author (Emmy Rannikko) presents the data from this publication that was generated at the Department of Neurodegeneration at H. Lundbeck A/S, Valby, Denmark in her PhD thesis entitled “Characterization of Parkinson's disease associated DJ-1 mutants and influence of α -synuclein on glial cells”

Valby 16/10-2013
Location, Date

Karina Fog
Karina Fog